

ALMA MATER STUDIORUM
UNIVERSITÀ DEGLI STUDI DI BOLOGNA
SEDE DI CESENA

Dipartimento di Elettronica Informatica e Sistemistica
Dottorato di Ricerca in Ingegneria Elettronica, Informatica
e delle Telecomunicazioni - XX Ciclo
SSD: ING-INF/03 - Telecomunicazioni

Cooperative Communication and
Distributed Detection in
Wireless Sensor Networks

Tesi di:
Ing. Matteo Lucchi

Relatore:
Chiar.mo Prof. Ing. Marco Chiani

Coordinatore:
Chiar.mo Prof. Ing. Paolo Bassi

Anno Accademico 2006–2007

Keywords

Telecommunications

Wireless Sensor Networks

Cooperative Diversity

Distributed Detection

Energy Efficiency

*To my girlfriend and future wife
Stefania*

Contents

Introduction	3
1 Wireless Sensor Networks	9
1.1 Main characteristics of Wireless Sensor Networks	11
1.2 Protocol Stack	13
1.2.1 The physical layer	14
1.2.2 The data link layer	15
1.2.3 The network layer	17
1.2.4 The transport and application layer	22
1.3 Applications of WSNs	23
1.3.1 Military applications	23
1.3.2 Environmental monitoring	23
1.3.3 Support for logistics	26
1.3.4 Human-centric and robotic applications	27
2 Cooperative Communication in Wireless Sensor Networks	29
2.1 System Description	30
2.1.1 Channel Model	30
2.1.2 Transmission Technique	32
2.1.3 Synchronization and Transmission Bandwidth Require- ments	34
2.1.4 Fusion Center Model	35
2.2 Performance Limits for Unconstrained Input Signaling	35
2.3 Performance Limits with Binary Signaling	38
2.3.1 Bit Error Probability Analysis	39
2.4 Numerical Results	41
2.4.1 Capacity and Throughput results	43
2.4.2 Bit Error Probability results	45
2.4.3 Scaling	48

3	Distributed Detection in Wireless Sensor Networks	53
3.1	First scenario: all nodes observing the same phenomenon . . .	55
3.1.1	Results	58
3.2	Second scenario: observation of a local phenomenon	67
3.2.1	Results	72
4	Experimental results of WSNs	75
4.1	Standard IEEE802.15.4	76
4.2	Description of two commercial WSN platforms	79
4.2.1	Crossbow Platform	79
4.2.2	Chipcon Platform	82
4.3	Application tests on Crossbow Micaz platform	84
4.3.1	Interference test	84
4.3.2	Radio distance	85
4.3.3	Energy consumptions	86
4.4	Agricultural Application	87
4.4.1	Results	88
4.5	Evolution: the path towards a dedicated platform	89
	Conclusion	92
	Acknowledgments	93

List of Figures

1.1	Typical wireless sensor networks scenario.	9
1.2	Units and subunits that composing a wireless sensor node. . .	12
1.3	Wireless sensor networks protocol stack.	14
1.4	Routing in WSNs.	19
2.1	The wireless sensor network and the UAV.	31
2.2	ELP representation of the Rake receiver adopted as fusion center.	33
2.3	Compact representation of the ELP transmission system. For simplicity, without loss of generality the matched filter and spreading/despreading blocks are not shown in the figure. The ideal Rake is represented as a MRC.	36
2.4	The sensors field with random positions of nodes (+) and the UAV trajectory (dashed line).	41
2.5	The normalized PDP of the channel when the UAV is in $x_{\text{UAV}} = -1500$ m, $y_{\text{UAV}} = 0$ m (outside the sensors field). . . .	42
2.6	The normalized PDP of the channel when the UAV is in $x_{\text{UAV}} = 0$ m, $y_{\text{UAV}} = 0$ m (above the sensors field).	43
2.7	The CDF of the inter-arrival time between adjacent paths in four different scenarios.	44
2.8	Average capacity profile $\overline{C}(s)$ as a function of the UAV position.	45
2.9	Average capacity profile $\overline{C}_{\text{BSC}}(s)$ as a function of the UAV position.	46
2.10	Average throughput per pass \overline{T} as a function of the trans- mitted symbol energy per node E_s , for different number of cooperative nodes in the network.	47
2.11	Average throughput per pass $\overline{T}_{\text{BSC}}$ as a function of the trans- mitted symbol energy per node E_s , for different number of cooperative nodes in the network.	48

2.12	Average bit error probability, equation (2.25), as a function of the UAV position for different number of cooperative nodes. Different values of E_s correspond to fixed average throughput $\bar{T}_{\text{BSC}} = 100$ bits/Hz.	49
2.13	The transmitted symbol energy per node E_s , required to reach the average throughput $\bar{T}_{\text{BSC}} = 100$ bits/Hz, as a function of the number of cooperative nodes N	50
2.14	Average bit error probability, equation (2.25), as a function of UAV position with $N = 100$ nodes, $E_s = 1.69$ pJ, and a PRake with N_{sel} fingers.	51
2.15	Average throughput per pass \bar{T}_{BSC} as a function of the number of selected nodes N_{sel} and the average energy consumption (as a percentage of the transmitted energy $E_s = 1.69$ pJ) required for the transmission.	52
3.1	Chain Network for Fire Detection.	55
3.2	Conditional p.d.f. of the observed phenomenon.	56
3.3	Markov chain used to describe the system.	57
3.4	Performance for the three schemes with $\pi_0 = \pi_1$ and SNR = -10dB.	60
3.5	Performance for the three schemes with $\pi_0 = \pi_1$ and SNR = 0dB.	60
3.6	Performance for the three schemes with $\pi_0 = \pi_1$ and SNR = 10dB.	61
3.7	Comparison of "Coordinated thresholds" scheme with Cover, Swaszek and optimum schemes.	62
3.8	Fixed threshold scheme for different a-priori probabilities.	63
3.9	Locally set thresholds scheme for different a-priori probabilities.	63
3.10	Coordinated thresholds scheme for different a-priori probabilities.	64
3.11	Comparison of the three cases with SNR= 0dB and $\pi_0 = 0.7$	64
3.12	ROC curves obtained with an SNR=10dB.	65
3.13	ROC curves obtained with an SNR=0dB.	66
3.14	ROC curves obtained with an SNR=-10dB.	66
3.15	ROC curves obtained with $\varepsilon = 3$ for different SNR values.	67
3.16	ROC curves obtained with SNR= 0dB for different values of ε	68
3.17	ROC curves obtained with $\varepsilon = 9$ and SNR=-10dB, for each stage of the chain.	68
3.18	ROC curves obtained with $\varepsilon = 3$ and SNR=0dB, for each stage of the chain.	69
3.19	Markov chain used to describe network in the second scenario.	70
3.20	Scheme of chain network used to evaluate P_{fa}	72

3.21	Scheme of chain network used to evaluate P_{md} .	72
3.22	ROC curves relative to the proposed decision criterion for different SNR values.	73
3.23	ROC curves to compare the two types of decision criterion.	74
4.1	Types of network defined by IEEE802.15.4 standard	77
4.2	Sensor board MTS300	79
4.3	Radio board MicaZ	81
4.4	Coordinator board MIB600	81
4.5	Crossbow network	82
4.6	Chipcon radio board	83
4.7	Chipcon smart evaluation board	84
4.8	WSN and WLAN overlapped channels frequencies	85
4.9	MTS420 sensor board	87
4.10	Comparison of energy consumptions of nodes with and without photovoltaic panels	88
4.11	Agricultural application scenario	89
4.12	Example of a network data displayed on the web site	90
4.13	Temperature values recorded over one month of monitoring	90
4.14	Humidity values recorded over one month of monitoring	91

List of Tables

3.1	Fusion rules for local phenomenon scenario	70
4.1	Results on distance test	85
4.2	Energy consumption on Micaz components	86
4.3	Sensor characteristics of MTS420 sensor board	87
4.4	Results on distance test with Chipcon nodes	90

Acronyms

UAV unmanned aerial vehicle

CD cooperative diversity

WSN wireless sensor network

UWB Ultrawide band

HAP high altitude platform

LOS line-of-sight

BSC binary symmetric channel

NLOS non-line-of-sight

SS spread spectrum

DSSS direct-sequence spread-spectrum

CDMA code division multiple access

BEP bit error probability

MRC maximal ratio combiner

LEO low earth orbit

MIMO multiple-input multiple-output

SIMO single-input multiple-output

MISO multiple-input single-output

MI mutual information

SISO single-input single-output

ISI intersymbol interference
PRake Partial Rake
PDP power dispersion profile
r.v. random variable
i.i.d. independent and identically distributed
p.d.f. probability distribution function
c.d.f. cumulative distribution function
ch.f. characteristic function
AWGN additive white Gaussian noise
BPSK binary phase shift keying
SNR signal-to-noise ratio
CIR channel impulse response
CSI channel state information
ELP equivalent low-pass
ADC analog-to-digital converter
ISM Industrial, Scientific and Medical
MAC medium access control
IR impulse radio
PPM pulse position modulation
QoS quality of service
TDMA time-division multiple access
FEC forward error correction
ARQ automatic repeat request
WPAN wireless personal area network
PHY physical layer

O-QPSK offset quadrature phase-shift keying

PSSS parallel sequence spread-spectrum

ASK amplitude shift keying

FFD full-function device

RFD reduced-function device

PER packet error rate

Introduction

Recent progress in microelectronic and wireless communications have enabled the development of low cost, low power, multifunctional sensors, which has allowed the birth of new type of networks named wireless sensor networks (WSNs). The main features of such networks are: the nodes can be positioned randomly over a given field with a high density; each node operates both like sensor (for collection of environmental data) as well as transceiver (for transmission of information to the data retrieval); the nodes have limited energy resources.

The use of wireless communications and the small size of nodes, make this type of networks suitable for a large number of applications. For example, sensor nodes can be used to monitor a high risk region, as near a volcano; in a hospital they could be used to monitor physical conditions of patients. For each of these possible application scenarios, it is necessary to guarantee a trade-off between energy consumptions and communication reliability.

This thesis investigates the use of WSNs in two possible scenarios and for each of them suggests a solution that permits to solve relating problems considering the trade-off introduced.

The first scenario considers a network with a high number of nodes deployed in a given geographical area without detailed planning that have to transmit data toward a coordinator node, named sink, that we assume to be located onboard an unmanned aerial vehicle (UAV). This is a practical example of reachback communication, characterized by the high density of nodes that have to transmit data reliably and efficiently towards a far receiver. It is considered that each node transmits a common shared message directly to the receiver onboard the UAV whenever it receives a broadcast message (triggered for example by the vehicle). We assume that the communication channels between the local nodes and the receiver are subject to fading and noise. The receiver onboard the UAV must be able to fuse the weak and noisy signals in a coherent way to receive the data reliably. It is proposed a cooperative diversity concept as an effective solution to the reachback problem. In particular, it is considered a spread spectrum (SS) transmission scheme in

conjunction with a fusion center that can exploit cooperative diversity, without requiring stringent synchronization between nodes. The idea consists of simultaneous transmission of the common message among the nodes and a Rake reception at the fusion center. The proposed solution is mainly motivated by two goals: the necessity to have simple nodes (to this aim we move the computational complexity to the receiver onboard the UAV), and the importance to guarantee high levels of energy efficiency of the network, thus increasing the network lifetime. The proposed scheme is analyzed in order to better understand the effectiveness of the approach presented. The performance metrics considered are both the theoretical limit on the maximum amount of data that can be collected by the receiver, as well as the error probability with a given modulation scheme. Since we deal with a WSN, both of these performance are evaluated taking into consideration the energy efficiency of the network.

The second scenario considers the use of a chain network for the detection of fires by using nodes that have a double function of sensors and routers. The first one is relative to the monitoring of a temperature parameter that allows to take a local binary decision of target (fire) absent/present. The second one considers that each node receives a decision made by the previous node of the chain, compares this with that deriving by the observation of the phenomenon, and transmits the final result to the next node. The chain ends at the sink node that transmits the received decision to the user. In this network the goals are to limit throughput in each sensor-to-sensor link and minimize probability of error at the last stage of the chain. This is a typical scenario of distributed detection. To obtain good performance it is necessary to define some fusion rules for each node to summarize local observations and decisions of the previous nodes, to get a final decision that it is transmitted to the next node.

The thesis outline is described next. In Chapter 1, the main characteristics of WSNs, the composition of protocol stack inherent to these networks and some applications are described. In Chapter 2, the first scenario presented is described with the approach proposed to reach the goals. Performance obtained through simulations are presented in order to evaluate the validity of the approach. The second scenario and fusion rules that guarantee good performance are presented in Chapter 3, where results obtained through simulations are compared with those present in literature. In Chapter 4, it is presented an experimental activity on WSNs. Here the main characteristics of the standard IEEE802.15.4 that defines the physical layer (PHY) and the medium access control (MAC) layer of wireless personal area networks (WPANs) are first summarized. Then two commercial WSN platforms and results relative on different types of tests are presented. Finally, it is de-

scribed the realization of an application of WSNs to an agricultural scenario.

Chapter 1

Wireless Sensor Networks

In recent years, advances in miniaturization; low-power circuit design; and simple, low power, yet reasonably efficient wireless communication equipment have been combined with reduced manufacturing costs to realize a new type of multifunctional sensor nodes that are small in size and communicate with each other through short radio distances. These tiny sensor nodes consist of sensing, data processing and communication components and have determined the birth of a new version of wireless networks named wireless sensor networks [1–5].

A WSN is composed of a large number of sensor nodes that are densely deployed either inside the phenomenon or very close to it. The position of sensor nodes can be predetermined to guarantee a uniformly sensing of a defined area or they can be randomly deployed in inaccessible terrains or in particular types of application as in disaster relief operations. In this last case it is necessary to create a sensor networks protocols and algorithms that possess self-organizing capabilities.

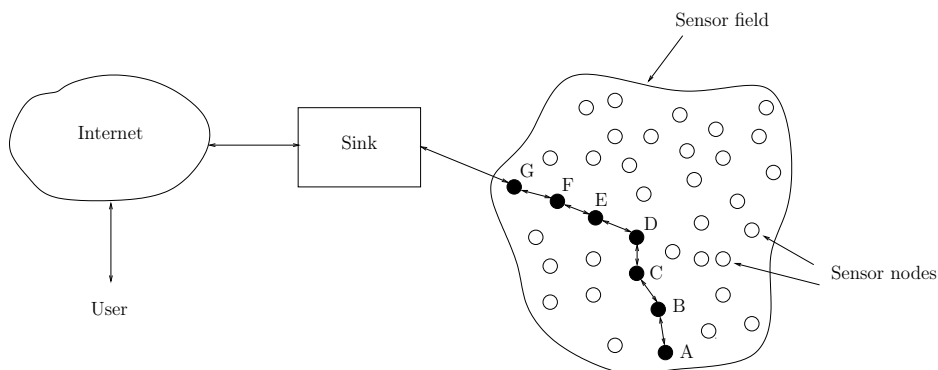


Figure 1.1: Typical wireless sensor networks scenario.

Typical application scenarios for WSNs (represented in Fig. 1.1) include a sink that acts as coordinator of the network and can trigger periodically the nodes, but especially collects the observations received by them and transmits the data to the user through wireless or wired link.

There are two main types of networks:

- Star network. Each sensor can transmit the observations directly to the sink.
- Mesh network. The nodes are positioned in a large area and the farther ones don't have a radio visibility with the coordinator. In this case each node acts both as sensor and as router to forward the data of the neighbor nodes toward the sink.

An important feature of sensor networks is the cooperative effort of sensor nodes. These instead of sending the raw data to the sink, use their processing capabilities to locally carry out simple computations and transmit only the required and partially processed data.

WSNs are suitable for a wide range of applications in military, health, home, industry, agricultural and a lot of other fields. For example in health, sensor nodes can be deployed to monitor and assist disabled or old patients.

Realization of this and other sensor network applications require ad-hoc networking techniques. Although many protocols and algorithms have been proposed for traditional wireless ad hoc networks, they are not well suited to the features and applications requirements of sensor networks. The main differences between these two types of networks are:

- The number of sensor nodes in a sensor network can be much higher than that in an ad-hoc network. These components are usually densely deployed.
- There is a high probability that sensor nodes can fail.
- In some cases the topology of a sensor network changes very frequently.
- Sensor nodes mainly use a broadcast communication, whereas most ad-hoc networks are based on point-to-point communications.
- Sensor nodes are limited in power, computational capacities, and memory.

1.1 Main characteristics of Wireless Sensor Networks

The main factors that it is important to consider to planning or to design algorithms and protocols for this type of networks are:

- **Fault Tolerance.** It is important to consider that some sensor nodes may fail or can be blocked due to lack of power, or have physical damage or environmental interference. The failure of sensor nodes should not affect the overall task of the network. Fault tolerance is the ability to sustain sensor network functionalities without any interruption due to sensor node failures.
- **Scalability.** The number of sensor nodes deployed in studying a phenomenon could be very high (of the order of hundred or thousand) for particular applications. Algorithms and protocols created for this type of networks must consider this aspect so as the high density that can range from few sensor nodes to few hundred in a region that can be less than 10m in diameter. Usually in those areas where there is a high density of nodes it is much easy to design energy-efficient algorithms, the great challenge is to design minimum-power-consumptions algorithms in that networks where there is a small redundancy of nodes.
- **Costs.** Since wireless sensor networks consist of a large number of sensor nodes, the cost of a single node is very important to justify the overall cost of the network. Obviously this cost has to be as low as possible. Actually the cost of a single wireless node is roughly 20 euros. The main producers are Texas Instruments, Crossbow, St Microelectronics, Zensys, FreeScale and others. With the development of technology the cost of a single node should be much less than 1 euro.
- **Hardware Constraints.** A typical structure of a sensor node is represented in figure 1.2. It is composed of four basic components: a sensing unit, a processing unit, a transceiver unit and a power unit. It is possible include additional components as a location finding system, a power generator and a mobilizer. Sensing units are usually composed of two subunits: sensors and analog-to-digital converters (ADCs). The sensors observe a determined phenomenon and produce the analog signals that are converted into digital form by the ADC, and subsequently are elaborated by the processing unit. This unit, which is generally associated with a small storage unit, manages the procedures both to extract information from the observations and for collaborate with the

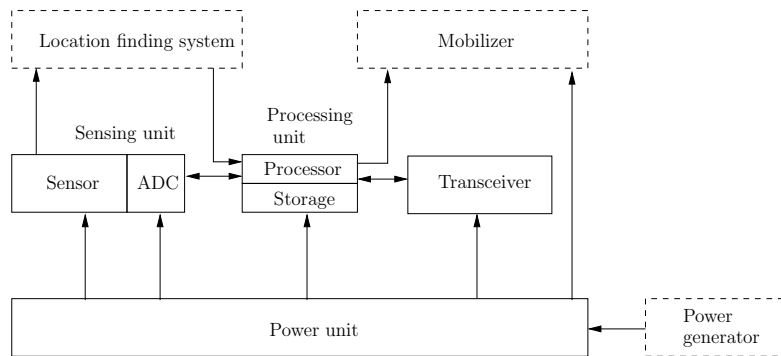


Figure 1.2: Units and subunits that composing a wireless sensor node.

neighbor nodes in the mesh networks, in order to guarantee reliable communications with minimum power consumptions. A transceiver unit connects the node to the network. It contains the transmitter and receiver usually tuned on Industrial, Scientific and Medical (ISM) frequency bands (433MHz, 800MHz and 2.4GHz). Power units may be supported by power scavenging units such as solar cells. Additional subunits are useful to particular types of application. Most of the sensor network routing techniques and sensing tasks require knowledge of location with high accuracy. In these types of applications, it is important that a sensor node has a location finding system. A mobilizer can be useful to move sensor nodes in those applications where it is required to monitor a mobile phenomenon. All of these units and subunits it is important that are included into a small module.

- Environment. Sensor nodes are usually densely deployed either very close or directly inside the phenomenon to be observed. Therefore, they usually work unattended in a remote geographic areas. They may be working in the interior of large machinery, at the bottom of an ocean, in a biologically or chemically contaminated field, in a battlefield beyond the enemy lines, and in a home or large building. For some of these scenarios, sensor nodes are thrown for example by an airplane and assume random positions. It is important that they can auto-organize in order to create an efficient and reliable network. In scenarios accessible by man, nodes are positioned one by one in the sensor field to create a desired network topology.
- Transmission Media. In a mesh network, communicating nodes are linked by a wireless medium. These links can be formed by radio, infrared, or optical media. To enable global operation of these networks,

the chosen transmission medium must be available worldwide. As above described, the three frequency bands actually utilized are 433MHz, 800MHz and 2.4GHz that are no licenses ISM bands. Another possible mode of internode communication in sensor networks is by infrared. Infrared communications is license-free and robust to interference from electrical devices. Moreover the transceiver are cheaper and easier to build. The big problem is that this type of transmission media require a line of sight between the sender and receiver (so as the optical media), that it is impossible to assure in environments as those described in the previous point.

- **Power Consumption.** Usually the wireless sensor node can only be equipped with a limited power source (in most cases two AA batteries). In some application scenarios, replenishment of power resources might be impossible. Sensor node lifetime, therefore has a strong dependence on battery lifetime. In a mesh network, each node plays the dual role of data originator and data router. The malfunctioning of a few nodes can cause significant topological changes and might require rerouting and reorganization of the network. Hence, power conservation and power management take an importance greater than reliability of communications. The main task of a sensor node in a sensor field is to detect events, perform quick local data processing, and then transmit the data. Power consumption can hence be divided into three domains: sensing, communication and data processing.

1.2 Protocol Stack

The protocol stack used by the sink and sensor nodes shown in Fig. 1.1 is that presented in Fig. 1.3. This scheme highlights as the algorithms and techniques used for each of the presented layers have to be designed considering three basic aspects: power management, mobility management and task management.

The physical layer addresses the needs of simple but robust modulation, transmission, and receiving techniques. Since the environment is noisy and sensor nodes can be mobile, the MAC protocol must be power-aware and able to minimize collision with neighbors' broadcasts. The network layer takes care of routing the data received by transport layer. The transport layer helps to maintain the flow of data if the sensor networks application require it. Depending on the sensing task, different types of application software can be built and used on the application layer. The power management plane

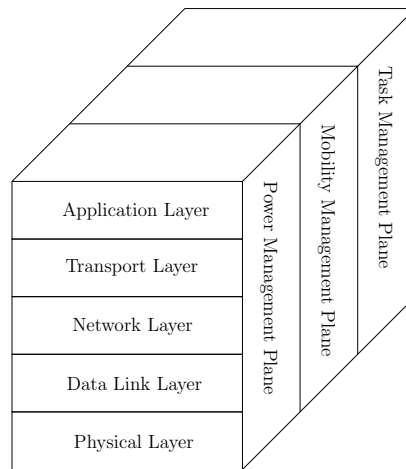


Figure 1.3: Wireless sensor networks protocol stack.

manages how a sensor node uses its power. For example, the sensor node may turn off its receiver after receiving a message from one of its neighbors. In this manner nodes don't receive duplicated messages. This orthogonal plane can also guarantee an efficient management of the network, for example when the power level of a sensor node is low, it broadcasts to its neighbors that it is low in power and cannot participate in routing messages. The remaining power is reserved for sensing. The mobility management plane detects and registers the movement of sensor nodes, so a route back to the user is always maintained and the sensor nodes can keep track of who their neighbor sensor node are. Through this knowledge each node can optimize power consumptions and task usage. The task management plane schedules the sensing task given to a specific region of sensor field. Not all sensor nodes in that region are required to perform the task more than others depending on their power level. These management planes are needed so that sensor nodes can work together in a power-efficient way, route data in a mobile sensor network, and share resources between sensor nodes.

1.2.1 The physical layer

The physical layer is responsible for frequency selection, carrier frequency generation, signal detection, modulation and data encryption. Actually, the 2.4 GHz ISM is the most used band. Frequency generation and signal detection depend on hardware and in particular on transceiver design. It is well known that long distance wireless communication can be expensive, in terms of both energy and implementation complexity. While designing the

physical layer for sensor networks, energy minimization assumes significant importance, over and above the propagation and fading effects. In general, the minimum output power required to transmit a signal over a distance d is proportional to d^n , where $2 \leq n < 4$. The exponent n is closer to four for low-lying antennae and near ground channels, as is typical in sensor network communication. This can be attributed to the partial signal cancellation by a ground-reflected ray. To guarantee reliable long communications and power efficiency it is important to use diversities where it is possible as in a research scenario presented in chapter 2. Multihop communication can overcome shadowing and path loss effects, but it is possible if the node density is high enough.

The choice of a good modulation scheme is critical for reliable communication in a sensor network. While an M-ary scheme can reduce the transmit on-time by sending multiple bits per symbol, it results in complex circuitry and increased radio power consumption. Usually for power dominant conditions, the binary modulation scheme is more energy-efficient.

Ultrawide band (UWB) or impulse radio (IR) has been used for baseband pulse radar and ranging systems, and has recently drawn considerable interest for communication applications, especially in indoor wireless networks. UWB employs baseband transmission and thus requires no intermediate or radio carrier frequencies. Generally, pulse position modulation (PPM) is used. The main advantage of UWB is its resilience to multipath. Low transmission power and simple transceiver circuitry make UWB an attractive candidate for wireless sensor networks.

1.2.2 The data link layer

The data link layer is responsible for the multiplexing of data streams, data frame detection, medium access and error control. It ensures reliable point-to-point and point-to-multipoint connections in a communication network.

The MAC protocol in a wireless multihop self-organizing sensor network must achieve two goals [6]. The first is the creation of the network infrastructure. Since thousand of sensor nodes are densely scattered in a sensor field, the MAC scheme must establish communication links for data transfer. This forms the basic infrastructure needed for wireless communication hop by hop and gives the sensor network self-organizing ability. The second objective is to fairly and efficiently share communication resources between sensor nodes.

MAC schemes adopted for other types of wireless networks are not suitable for wireless sensor networks. In particular the differences with the two most used MAC schemes are:

- Cellular system. In this type of networks, the base stations form a wired backbone. A mobile node is only a single hop away from the nearest base station. The primary goal of the MAC protocol in such systems is the provision of high quality of service (QoS) and bandwidth efficiency. Power conservation assumes only secondary importance since base stations have unlimited power supply and the mobile user can replenish exhausted batteries in the handset. Hence, medium access is invariably inclined toward a dedicated resources assignment strategy. Such an access scheme is impractical for sensor networks since there is no central controlling agent like the base station. This makes networkwide synchronization a difficult task. Moreover, power efficiency directly influences network lifetime in a sensor network and hence is of prime importance.
- Bluetooth and mobile ad hoc network. Bluetooth is an infrastructure-less short-range wireless system intended to replace the cable between electronic user terminals with radio-frequency links. The Bluetooth topology is a star network where a master node can have up to seven slave nodes wirelessly connected to it to form a piconet. Each piconet uses a centrally assigned time-division multiple access (TDMA) schedule and frequency hopping pattern. Transmission power is typically around 20 dBm and the transmission range is on the order of tens of meters. The MAC protocol in ad hoc networks has the task of forming the network infrastructure and maintaining it in the case of mobile nodes. Hence, the primary goal is the provision of high QoS under mobile conditions. Although the nodes are portable battery-powered devices, they can be replaced by the user, and hence power consumption is only of secondary importance. In contrast to these two systems, the sensor network may have a much larger number of nodes. The transmission power (~ 0 dBm) and radio range of a sensor node is much less than those of Bluetooth or ad hoc network. Topology changes are more frequent in a sensor network and can be attributed to both node mobility and failure. The mobility rate can also be expected to be much lower than in ad hoc networks. In essence, the primary importance of power conservation to prolong network lifetime in a sensor network means that none of the existing Bluetooth or ad hoc network MAC protocols can be directly used.

In literature there are several MAC protocols proposed for wireless sensor networks, that have different characteristics but two common points. First of all it is important to minimize messaging overhead and link setup delay. In the second instance power conservation is achieved by the use of power saving

operation modes and by preferring timeouts to acknowledgment, wherever possible. It is obvious that to conserve power supply we have to turn off the transceiver when it is not used. Power saving operation modes consider to turn off not only the transceiver but also the others hardware parts of sensor node as CPU, sensing unit, ADC unit etc. MAC protocol must define two phases, in the first one the nodes is active and carry out sensing, processing and receiving/transmitting operations, in the second one it is in power saving mode characterized by very low consumptions. The duty-cycle between these two phases depends on the application. Minimizing the active period allows to increase nodes lifetime. Turning off sensor hardware units during idle periods may not always be efficient due to energy spent in turning they back on each time, this is the case of applications that require frequent sensor transmissions. In general operation in power-saving mode is energy-efficient only if the time spent in that mode is greater than a certain threshold. There can be several power saving modes, each of them consider to turn off in the idle period different parts of the node. Each of these modes can be characterized by its power consumption and latency overhead, which is the transition power to and from that mode. The power saving operations usage increase synchronization algorithms complexity. To limit messaging overhead sensor nodes communicate using short data packets.

Another important function of the data link layer is the error control of transmission data. Two important modes of error control in communication networks are forward error correction (FEC) and automatic repeat request (ARQ). The usefulness of ARQ in multihop sensor network environments is limited by the additional retransmission energy cost and overhead. On the other hand, the decoding complexity is greater in FEC since error correction capabilities need to be built in. Considering this, simple error control codes with low-complexity encoding and decoding might present the best solutions for sensor networks.

1.2.3 The network layer

Sensor nodes are usually scattered densely in a field either close to or inside the phenomenon, as shown in Fig. 1.1. In this scenario multihop wireless routing protocols between the sensor nodes and the sink are needed. The networking layer of sensor networks is usually designed according to the following principles:

- Power efficiency is a primary aspects in this type of networks.
- Sensor networks are mostly data-centric.

- Data aggregation is useful only when it does not hinder the collaborative effort of the sensor nodes.
- An ideal sensor network has attribute-based addressing and location awareness.

Figure 1.4 represent an example of WSN where node T is the source node that sense the phenomena and has to transmit data to the sink. An energy-efficient route inside a WSN is selected using different approaches based on two parameters inherent at each node:

- Available power defined as PA in Fig. 1.4
- Energy required for a single transmission in sensor-to-sensor links defined as α in Fig. 1.4.

The main approaches used to define algorithms to find the best route in a WSN are:

- Maximum available power route. Algorithms that choose this approach define routes that use nodes that have high energy resources so that the sum of available power from each node of the route is the maximum. Based on this approach route T-C-B-A is selected in Fig. 1.4. As we can see, this criterion can consider long routes, but have the goal to uniformly distribute the consumptions of the entire network.
- Minimum energy route. Algorithms that choose this approach select routes that consider short sensor-to-sensor links in order to minimize the energy spent from each transmission. Based on this approach route T-B-A is selected in Fig. 1.4. In the case of static network (no mobile nodes) this criterion determines the usage of the same route until some nodes of this preferred route dead (malfunctioning or low energy resources).
- Minimum hop route. In this approach, algorithms choose the shortest route, that is the route that considers the minimum number of hops to reach the sink. Based on this approach route T-D is selected in Fig. 1.4. In the case where the same amount of energy is used for transmission on every link this criterion is equal to that named minimum energy route.
- Maximum minimum available power node route. Algorithms that choose this approach define routes where the node with minimum available power is that with a maximum energy resources in comparison with

minimum available power nodes of other routes. Based on this approach route T-D is selected in Fig. 1.4 and route T-B-A is the second most efficient. In this criterion routes must be often redefined because nodes with minimum available power discharge rapidly.

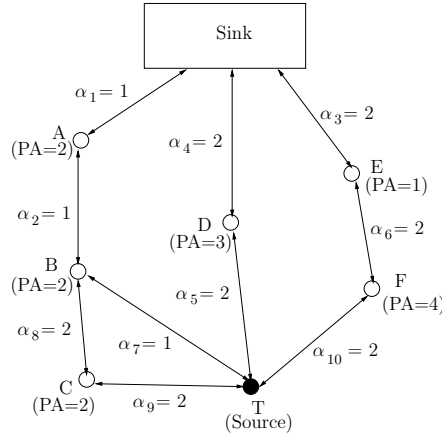


Figure 1.4: Routing in WSNs.

Another important issue is that routing may be based on data-centric approach. In data-centric routing, interest dissemination is performed to assign the sensing task to the sensor nodes. There are two approaches used for interest dissemination: sink broadcast the interest, and sensor nodes broadcast an advertisement for the available data and wait for a request from the interested nodes. Data-centric routing requires attribute-based naming. In other words, the users are interested in querying an attribute of the phenomenon, rather than querying an individual node. For instance, "the areas where temperature is over 50° C" is a common query.

Data aggregation is a technique used to solve the problems in data-centric routing [7]. In this technique a sensor network is usually perceived as a reverse multicast tree where the sink asks the sensor nodes to report the environment condition of the phenomena. Data coming from multiple sensor nodes are aggregated as if they are about the same attribute of the phenomenon when they reach the same routing node on the way back to the sink. Data aggregation can be perceived as a set of automated methods of combining the data that comes from many sensor nodes into a set of meaningful information. More generally data aggregation is known in literature as *data fusion*.

One other important function of the network layer is to provide inter-networking with external networks such as other sensor networks, command and control systems, and the Internet. In one scenario, the sink nodes can

be used as a gateway to other networks. Another scenario is creating a backbone by connecting sink nodes together and making this backbone access other networks via a gateway.

The main schemes inherent to network layer proposed for sensor networks are:

- Flooding. Flooding is an old technique that can also be used for routing in sensor networks. In this scheme, each node receiving a data or management packet repeats it by broadcasting, unless a maximum number of hops for the packet is reached or the destination of the packet is the node itself. Flooding is a reactive technique, and it does not require costly topology maintenance and complex route discovery algorithms. However, it has several deficiencies such as:
 - It is possible that duplicated messages are sent to the same node. For example, if sensor node A has N neighbor nodes that are also the neighbors of sensor node B, this one will receive N copies of the message sent by sensor node A.
 - If two nodes share the same observing region, both of them may sense the same phenomenon at the same time. As a result, neighbor nodes receive duplicated messages.
 - The flooding protocol does not take into account the available energy resources.
- Gossiping [8]. This scheme is a derivation of flooding where nodes do not broadcast but send the incoming packets to a randomly selected neighbor. A sensor node randomly selects one of its neighbors to send the data. Once the neighbor node receive the data, it randomly selects another sensor node. Although this approach avoids the problem of duplicated messages because each node will has one copy of a message, it takes a long time to propagate the message to all sensor nodes.
- Negotiation [9]. This scheme is designed to address the deficiencies of *classic flooding* introducing a negotiation phase between nodes and resource adaptation. The family of protocols that use this scheme are designed based on two basic ideas: sensor nodes operate more efficiently and conserve energy by sending a preliminary packet that describe the data instead of sending all the data. In other words, before to transmit a data packet two nodes exchange other short packets in order to understand if that determined information has to be transmitted (if the receiving node is interested in that data).

- Clustering. This scheme has the goal to minimize energy dissipation in sensor networks. The idea is to randomly select sensor nodes as clusterheads and then divide sensor field into different areas. A single node communicates only to a clusterhead with minimum energy consumption and clusterheads communicate data to the sink. The random choice of clusterhead allow to uniformly discharge the energy of the entire network. In this scheme it is possible to define two phases, named setup phase and steady phase. The duration of the steady phase is longer than the duration of the setup phase in order to minimize overhead. During the setup phase, a sensor node chooses a random number between 0 and 1. If this number is less than a defined threshold this sensor node will be a clusterhead. The threshold is calculated to guarantee that each node of the network become clusterhead before other nodes keep this role for the second time. After the clusterheads are selected, they advertise all sensor nodes of the network of their election. Once the sensor nodes receive the advertisement, they determine the cluster to which they want to belong, based on the signal strength of the advertisement. Then sensor nodes inform the appropriate clusterhead that they will be a member of the cluster. Afterwards, the clusterheads assign the time on which the sensor nodes can send data to the clusterheads based on a TDMA approach. During the steady phase, the sensor nodes can begin sensing and transmitting data to the clusterheads. These last ones aggregate data from the nodes in their cluster and send them to the base station. After a certain period of time spent on steady phase, the network goes into the setup phase again and begins another round of selecting clusterheads.

- Directed diffusion. In this scheme the sink send out an *interest* packet, which is a task description, to all sensors. The task descriptors are named by assigning attribute-value pairs that describe the task. Each sensor node then stores the interest entry in its cache. The interest entry contains a timestamp field and several gradient fields. As the interest is propagated throughout the sensor network, the gradients from the source back to the sink are set up. When the source has data for the interest, it sends the data along interest's gradient path. The sink must refresh and reinforce the interest when it starts to receive data from the source.

1.2.4 The transport and application layer

The transport layer is especially needed when the system is planned to be accessed through the Internet or other external networks. TCP with its transmission window mechanisms may be needed to make sensor networks interact with other networks such as the Internet. Communication between the user and the sink node is by UDP or TCP via the Internet or satellite; on the other hand, communication between the sink and sensor nodes may be purely by UDP-type protocols, because each sensor node has limited memory. Factors such as power consumption and scalability, and characteristics like data-centric routing mean sensor networks need a particular handling in the transport layer. Due to limited power and memory capacity each sensor node cannot store large amounts of data like a server in the Internet, and acknowledgements are too costly for sensor networks.

The application layer protocols depend on single application requirements. Three example of protocols for this layer are:

- Sensor management protocol (SMP). An application layer management protocol makes the hardware and software of the lower levels transparent to the sensor network management applications. System administrators use this protocol to interact with sensor networks. Unlike many other networks, WSNs consist of nodes that do not have global identifications and are usually infrastructureless. Therefore, SMP needs to access the nodes by using attribute-based naming and location-based addressed.
- Task assignment and data advertisement protocol. Another important operation in the sensor networks is interest dissemination. Users send their interest to a sensor nodes, a subset of the nodes, or the whole network. This interest may be about a certain attribute of the phenomenon or a triggering event. Another approach is the advertisement of available data in which the sensor nodes advertise the available data to the users, and the users query the data in which they are interested.
- Sensor query and data dissemination protocol. This type of protocol provides user application with interfaces to issue queries, respond to queries and collect incoming replies. These queries are generally not issued to particular nodes. Instead, attribute or location based naming is usually preferred. For instance, *"the location of the nodes that sense temperature higher than 50°C"* is an attribute-based query. Similarly, *"temperatures read by the nodes in region A"* ia an example of location-based naming.

1.3 Applications of WSNs

Due to the characteristics above described, in particular the short dimensions, the capability of processing and the use of wireless communications, WSN are suitable for a high number of applications [10]. It is possible to classify them in appropriate categories.

1.3.1 Military applications

It is very difficult to say for sure whether sensor nodes were developed because of military and air defense needs or whether they were invented independently and were subsequently applied to army services. Regarding military applications, the area of interest extends from information collection, generally, to enemy tracking, battlefield surveillance or target classification [11]. Classification algorithms use, for instance, input data that come from seismic and acoustic signal sensing. For example, mines may be regarded as dangerous and obsolete in the future and may be replaced by thousands of dispersed wireless sensor nodes that will detect an intrusion of hostile units [12]. Then, the prevention of intrusion will be the response of the defence system. Another demonstration deals with multi-vehicle tracking in the framework of a pursuit-evasion game [13]. There are two competitive teams: the pursuers and the evaders. A third part is a sensor network which is used to help pursuers locate their opponents. The sensor network informs the pursuers about the relative positions and movements of the enemy units. So, the WSN augments the "vision" of the pursuers team and reveals their rivals. Another possible application is relative to detect metallic objects. The ultimate objective was the tracking and classification of moving objects with significant metallic content and specifically the tracking of vehicles and armed soldiers. Other beings (e.g. civilians) were ignored by the system.

1.3.2 Environmental monitoring

This is a big category that can be divided into two subcategories.

Indoor environmental monitoring and emergency services

The capability of sensing temperature, light, status of frames (windows, doors), air streams and indoor pollution can be utilized for optimal control of the indoor environment. Moreover, a major waste of energy occurs through unnecessary heating or cooling of buildings. Wireless sensor nodes can help in using heaters, fans and other relevant equipment at a reasonable

and economic way, leading to a healthier environment and greater level of comfort for residents. Other indoor applications can be mitigation of fire and earthquake damages. Fire and smoke detection is something common, nowadays, in building and in most countries it is imposed by relevant laws. The existence, also, of light-signals indicating exits is, usually, obligatory in big buildings. The installation of WSNs in buildings can lead to the integration of these two systems. So, the role of a sensor network is to guide the trapped residents through the safest route and save their lives. Sensor networks may also be useful after an earthquake. Civil engineering research has shown that the inspection of structures based on vibrations is possible [14]. Based on this observation, the incorporation of wireless sensors inside cement blocks during construction, or their attachment to structural units makes sense. The recording of vibrations during the life of a building can function as the identity of the building. The inspection of a building after an earthquake, by the use of this system, will not be restricted to evaluation of cracks and damages, but will be accompanied by real data. Computation of average and maximum values of vibrations maybe done by each node, so the inspection can be done faster and the determination for any repairs can be more precise.

Outdoor Monitoring - Application to Ecology

Outdoor monitoring is another vast area for applications of WSNs. One of the first practical example of environmental monitoring is that on Great Duck Island [15], this network was used for habitat monitoring. The sensors that were used were able to sense temperature, barometric pressure, and humidity. In addition, passive infrared sensors and photoresistors were used. The aim was to monitor the natural environment of a bird and its behavior according to climatic changes. For that reason, some sensor nodes were installed inside birds' burrows, to detect the bird's presence, while the rest were deployed in the surrounding area. Data are aggregated via sensor nodes and are passed through to a gateway. The role of the gateway is to transmit data using a higher-level network to a local base station (database). The database is accessible through the Internet and is replicated for safety. This application provides an example for monitoring using a heterogeneous, multi-level network. As other example of environmental monitoring application, North Carolina State University is conducting a study of the red wolf, an endangered species. The plan is to attach a node to each animal, in order to record information about its condition and behavior. The inability of sensor nodes to transmit over large distances and their energy constraints implies that it is unfeasible to keep all the nodes online at all times. To overcome this problem, the network contains two types of nodes: mobile and static.

The concept is that a moving node collects and stores information until the animal runs across a static node. The static node triggers the communication capabilities of the moving node and the latter establishes a connection and uploads the stored data. Other applications pertaining to outdoor monitoring that have been implemented concern environmental observations and forecasting weather phenomena. In these applications usually the time scales are much slower, because climatic changes are expected to be sluggish, and the area covered is vast. Finally it is possible to use WSN for the monitoring of forest fires, floodings and landslides. To sum up, WSNs are ideal for remote monitoring and event detection in geographically large regions or inhospitable areas.

Outdoor Monitoring - Applications to agriculture

In this types of applications the idea is to use WSNs to enhance the efficiency and growth of cultivations. Using these networks it is possible to effect a punctual and real time monitoring that is useful to know the different microclimates that can be present in cultivations. The first works have been done on vineyard [16]. The original idea was that a survey of microclimates would improve productivity and would be useful for farmers. Consequently, the prototype platform were equipped initially with temperature sensors. However, interviews with farmers led to the conclusion that another source of raw data was practically useless for them. The perspective changed as a result. The sensor network turned out to be a component of a system that could be useful for every participant in the wine making process, from the time of growing the grapes to wine production and marketing. Many activities like filling out of time sheets, automatic calculation of salaries overtime and billing, time-programming and monitoring of tasks such as pruning (by attaching sensors to tools such as pruning shears), targeting of chemicals and pesticides to selected points (by forecasting diseases through monitoring of temperature and humidity) and harvest timing (observing the ripeness of grapes). In the last chapter of this thesis it is presented a practical realization of agricultural application similar to that here described. Another interesting WSN agricultural application is inherent to irrigation management. Water usage can be controlled in a more efficient and economic way by monitoring moisture on soil, air humidity and weather forecasting. Other goals of the system are frost detection and warning and, as before, pesticide application and disease detection. Generally, crop management, lowering costs and increasing quality is in the scope of applying sensors network technology to agriculture.

1.3.3 Support for logistics

Inventory control is a major problem for big companies. Management of assets (pieces of equipment, machinery, different types of stock or products) can be a predicament. The problem is highly distributed, as these companies expand all over the world. A promising way to achieve asset tracking and cope with this problem is believed to be the use of RF-ID tags and WSNs. A possible application is related to warehouse and storage management of barrels. The concept is that sensor nodes attached to barrels will be capable of locating nearby objects (other barrels), detecting their content and alerting in case of incompatibility with their own (danger of a chemical reaction), aging effects of the enclosure etc. This will enhance safety and guarantee product quality. Tracing of lorries and railcars and tracking of parameters regarding carried goods is possible through sensor nodes and GPS system. So, telemetry and wireless sensing can be combined to build smart objects and vehicles. Intel research deploys a WSN to monitor the condition of semiconductor fabrication equipment. Nodes in this case sense vibrations. More specifically, the plan is to make feasible the detection of faulty parts, which need repair or changing, by analyzing their "vibration signature". Other possible industry applications can regard monitoring of supermarket, monitoring of the process of paper production (measuring temperature in order to control heating of rolls in the paper drying stage), monitoring condition of pumps at gas stations. Researchers at UC Berkeley have also proposed an application based on "wearable nodes". The integration of a wireless sensor node to a part of the equipment that firemen wear, not only makes the coordination of fire-extinguishing easier and more effective, but can also act as a supplementary safety measure by revealing the exact location of each fireman. In case of an accident, rescue crews can act more effectively. Delivery and distribution systems are another area of applications for WSNs. British Petroleum use this technology for managing the delivery of liquefied petroleum gas to its clients. The content of each customer's tank is monitored so that the supply department of the company knows the remaining quantity. That is useful in programming the trips of supply tank-trucks and consequently increases the efficiency of the delivery system. Electric energy system can also benefit from deploying sensor nodes to households and, generally, to consumers of electric power. "Electric economy" always deals with maximum values of electricity consumption. This value has to be kept as low as possible for economic reasons relevant to production. Peaks in electricity demand can be diminished by attaching wireless sensors as components of smart appliances. In a program, smart energy distribution and consumption is deployed in three stages. First, the end user monitors their appliances

and finds out defective or energy exorbitant-consumers. Next, feedback is employed between end user and supplier (real-time pricing). Finally, measuring of environmental parameters slips into the system operation. In this phase the indoor environmental monitoring application described earlier is encountered.

1.3.4 Human-centric and robotic applications

Human-centric applications

Health science and the health care system can also benefit from the use of WSNs [17]. For example this technology can be used for monitor senior citizens and their problems. Cognitive disorders, which perhaps lead to Alzheimer's, can be monitored and controlled at their early stages, using wireless sensors. The nodes can be used to record recent actions (taking medication, last visitor, etc.) and remind senior citizens, indicate the person's real behavior, or detect an emerging problem. Sensor nodes can also be used in order to study the behavior of young children [18]. For future application it is possible to think that nodes will be implanted to human organs to support a function. Others applications of these networks to health care include tracking and monitoring doctors and patients, or tracking drug inside hospitals.

Application to robotics

Usually in these application the idea is to have dense measurements over a wide area. Robots can use the collaboration of wireless sensors to explore the environment and to act as beacons that help them to define directions. In the range between robotics and medical applications it is interesting the virtual keyboard project. This is a system of wearable wireless nodes sensing acceleration. Six nodes are attached to a glove, one for each finger and one at the wrist. The objective is the understanding of the relevant movements of fingers so that gestures can be recognized [19]. Applications could be a wireless wearable mouse/keyboard, or a pointing device, hand motion and gesture recognition for the disabled, virtual musical instruments and work training in a simulated environment.

Chapter 2

Cooperative Communication in Wireless Sensor Networks

As described in detailed manner in chapter 1, wireless sensor networks are suitable for a high number of applications. It is also shown that typical scenarios include a sink, which periodically triggers the WSN, and a large number of nodes deployed in a given geographical area without detailed planning. In such scenarios, the goal is to collect observations from all sensors to a far receiver [20,21]. In this chapter is presented the case where the receiver is located onboard an unmanned aerial vehicles (UAVs) [22]. This is a practical example of *reachback* communication, characterized by the high density of nodes that transmit data reliably and efficiently towards a far receiver. This problem has been investigated from the information-theoretic point of view in [23–25].

In the literature a few technical solutions have been proposed. The aggregate transmission of relay nodes is proposed in [26], while a distributed algorithm for a broadcast communication is presented in [23]. In [22], a different solution based on the UWB transmission technique that does not require stringent network synchronization [27, 28], is proposed and analyzed. The problem of transmitting information from a sensor to a far receiver lies in the more general framework of cooperative communications. This paradigm has recently attracted considerable attention in wireless cellular and ad-hoc networks as a way to share resources through distributed transmission and processing. Through this concept, it is possible to realize a new form of diversity to mitigate the effects of severe fading that has been termed *cooperative* diversity. With the aim to increase network capacity and reliability, the cooperation can be realized in various forms: for example through the adoption of distributed space-time codes in wireless ad-hoc networks [29,30], the use of code division multiple access (CDMA) signaling [31, 32], or by

means of practical opportunistic relaying [33–35].

In this chapter it is considered a scenario in which each node transmits a common shared message directly to the receiver onboard the UAV whenever it receives a broadcast message (triggered for example by the vehicle). This common message can be obtained by a “Gossip Phase” where the information is shared among sensors via efficient flooding as mentioned in chapter 1. We assume that the communication channels between the local nodes and the receiver are subject to fading and noise. The receiver onboard UAV which we will refer to as fusion center, must be able to fuse the weak and noisy signals in a coherent way to receive the data reliably.

In this work, it is analyzed a cooperative diversity concept as an effective solution to the reachback problem. In particular, it is proposed a SS transmission scheme in conjunction with a fusion center that can exploit cooperative diversity, without requiring stringent synchronization between nodes. The idea consists of simultaneous transmission of the common message among the nodes and a Rake reception at the fusion center. The proposed solution is mainly motivated by two goals: the necessity to have simple nodes (to this aim the computational complexity is moved to the receiver on board the UAV), and the importance to guarantee high levels of energy efficiency of the network, thus increasing the network lifetime. The proposed scheme is analyzed in order to better understand the effectiveness of the approach presented. The performance metrics considered here are both the theoretical limit on the maximum amount of data that can be collected by the fusion center, as well as the error probability with a given modulation scheme. Since we deal with a WSN, both of these performance are evaluated taking into consideration the energy efficiency of the network.

2.1 System Description

We consider a WSN with N nodes deployed randomly over a wide planar area (Fig. 2.1). These nodes collect data (e.g., environmental such as temperature, pressure, humidity, etc.) that need to be transmitted to the fusion center onboard the UAV whenever a message triggered from the vehicle is received by the nodes. As previously stated, all nodes share the same data.

2.1.1 Channel Model

The channel for each communication link between a node and the fusion center is modelled with path-loss and fading. In particular, we consider a free-

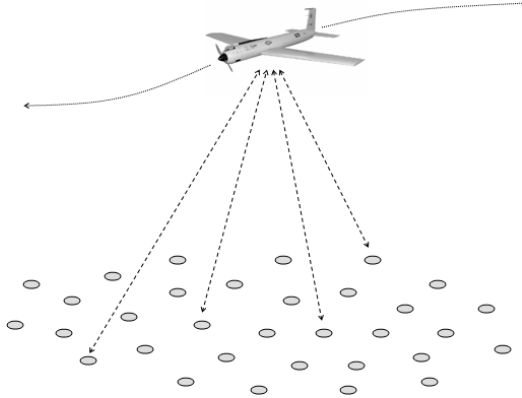


Figure 2.1: The wireless sensor network and the UAV.

space path-loss model for the link between the i^{th} node (with $i = 1, \dots, N$) and the UAV, given by

$$\text{PL}(d_i) = \frac{1}{G_{\text{T}}G_{\text{R}}} \left(\frac{4\pi d_i f_0}{c} \right)^2 \quad (2.1)$$

where G_{T} and G_{R} are the transmitting and receiving antenna gains, respectively, c is the speed of light, and f_0 is the carrier frequency. The distance d_i between the i^{th} node and the receiver can be written as

$$d_i = \sqrt{(x_i - x_{\text{UAV}})^2 + (y_i - y_{\text{UAV}})^2 + z_{\text{UAV}}^2}, \quad (2.2)$$

where $(x_i, y_i, 0)$ are the coordinates of the i^{th} node and $(x_{\text{UAV}}, y_{\text{UAV}}, z_{\text{UAV}})$ are the coordinates of the UAV with respect to a reference coordinate system.

Aeronautical channel models have attracted attention for their peculiar propagation characteristics owing to a strong direct line-of-sight (LOS) component in addition to many weaker random components due to local scattering [36]. Accordingly, it has been shown recently that Rician fading is a good model for aeronautical [37] and ship-to-ship radio [38] channels. The Rice fading is characterized by a Rice factor K which is the ratio of the power of the LOS and that of the non-line-of-sight (NLOS) components.

Therefore, in our analysis we consider independent frequency-flat Rician fading channels between the nodes and the UAV. In particular, the equivalent low-pass representation of the channel between the i^{th} node and the UAV is modelled by a complex gain $h_i = |h_i| \cdot e^{j\theta_i}$ with phases θ_i uniformly distributed between 0 and 2π , and Rice distributed amplitudes $|h_i|$.

For the sake of convenience we include the path-loss in the fading model as¹

$$\Omega_i = \mathbb{E} \{|h_i|^2\} = \frac{1}{\text{PL}(d_i)}, \quad (2.3)$$

and we consider the scenario in which all the N channels have the same Rice factor K [39].

2.1.2 Transmission Technique

We consider a direct-sequence spread-spectrum (DSSS) transmission scheme such as in CDMA [40] or impulse radio UWB [41–43]. In this case, the equivalent low-pass (ELP) representation of the transmitted signal from the i^{th} node can be written as

$$s^{(i)}(t) = \sqrt{2} \sum_j a_j C(t - jT_s - \delta_i), \quad (2.4)$$

where a_j is the j^{th} transmitted symbol with $\mathbb{E} \{|a_j|^2\} = P_T$, and the delays δ_i , $i = 1, \dots, N$, account for the asynchronism among the nodes. The spreading waveform is composed of M chips with duration T_c as

$$C(t) = \sum_{k=0}^{M-1} c_k g(t - kT_c), \quad (2.5)$$

where $c_k \in \{-1, 1\}$. The symbol duration is thus $T_s = MT_c$ and $g(t)$ represents the chip waveform with energy $\int_{-\infty}^{+\infty} g^2(t) dt = T_c$. We assume that each node transmits with the same power and same spreading sequence $\{c_k\}_{k=0}^{M-1}$. In the following, we denote by $E_s = P_T/R_s$ the transmitted energy per symbol of each node, where $R_s = 1/T_s$ is the symbol rate.

Now, considering the channel model adopted, the ELP received signal at the fusion center can be written as

$$s_r(t) = \sum_{i=1}^N h_i s^{(i)}(t - \tau_i) + \nu(t), \quad (2.6)$$

where h_i is the complex channel gain between the i^{th} node and the fusion center, τ_i is the propagation delay between the i^{th} node and the UAV, and $\nu(t)$ is the complex additive white Gaussian noise (AWGN) with two-sided power spectral density $2N_0$. The instantaneous received power at the fusion

¹We use $\mathbb{E} \{\cdot\}$ to denote the expectation operator.

center from the i^{th} node is $P_R^{(i)} = P_T |h_i|^2$, and, due to (2.3), the average received power is therefore $\bar{P}_R^{(i)} = P_T / \text{PL}(d_i)$.

It is clear from (2.6) that the received signal $s_r(t)$ is the result of the superposition of the common message transmitted from different signal nodes. Since all nodes use the same spreading sequence this composite signal, although individual signals experiences independent flat-fading, can be thought as the signal received from a single node through a “virtual” frequency-selective multipath channel. That is, the received signal is composed of replicas of the same transmitted signal with different amplitudes, delays, and phases. As a result we can employ a Rake receiver as fusion center to combine these replicas to decode the data as shown in Figure 2.2.

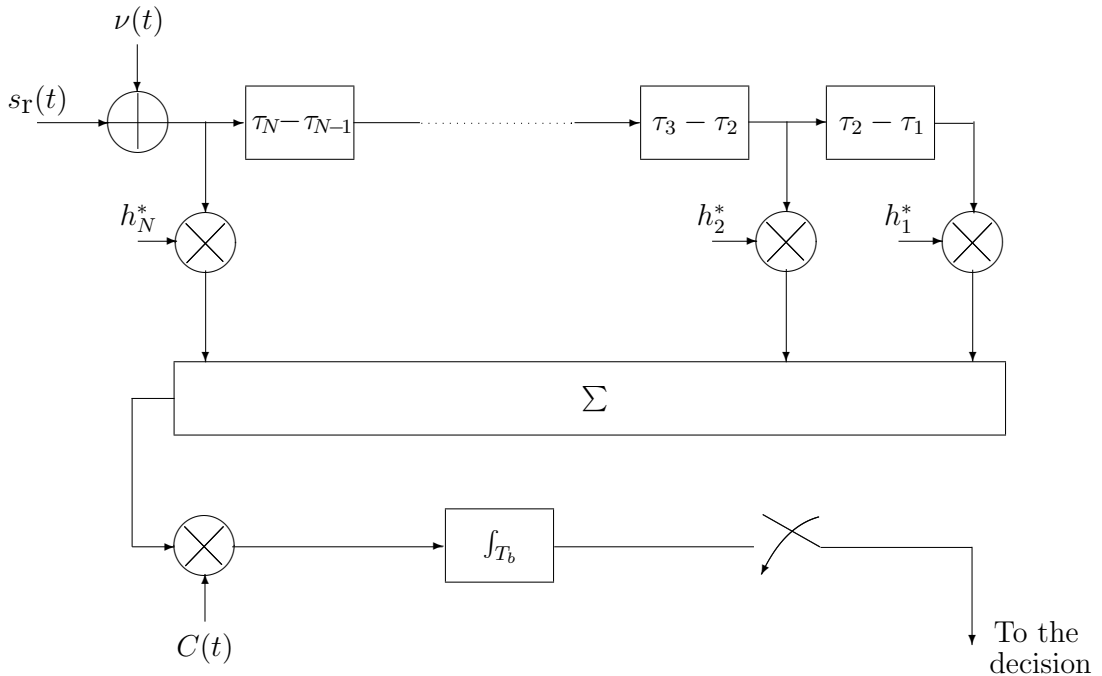


Figure 2.2: ELP representation of the Rake receiver adopted as fusion center.

However, this choice introduces an increasing complexity of the receiver when the number of nodes becomes high, since it requires a Rake receiver with N fingers. In [22] the UWB transmitted-reference impulse radio is proposed as a transmission technique able to combine in a non-coherent way all the received replicas. This scheme has the great advantage of low complexity due to a simple reception based on the correlation of the received signals with its delayed versions at the expense of suboptimal performance due to noisy template [27]. In this work, we propose to use the optimal coherent reception

via Rake receiver in order to save transmission power and then increase the network lifetime.

In order to keep the complexity low, we propose two solutions depending on the specific application of the network. The first one is devoted to applications where an instantaneous detection of the signal is not required. In fact, some applications can tolerate great delays, so in principle data can be collected by the UAV and decoded “off-line”. In this case, the fusion center can be implemented via software. Therefore, the receiver complexity could be overcome by a software implementation of the receiver (including channel estimation, synchronization, combining, etc.) at the expense of a non real time availability of the data. Conversely, if the application requires stringent delay constraints, it is possible to use a Rake with a limited number of fingers (equals to N_{sel}) that combines only the N_{sel} signals, namely Partial Rake (PRake) [44]. As we will show in the following, the latter solution gives a good trade-off between reliability and energy consumption.

2.1.3 Synchronization and Transmission Bandwidth Requirements

As previously stated, the Rake receiver can combine coherently the signals from all nodes provided that they are resolvable. Due to the properties of the Rake receiver, this does not require any form of coordination among the nodes prior to transmission. Such asynchronous transmission results in simple network design, provided that the maximum excess delay is significantly smaller than the symbol duration, T_s .

To understand typical values of the maximum excess delay, i.e., the delay between the first and the last received replicas, let us consider a scenario where nodes are positioned on a square area with side L . Each node transmits to the UAV whenever it receives a trigger message from the vehicle. When the UAV is located at the center of the sensors field at an altitude z_{UAV} , the path lengths difference between the closest node (at the center of the area) and the farthest one (at the corner of the area) is $\Delta d = \sqrt{z_{\text{UAV}}^2 + L^2/2} - z_{\text{UAV}}$. Therefore, the time difference between the reception of the symbol from the two nodes is $\Delta t = 2\Delta d/c$, where the factor 2 accounts for the round trip delays. For example, $L = 1 \text{ Km}$ and $z_{\text{UAV}} = 1 \text{ Km}$ correspond to $\Delta t = 1.4 \mu\text{s}$ which is typically encountered in outdoor propagation environments, where the Rake receiver is used to exploit multipath fading. This means that in order to reduce intersymbol interference (ISI), without requiring synchronization among nodes, the symbol rate R_s should be much less than $1/\Delta t$, i.e., $R_s \ll 714 \text{ Kbit/s}$. For sensor network applications that does not require

high data rate, this is a reasonable limit for R_s . In this case, the synchronization is guaranteed by the geometry of the network itself. Otherwise, it would require some form of synchronization among the nodes.

As far as the required bandwidth of the SS signal is concerned, it is important to note that in order to guarantee resolvable paths, the chip duration T_c should be less than most of the inter-arrival times, between the adjacent paths. Since nodes positions are random, the corresponding delays $\tau_i = d_i/c$ are random variables (r.v.s). Note that the statistical distribution of inter-arrival time is dependent on the sensor field geometry, the nodes density (i.e., nodes per unit area) and the UAV position. In general, we can state that the average inter-arrival time increases as the nodes density decreases.

2.1.4 Fusion Center Model

Since all nodes transmit the same message toward the UAV, the transmission scheme can be represented conveniently as a single-input single-output (SISO) system where a single transmitting “virtual” source, transmits over a single “virtual” frequency-selective multipath channel to the fusion center, represented by a Rake receiver. The virtual frequency-selective fading channel can be represented by a channel impulse response (CIR) with N paths, and the corresponding power dispersion profile (PDP).

For the spreading waveforms with ideal correlation properties, ISI and self-interference are negligible, and thus the Rake receiver can be represented as a maximal ratio combiner (MRC). Such a representation is depicted in Fig. 2.3. In the figure, n_i with $i = 1, \dots, N$, represent the noise terms at the output of each finger.

2.2 Performance Limits for Unconstrained Input Signaling

The signal at the output of the Rake combiner at the sampling instant will be

$$Y = X \cdot \sum_{i=1}^N |h_i|^2 + \sum_{i=1}^N |h_i|^2 n_i, \quad (2.7)$$

where X is the transmitted signal and the second term represent the thermal noise at the combiner output with power

$$\sigma^2 = \sum_{i=1}^N |h_i|^2 \mathbb{E} \{ |n_i|^2 \} = \sigma_n^2 \cdot \sum_{i=1}^N |h_i|^2, \quad (2.8)$$

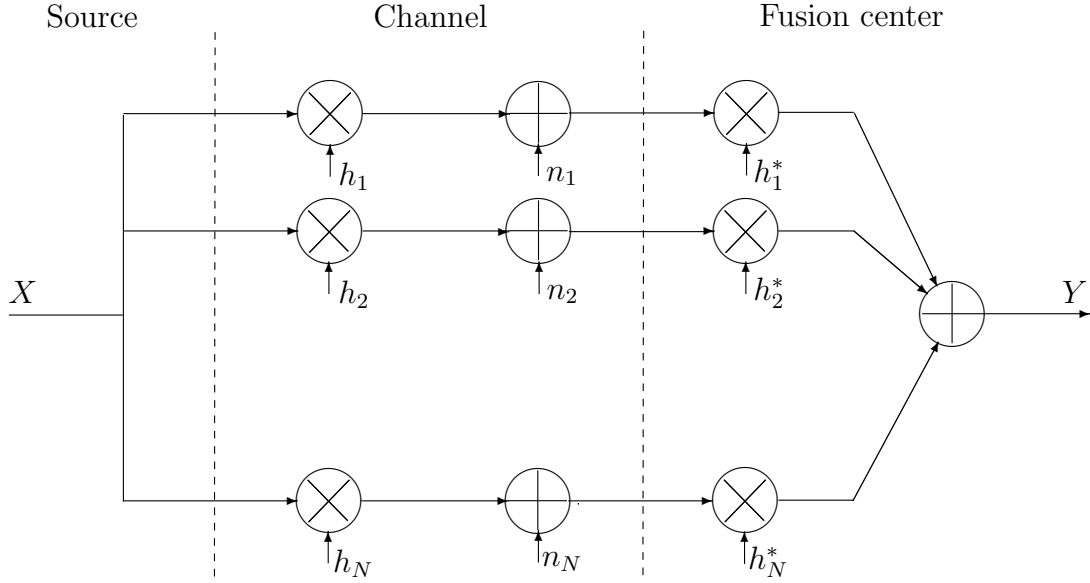


Figure 2.3: Compact representation of the ELP transmission system. For simplicity, without loss of generality the matched filter and spreading/despreading blocks are not shown in the figure. The ideal Rake is represented as a MRC.

and $\sigma_n^2 = \mathbb{E}\{|n_i|^2\} = N_0 R_s$ is the noise power of each path before the MRC. For a given instantaneous channel gains $\mathbf{h} \triangleq (h_1, h_2, \dots, h_N)$, the transmission scheme considered is equivalent to a SISO system affected by AWGN with power σ^2 , and the instantaneous capacity, when channel state information (CSI) is available at the receiver, is

$$C(\mathbf{h}) = \log_2(1 + \text{SNR}(\mathbf{h})) , \quad [\text{bits/s/Hz}] \quad (2.9)$$

where $\text{SNR}(\mathbf{h})$ is the instantaneous signal-to-noise ratio (SNR) given by

$$\text{SNR}(\mathbf{h}) = \rho \cdot \sum_{i=1}^N |h_i|^2 , \quad (2.10)$$

with $\rho = \mathbb{E}\{|X|^2\} / (N_0 R_s) = E_s / N_0$. Since the channel gains depend on the relative positions between the nodes and the UAV, i.e., $\mathbf{h} = \mathbf{h}(s, \mathbf{p})$ with s the distance covered by the UAV from the beginning of the trajectory and $\mathbf{p} = (x_1, y_1, x_2, y_2, \dots, x_N, y_N)$ the vector of nodes positions², the expression

²For the sake of convenience, the position is denoted by s instead of the coordinates $(x_{\text{UAV}}, y_{\text{UAV}}, z_{\text{UAV}})$.

of the instantaneous capacity can be rewritten as

$$C(s, \mathbf{p}, \mathbf{h}) = \log_2 (1 + \rho \|\mathbf{h}(s, \mathbf{p})\|^2) , \quad (2.11)$$

where $\|\cdot\|^2$ denotes the norm squared of a given vector.

Another interesting metric related to the capacity is the throughput defined as the total amount of bits per unit bandwidth that the sensors network can reliably transmit to the UAV in a single passage over the sensor field. In particular, our goal is to evaluate the average capacity and throughput where averages are over random fluctuations of the channel and random positions of the nodes. The approach used to achieve this goal consists in three steps:

1. Compute the *local ergodic capacity* (averaging over fading),

$$\bar{C}(s, \mathbf{p}) = \mathbb{E}_{\mathbf{h}}\{C(s, \mathbf{p}, \mathbf{h})\} \quad [\text{bits/s/Hz}] \quad (2.12)$$

for a fixed s and \mathbf{p} ;

2. For a uniform UAV speed v [m/s] over the trajectory, we can integrate the local ergodic capacity over the pass in order to calculate the *throughput* per pass as [45]

$$\mathcal{T}(\mathbf{p}) \triangleq \int_{\text{flying time}} \bar{C}(v \cdot t, \mathbf{p}) dt = \int_{\text{trajectory}} \bar{C}(s, \mathbf{p}) \frac{ds}{v} \quad [\text{bits/Hz}] \quad (2.13)$$

i.e., the total amount of data transmitted per unit bandwidth³;

3. Compute the *average throughput per pass*

$$\bar{\mathcal{T}} = \mathbb{E}_{\mathbf{p}}\{\mathcal{T}(\mathbf{p})\} \quad [\text{bits/Hz}] \quad (2.14)$$

over random positions of nodes.

In general, the term $\|\mathbf{h}(s, \mathbf{p})\|^2$ that appears in (2.11) represents a r.v. for a fixed position of the UAV and nodes, and it can be viewed as a random process in time (or space) as the UAV moves along its trajectory, i.e., by varying s . Thus capacity in (2.11) can also be viewed as a random process as was observed in [46–48]. Looking at the geometry of the scenario considered and the finiteness of the sensor field, we note that the instantaneous capacity (2.11) is not a stationary process when the UAV moves along its trajectory.

³In this work we define the throughput according to [45], as volume of data transferred; other possible definitions are in terms of transfer rate.

Despite this, it is reasonable to assume that the instantaneous capacity is ergodic in a certain temporal (or spatial) interval around a given UAV position. With this assumption, we assume that the channel is “quasi-static”, i.e., varies randomly from burst to burst. Within a burst, the channel is assumed fixed and it is also assumed that sufficient bits are transmitted for the standard infinite time horizon of information theory to be meaningful.

Once the local ergodic capacity is evaluated in the first step, we can then integrate the capacity over the trajectory, i.e., by varying the position s , in order to obtain the throughput. In practice, we decompose the UAV trajectory into a number of segments in which the capacity is assumed ergodic. Note that, the throughput is a r.v. due to the random position of the nodes.

We can also analyze the outage throughput, namely the probability that the throughput is below a certain threshold. It will be apparent that the average throughput, instead of its outage, is sufficient as the number of nodes becomes large ($N > 10$), i.e., the variance of the throughput becomes small, and thus its average becomes representative of the performance of the system.

Similarly, it is interesting to evaluate the average capacity at a given UAV position, s , averaged over the fading and nodes positions as

$$\overline{\overline{C}}(s) = \mathbb{E}_{\mathbf{p}}\{\overline{C}(s, \mathbf{p})\} . \quad (2.15)$$

We will use (2.14) and (2.15) in Section 2.4 to investigate the maximum attainable capacity.

2.3 Performance Limits with Binary Signaling

The capacity limits described in Section 2.2 are achieved with Gaussian signaling, i.e., with symbols X having a Gaussian distribution. Following a similar method, here we evaluate the performance limits of the network under the constraint of binary signaling. Complementary to the results in previous section, the analysis with binary modulation is useful to evaluate practical performance limits when energy consumption and complexity of nodes are major issues.

In particular, restricting the possible symbols to binary signaling $X \in \{-\sqrt{P_T}, +\sqrt{P_T}\}$, and assuming hard decision on the output Y , the transmission system can be modelled as a binary symmetric channel (BSC) with crossover probability P_e . We now evaluate the throughput per pass and the average bit error probability (BEP) for this transmission scheme.

Let us start by defining the instantaneous SNR for the i^{th} Rake finger as

$$\gamma_i = \frac{P_T |h_i|^2}{N_0 R_s} = \frac{E_s}{N_0} |h_i|^2. \quad (2.16)$$

The BEP conditioned on the channels amplitudes on each finger can be written as

$$P_e(s, \mathbf{p}, \mathbf{h}) = \mathcal{Q} \left(\sqrt{2 \frac{E_s}{N_0} \|\mathbf{h}(s, \mathbf{p})\|^2} \right), \quad (2.17)$$

where $\mathcal{Q}(\cdot)$ is the Gaussian Q -function defined in [49]. Considering that $P_e(s, \mathbf{p}, \mathbf{h})$ is the crossover probability of the equivalent BSC, the instantaneous capacity can be written as

$$C_{\text{BSC}}(s, \mathbf{p}, \mathbf{h}) = 1 + P_e \log_2(P_e) + (1 - P_e) \log_2(1 - P_e) \quad [\text{bits/s/Hz}]. \quad (2.18)$$

Using (2.18) in steps 1)–3) of Section 2.2, the average throughput of the network can be obtained as follows: first evaluating the capacity $\overline{C}_{\text{BSC}}(s, \mathbf{p})$ averaged over fading as in (2.12), then integrating it over the trajectory $\mathcal{T}_{\text{BSC}}(\mathbf{p})$ as in (2.13), and finally obtaining the average throughput over nodes positions $\overline{\mathcal{T}}_{\text{BSC}}$ as in (2.14). Moreover, the average capacity $\overline{\overline{C}}_{\text{BSC}}(s)$ along the trajectory can be evaluated by further averaging over nodes positions as in (2.15).

2.3.1 Bit Error Probability Analysis

Starting from the expressions (2.16) and (2.17), the BEP conditioned on the channels amplitudes or equivalently the SNR in each path $\boldsymbol{\gamma} \triangleq (\gamma_1, \dots, \gamma_N)$ can be rewritten as

$$P_e(\boldsymbol{\gamma}) = \mathcal{Q} \left(\sqrt{2 \sum_{i=1}^N \gamma_i} \right). \quad (2.19)$$

Then, the BEP averaged over the Rice fading, can be obtained by averaging $P_e(\boldsymbol{\gamma})$ over the distribution of the γ_i 's with probability distribution function (p.d.f.)

$$f_{\gamma_i}(\gamma) = \frac{K+1}{\overline{\gamma}_i} \exp \left(-K - (1+K) \frac{\gamma}{\overline{\gamma}_i} \right) I_0 \left(2 \sqrt{K(1+K)} \frac{\gamma}{\overline{\gamma}_i} \right), \quad \gamma \geq 0, \quad (2.20)$$

where the term $\bar{\gamma}_i$ is the average SNR per path (or finger)

$$\bar{\gamma}_i = \mathbb{E} \{ \gamma_i \} = \frac{E_s}{N_0} \frac{1}{\text{PL}(d_i)}. \quad (2.21)$$

Unfortunately, this cannot be performed in closed-form due to the difficulties in evaluating the integrals involved. In order to obtain a useful closed-form formula, we compute the average error probability $\bar{P}_e(s, \mathbf{p}) = \mathbb{E}_{\gamma} \{ P_e(\gamma) \}$ by introducing the approximation proposed in [50]

$$\mathcal{Q}(x) \cong \frac{1}{12} \exp\left(-\frac{1}{2}x^2\right) + \frac{1}{4} \exp\left(-\frac{2}{3}x^2\right), \quad (2.22)$$

that avoids problems with the averaging of the error function over Rice fading. Therefore, the average BEP can be well approximated as

$$\bar{P}_e(s, \mathbf{p}) \cong \frac{1}{12} \mathbb{E}_{\gamma} \left\{ \prod_{i=1}^N \exp(-\gamma_i) \right\} + \frac{1}{4} \mathbb{E}_{\gamma} \left\{ \prod_{i=1}^N \exp(-4\gamma_i/3) \right\}. \quad (2.23)$$

For independent Rice distributed fading in each path, the average BEP becomes

$$\begin{aligned} \bar{P}_e(s, \mathbf{p}) \cong & \frac{1}{12} \prod_{i=1}^N \frac{1+K}{1+\bar{\gamma}_i+K} \exp\left(-\frac{\bar{\gamma}_i K}{1+\bar{\gamma}_i+K}\right) + \\ & + \frac{1}{4} \prod_{i=1}^N \frac{3(1+K)}{3+4\bar{\gamma}_i+3K} \exp\left(-\frac{4\bar{\gamma}_i K}{3+4\bar{\gamma}_i+3K}\right). \end{aligned} \quad (2.24)$$

This formula gives the BEP expression as a function of the average SNRs (2.21), which in turns depend on the distances, (2.2), between the nodes and the UAV. Similarly to (2.15), we can obtain average performance over nodes positions by further averaging (2.24) as

$$\bar{\bar{P}}_e(s) = \mathbb{E}_{\mathbf{p}} \{ \bar{P}_e(s, \mathbf{p}) \}. \quad (2.25)$$

In the next section we illustrate the results of several simulations for the Rake-based cooperative scheme proposed, with a number of fingers equal to the number of nodes N in the network.

Moreover, as previously mentioned, to counteract the receiver complexity in those scenarios where stringent delay constraints require an hardware implementation of the fusion center, we analyze the PRake with binary signaling. As shown in the following, this solution gives a good trade-off between complexity, reliability and energy consumption. In this case, the analysis can be conducted by means of the expressions (2.19) and (2.24) by replacing N with N_{sel} .

2.4 Numerical Results

We consider a scenario that consists of a square area with side $L = 1$ Km, $N = 100$ uniformly distributed nodes, and an UAV that flies with speed $v = 100$ Km/h for a trajectory with length $S = 3$ Km at a constant altitude $z_{\text{UAV}} = 1$ Km over the area. Fig. 2.4 shows an example of the sensors field and the UAV trajectory. The carrier frequency of the transmission is $f_0 = 2.4$ GHz. The free space path-loss model in (2.1) and Ricean fading with $K = 10$ dB are assumed. The antenna gains are $G_T = 0$ dB for the nodes and $G_R = 6$ dB for the receiver. The one-sided power spectral density of the AWGN at the fusion center is $N_0 = K_B T_{\text{sys}}$, where $K_B = 1.38 \cdot 10^{-23}$ J/K is the Boltzmann constant and $T_{\text{sys}} = T_0 F$ is the noise temperature with $T_0 = 290$ K and a receiver noise figure $F = 5$ dB. Supposing that all the nodes transmit with the same energy per symbol E_s , the total energy per symbol spent by the WSN is $E_s^{\text{tot}} = N \cdot E_s$. Unless otherwise stated, we assume $E_s = 10$ pJ and a Rake receiver with a number of fingers equal to the number of nodes N .

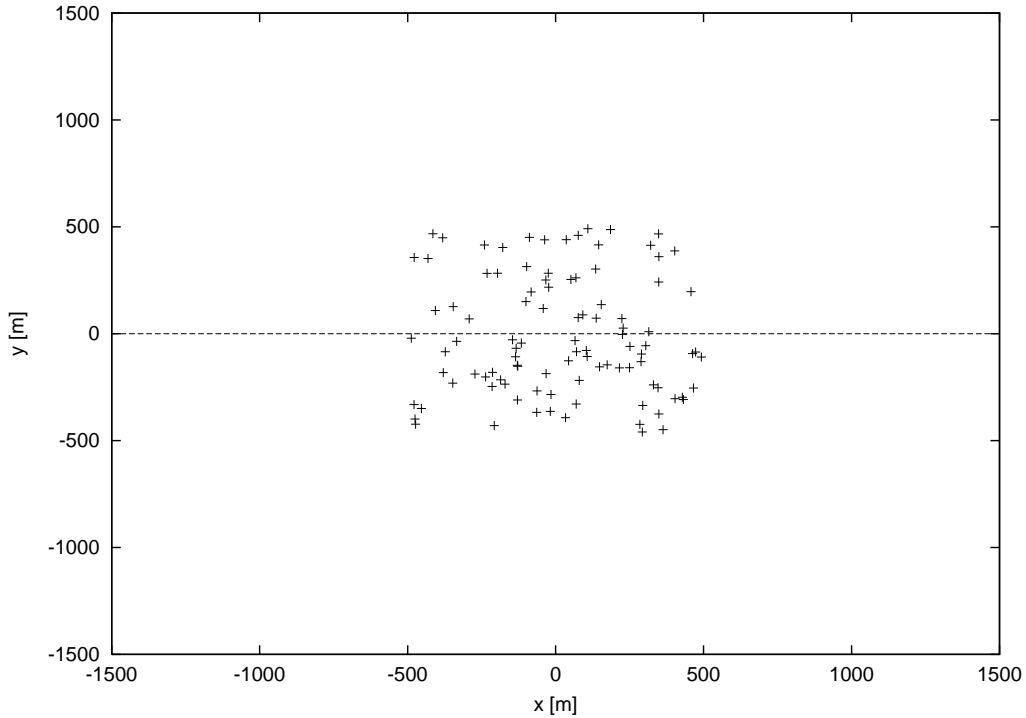


Figure 2.4: The sensors field with random positions of nodes (+) and the UAV trajectory (dashed line).

As explained, the capacity expression in (2.12) and the average BEP

formula in (2.24) are conditioned on the PDP, or more explicitly on the power of each path, (2.3), that depends on nodes positions, the scenario geometry, etc. This profile can be evaluated numerically for a given sensor field, UAV altitude and trajectory, the number and positions of the nodes, and the path-loss model adopted. Figs. 2.5 and 2.6 show two normalized PDPs for two different UAV positions. In these figures the normalization is carried out with respect to the first path indexed by $i = 1$, which has the maximum power and minimum delay, i.e., PDP is given by $\alpha_i^2 \triangleq \Omega_i/\Omega_1$ as a function of the excess delays $\tau_i - \tau_1$ with $i = 1, \dots, N$. Comparison between these figures shows that the second profile has powers roughly equal in amplitude, while in the first one, differences are much more pronounced. The reason behind these differences is related to the position of the UAV, and in fact Fig. 2.5 corresponds to the UAV that is far from the sensors field while Fig. 2.6 corresponds to the UAV above the network, $x_{\text{UAV}} = y_{\text{UAV}} = 0$.

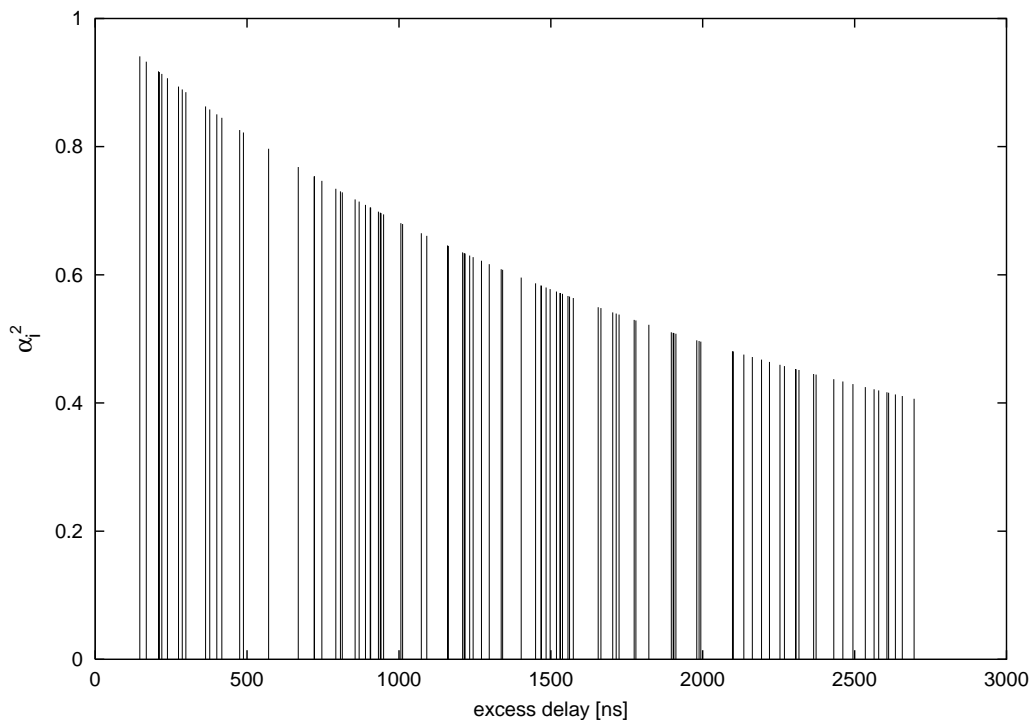


Figure 2.5: The normalized PDP of the channel when the UAV is in $x_{\text{UAV}} = -1500$ m, $y_{\text{UAV}} = 0$ m (outside the sensors field).

To evaluate the bandwidth required to resolve adjacent paths, Fig. 2.7 shows the cumulative distribution function (CDF) of the inter-arrival time be-

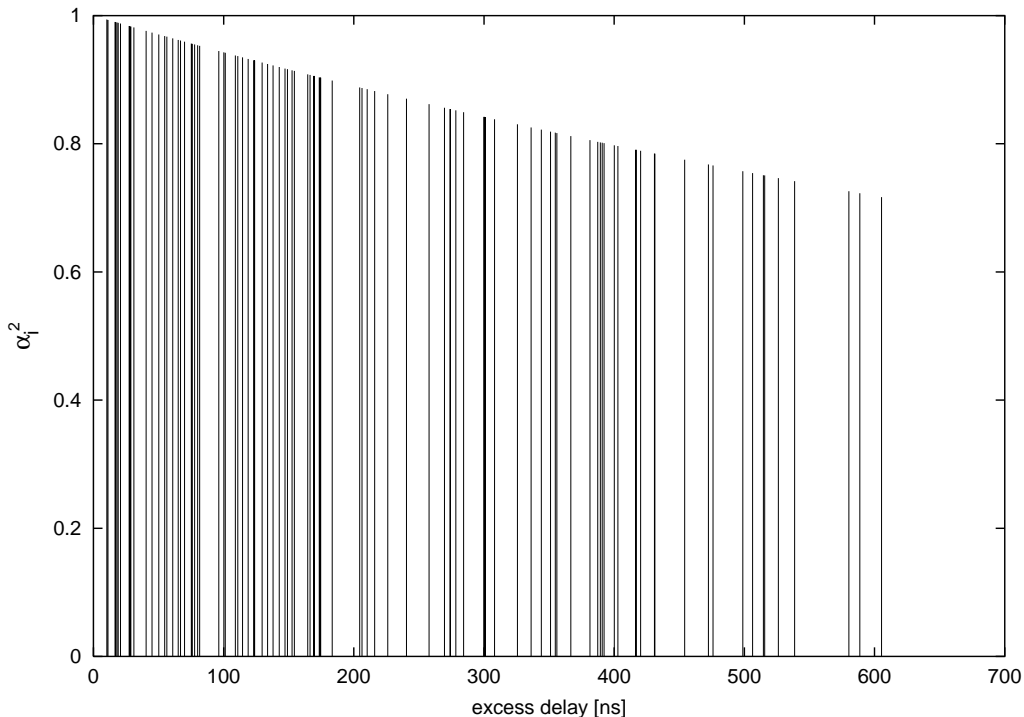


Figure 2.6: The normalized PDP of the channel when the UAV is in $x_{\text{UAV}} = 0$ m, $y_{\text{UAV}} = 0$ m (above the sensors field).

tween the received replicas, for the two UAV positions considered in Figs. 2.5 and 2.6, and for different number of nodes. For example, considering a scenario with $N = 30$ nodes with the UAV located at the beginning of the trajectory, we observe that 20% of paths have an inter-arrival time lower than 20 ns, which corresponds to a bandwidth in the order of 50 MHz. On the other hand, when the UAV is above the network and $N = 100$, the corresponding minimum resolvable delay must be around 2 ns, that correspond to a bandwidth of 500 MHz. In this case, the UWB impulse radio technology is mandatory to support the cooperative communication proposed.

2.4.1 Capacity and Throughput results

For the evaluation of the throughput, as we have explained before, in addition to the parameters expressed, we need to set the number of trajectory samples n_s and the number n_t of scenarios considered for the Monte Carlo simulation. In the following, we assume $n_s = 100$ samples and $n_t = 100$ scenarios.

Following the approach developed in Section 2.2 and 2.3, we plot the

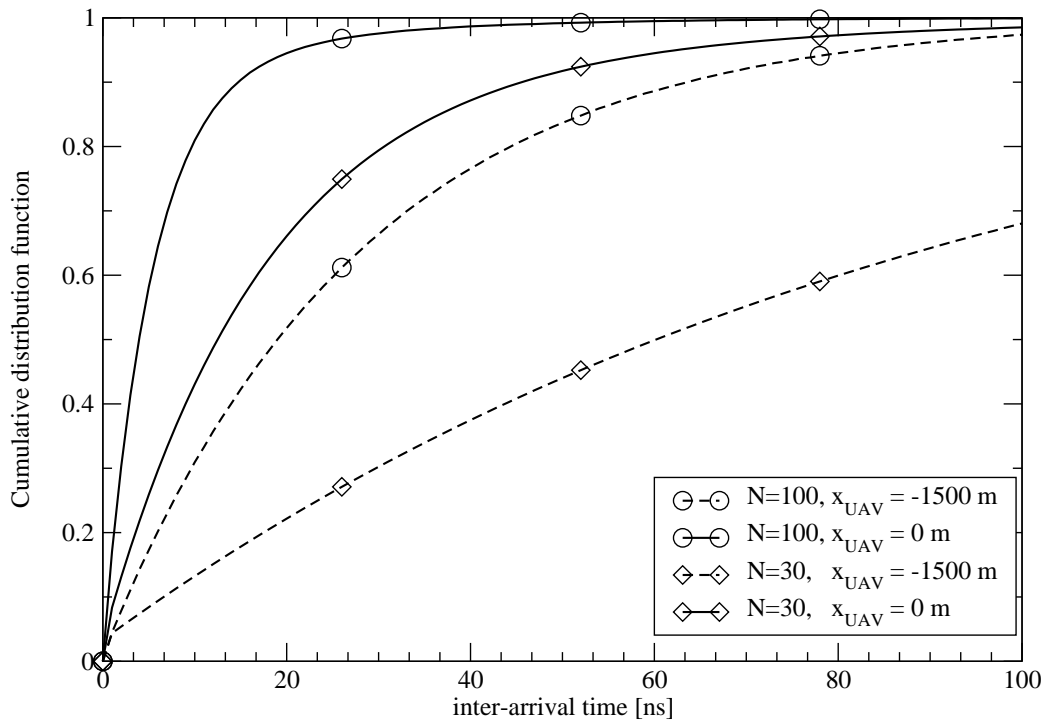


Figure 2.7: The CDF of the inter-arrival time between adjacent paths in four different scenarios.

capacity along the UAV trajectory for both signaling schemes considered. In particular, as shown in Figs. 2.8 and 2.9, $\overline{C}(s)$ and $\overline{C}_{\text{BSC}}(s)$ are plotted as a function of UAV position $s = x_{\text{UAV}}$ for different number of nodes, fixing the energy per transmitted symbol E_s . Due to the symmetry of the scenario, the curves presented are symmetric. Moreover, as expected, with binary signaling (Fig. 2.9) the capacity saturates to 1 bit/s/Hz when N , or equivalently the signal-to-noise ratio, becomes high.

The average throughput as a function of the energy per transmitted symbol E_s is plotted in Fig. 2.10 for different number of nodes. As shown in Fig. 2.10, the amount of information bits per unit bandwidth for a given number of nodes, is directly proportional to the transmit energy E_s , and approaches a linear behavior for large energy values. This linear behavior is justified by the fact that, as shown in equation (2.11), the capacity has a logarithmic dependence with E_s and the energy plotted in Fig. 2.10 is in logarithmic scale. Note that for a given E_s , equivalently the node (or network) lifetime, there is a significant improvement in throughput obtained by increasing the number of nodes. Alternatively, it is possible to keep constant

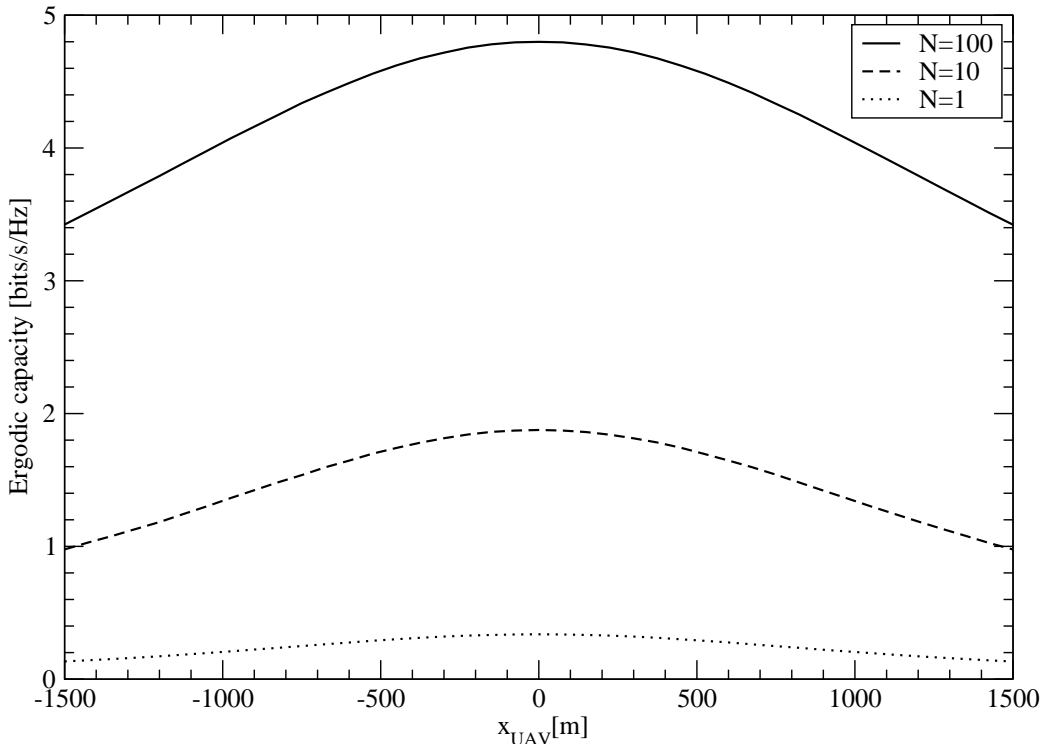


Figure 2.8: Average capacity profile $\bar{C}(s)$ as a function of the UAV position.

the average throughput and reduce the transmit energy, by simply increasing the number of nodes. For instance, a throughput of 440 bits/Hz can be obtained by a single node with energy $E_s = 1$ nJ or by 10 nodes with energy $E_s = 83$ pJ, thus increasing the network lifetime considerably. This throughput, with a symbol-rate equal to $R_s = 1$ Msymbols/s, means that it is possible to collect data volumes up to 55 Mbytes/pass. Obviously, this result is derived under an information-theoretic framework, thus it should be considered as an upper bound of practical attainable performance. Adopting a binary signaling the average throughput \bar{T}_{BSC} evaluated using expression (2.14) is depicted in Fig. 2.11. As we can see, the amount of information bits per unit bandwidth is directly proportional to the energy E_s and N , but saturates accordingly to the capacity behavior.

2.4.2 Bit Error Probability results

In Fig. 2.12, the average BEP (2.25) as a function of UAV position, for different number of nodes in the network, is reported. In the figure, different values of E_s correspond to the same average throughput $\bar{T}_{\text{BSC}} = 100$. The

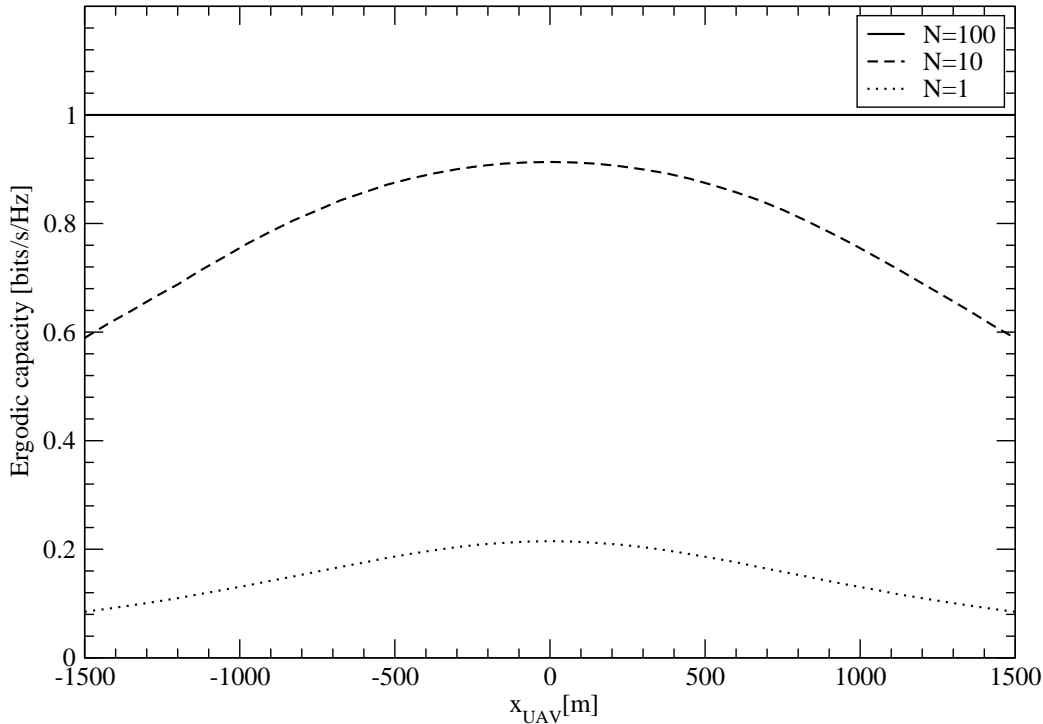


Figure 2.9: Average capacity profile $\overline{\overline{C}}_{\text{BSC}}(s)$ as a function of the UAV position.

figure confirms that the proposed cooperative approach offers good results, both in terms of communication reliability and energy efficiency. For example, we can guarantee the same average throughput with a single node and a transmitted energy $E_s = 231$ pJ, or with $N = 5$ nodes and $E_s = 35.7$ pJ. Looking at the total energy spent by the network E_s^{tot} , we can note that increasing the number of nodes decreases the total energy owing to the diversity provided by our scheme. Keeping fixed the throughput, in Fig. 2.13 we report the node energy as a function of the number of nodes. As we can see, the required symbol energy decreases as the number of cooperative nodes increases.

Finally, to overcome the drawback of high receiver complexity, we consider a PRake with a limited number of fingers $N_{\text{sel}} < N$ which is able to fuse only the first (or strongest on average) N_{sel} paths. The adoption of a PRake scheme could be also useful to reduce the energy consumption of the network in those scenarios where only a limited number of nodes transmits its data in a passage. In other words, a possible way to increase the network lifetime at the expense of reducing the throughput of the network, could be to select N_{sel} nodes among N to transmit in a given passage. By selecting

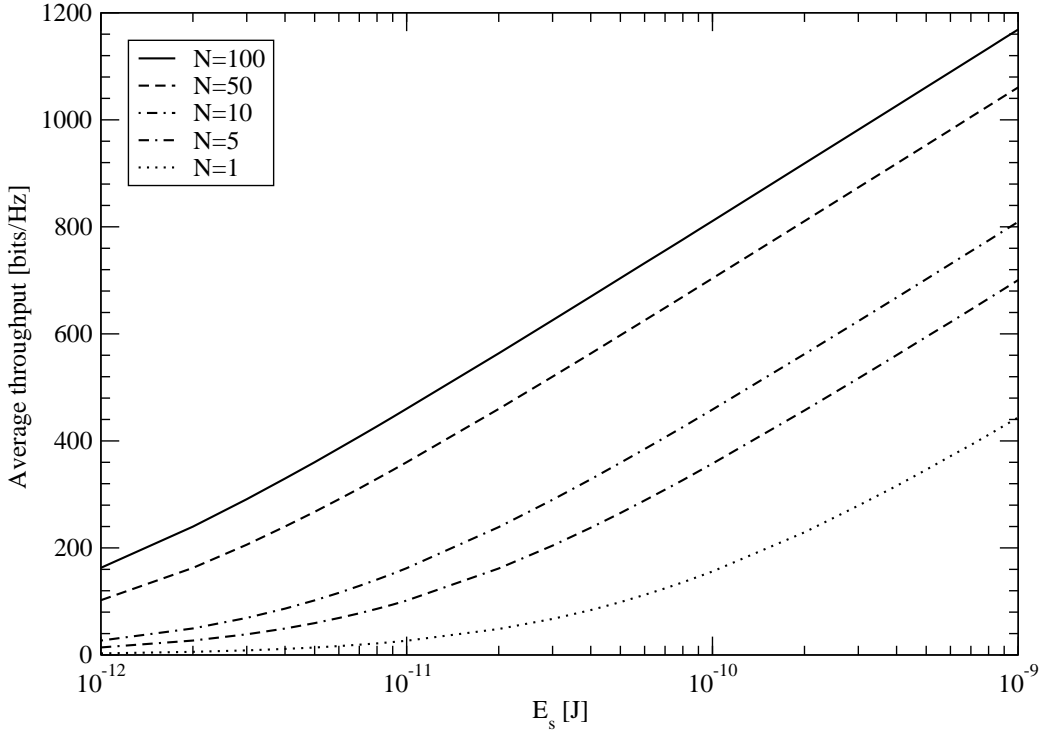


Figure 2.10: Average throughput per pass $\bar{\mathcal{T}}$ as a function of the transmitted symbol energy per node E_s , for different number of cooperative nodes in the network.

different subsets of N_{sel} nodes in each passage, the energy consumption will be distributed among all N nodes, thus reducing the energy consumption by a factor N/N_{sel} . Fig. 2.14 shows the result obtained with this receiver considering a WSN with $N = 100$ nodes and different number of fingers. This figure quantify the trade-off between complexity and energy consumption. As previously explained, the adoption of a PRake could be useful to reduce the energy consumption of the network when combined with a scenario where for each UAV passage only a selected number of nodes transmit its data. Fig. 2.15 shows the average throughput $\bar{\mathcal{T}}_{\text{BSC}}$ as a function of the number of selected nodes N_{sel} that transmit and the average energy consumption for the transmission. This figure shows that we can achieve an energy saving (as a percentage of E_s) selecting a low number of transmit nodes at the expense of a reduced throughput.

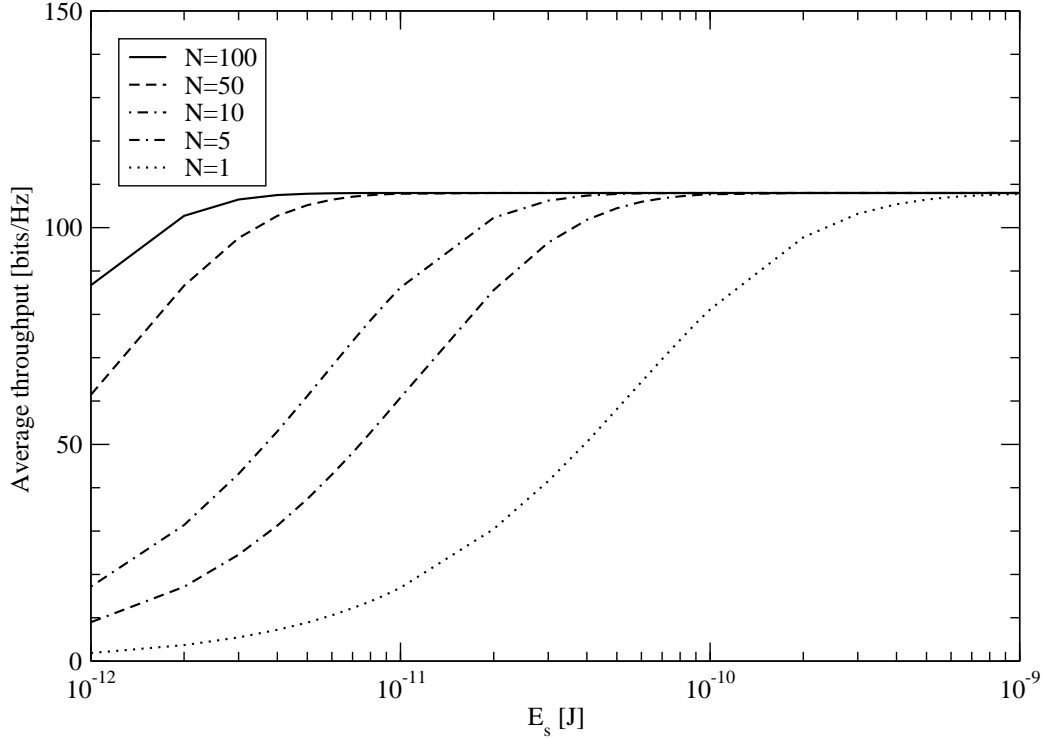


Figure 2.11: Average throughput per pass \bar{T}_{BSC} as a function of the transmitted symbol energy per node E_s , for different number of cooperative nodes in the network.

2.4.3 Scaling

For the sake of simplicity, the previous results are derived with parameters such as the UAV altitude and the area of the network that are reasonable for practical applications in the scenario considered. These numerical results can be easily extended by means of proper scaling factors to other similar scenarios. For instance, if we change the noise power spectral density by a factor Υ , i.e., $N'_0 = N_0 \cdot \Upsilon$, to obtain the same network performance we need to have an energy scaled by the same factor, $E'_s = E_s \cdot \Upsilon$. Similarly, for a given geometry of the scenario, i.e., the ratios z_{UAV}/L and S/L , changing all the distances by a factor Υ we have to scale the energy, $E'_s = E_s \cdot \Upsilon^2$, to maintain the same performance. As far as the UAV speed is concerned, replacing the speed with $v \cdot \Upsilon$ the corresponding throughput will be scaled by a factor $1/\Upsilon$.

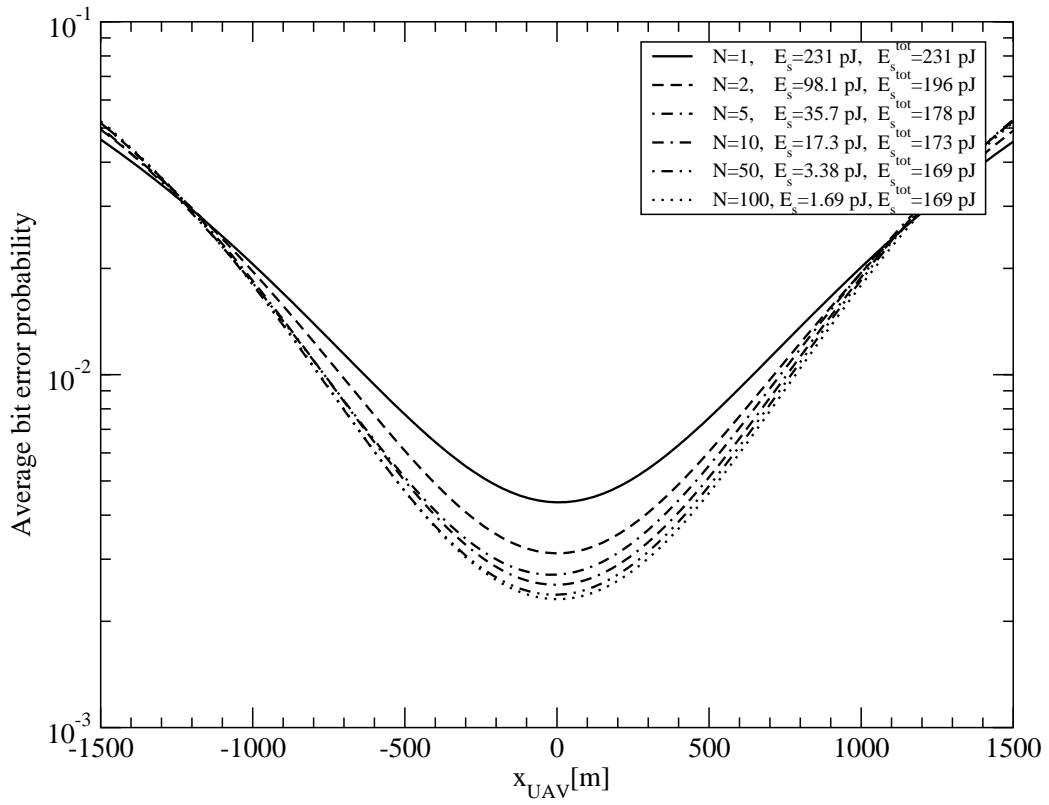


Figure 2.12: Average bit error probability, equation (2.25), as a function of the UAV position for different number of cooperative nodes. Different values of E_s correspond to fixed average throughput $\bar{\mathcal{T}}_{\text{BSC}} = 100$ bits/Hz.

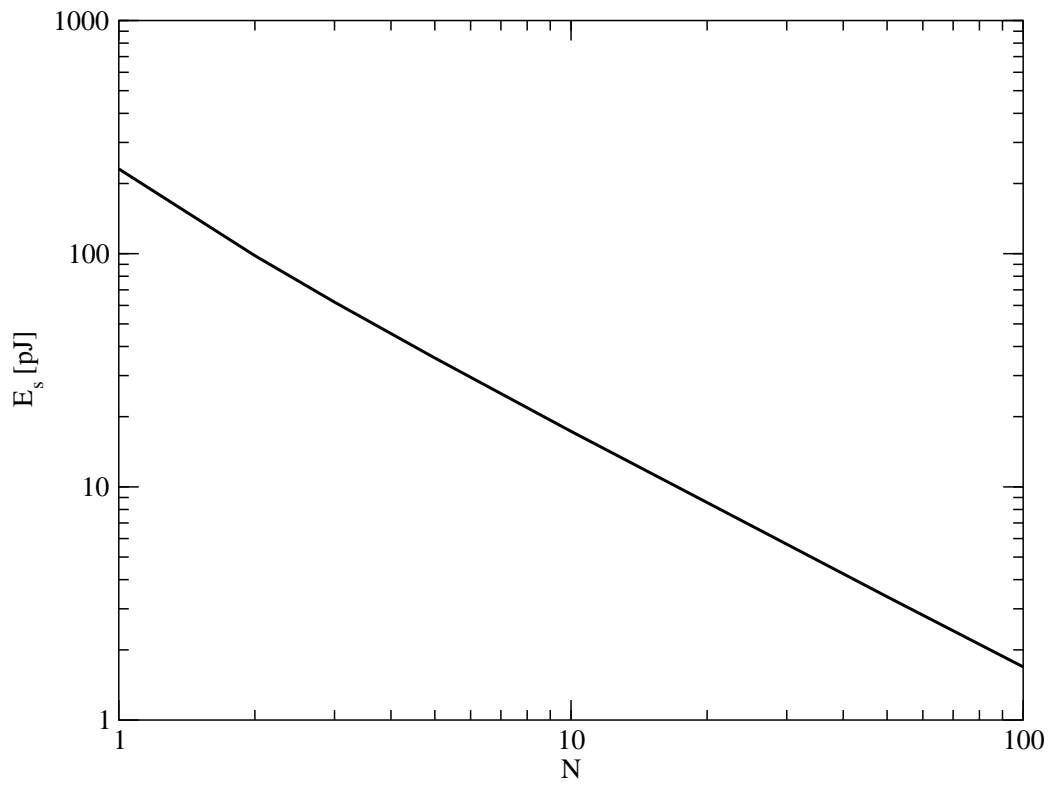


Figure 2.13: The transmitted symbol energy per node E_s , required to reach the average throughput $\bar{\mathcal{T}}_{\text{BSC}} = 100$ bits/Hz, as a function of the number of cooperative nodes N .

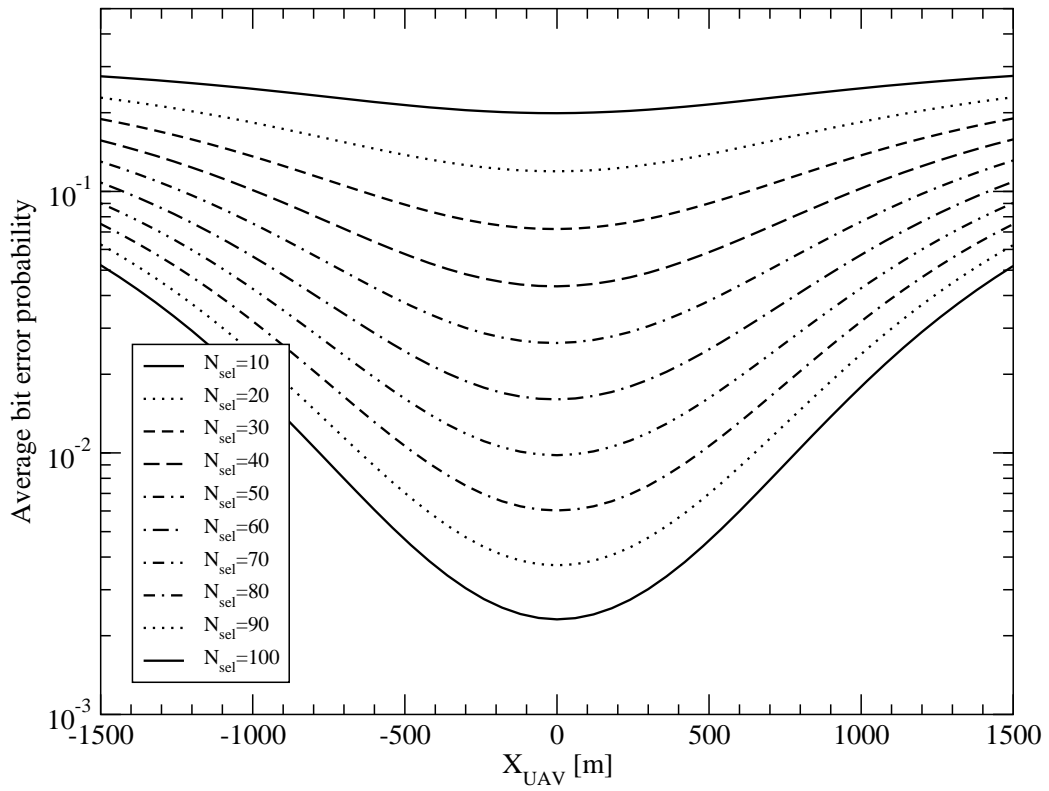


Figure 2.14: Average bit error probability, equation (2.25), as a function of UAV position with $N = 100$ nodes, $E_s = 1.69$ pJ, and a PRake with N_{sel} fingers.

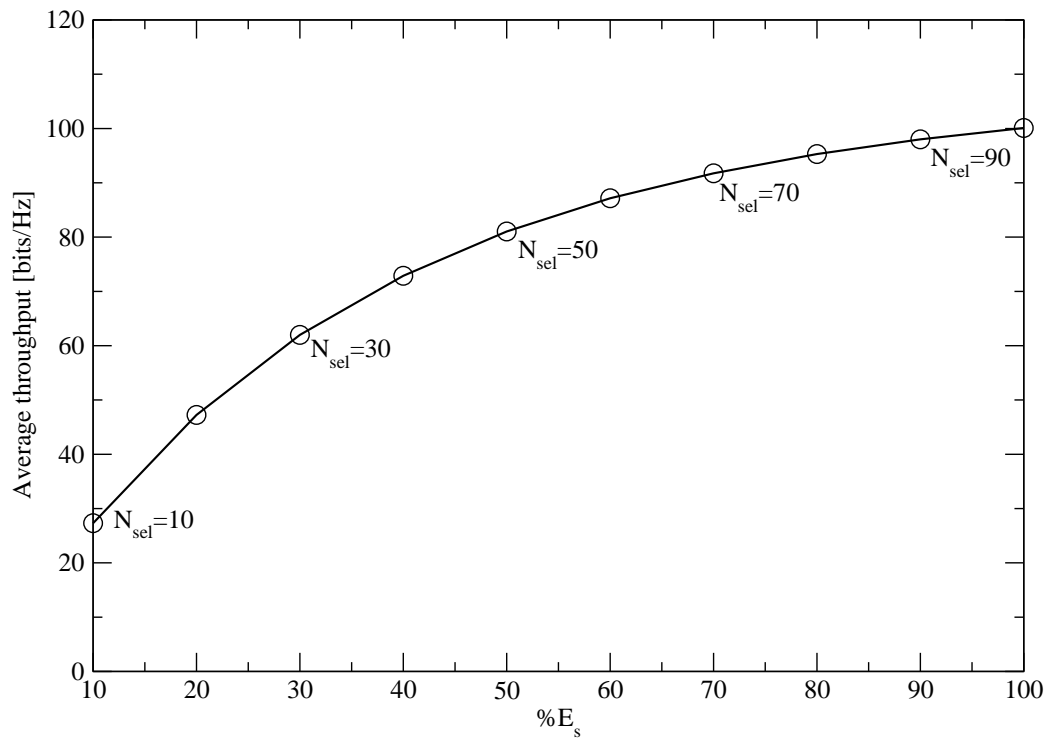


Figure 2.15: Average throughput per pass $\bar{\mathcal{T}}_{\text{BSC}}$ as a function of the number of selected nodes N_{sel} and the average energy consumption (as a percentage of the transmitted energy $E_s = 1.69$ pJ) required for the transmission.

Chapter 3

Distributed Detection in Wireless Sensor Networks

One of the most interesting application scenario for WSNs is that of fires detection. At the moment, the systems used to detect forest fires are a satellite-based monitoring methods and other systems that usually cannot forecast forest fires before the fire is spread uncontrollable. Using a large number of sensor nodes densely deployed in a risk environment it is possible to create a real time system monitoring that allows to predict fire promptly and accurately [51, 52].

Typical applications that use the WSN technology consider a network whose data have to be transmitted toward a node coordinator, which by means of radio links as GPRS or UMTS transmits these information to the final user. If the node coordinator is near to each sensor of the network (in terms of radio distance) we consider a star network where each node transmits its data directly to the coordinator. When this assumption is not true, we need to consider another type of scenario. In fact, considering that energy efficiency is the most important requirement in WSNs, to minimize the energy consumptions of nodes (and then maximize the lifetime) it is important to limit the distance of transmissions. Consequently, the data will have to be sent to the coordinator of the network using the multi-hop technique. A typical scenario considers the coordinator at the border of the monitoring area, and a high number of sensors positioned randomly that have a double function: collect information about a determined phenomenon (sensor function) and send the data of neighbor nodes toward the coordinator (routing function).

Usually, to increase the lifetime of the entire network, routing algorithms at regular intervals select a limited number of sensors that collect information and define a route until the coordinator. In this manner for each of these

intervals, we can see the network as a chain.

We here propose the use of a chain network for the detection of fires.

In these types of networks the goals are to limit throughput in each sensor-to-sensor link (also to save energy) and minimize the probability of error at the last stage of the chain. We can define two types of error: when the fire is present but the network doesn't detect it (miss detection), and when the fire is absent but the network detects it (false alarm). The problem is similar to that of storing data in limited capacity memory, studied in [53] where it is proposed a finite statistic to summarize a number of observations. In that work it is presented an algorithm with a four-valued statistic which achieves a limiting probability of error under binary hypothesis.

This is a typical scenario of distributed detection [54–69, 69–95], where the single nodes sense the environment independently to detect a natural phenomenon and make a local binary decision of target absent/present (according to the literature in detection, we use the term target instead of fire or natural phenomenon). To limit the number of transmissions, each node waits the decision made by the previous node in the chain and using some fusion rules compares its observation with the received decision to derive a final decision that it is transmitted to the next node. To reach the two above described goals it is important that each node uses optimized fusion rules.

In Fig. 3.1 it is shown the scenario considered, where there are N sensors and a set of hypotheses $\mathcal{H} = \{H^{(1)}, H^{(2)}, \dots, H^{(N)}\}$ with the state of the nature for the i^{th} node as $H^{(i)} \in \{H_0, H_1\}$. In what follows the term $H_j^{(i)}$ stands for $H^{(i)} = H_j$. Hypothesis H_0 denotes the absence of fire whereas H_1 denotes the presence of fire. With $r^{(i)}$ we define the observation of the i^{th} node used to make a local decision, while $u^{(i)}$ represents the final decision derived from the use of fusion rules. Considering that decisions are related to absence/presence of a natural phenomenon, terms $u^{(i)}$ constitute a sequence of 0/1 bits. Our aim is to limit the throughput, that means minimizing the number of these bits in each sensor-to-sensor link. In this work we consider the observations $r^{(i)}$ to be statistically independent. They are also identically distributed when nodes observe a phenomenon relative to the same hypothesis.

In a more realistic setting we can think that observations $r^{(i)}$ are related to the sensing of environmental temperature and for the local decision a single node decides for H_1 (fire present) if this sensed temperature exceeds a determined threshold value. Usually these observations are affected by Gaussian estimation error. Nevertheless, next considerations are without considering a particular estimation error distribution, so they are valid for Gaussian, Laplacian and any other distribution.

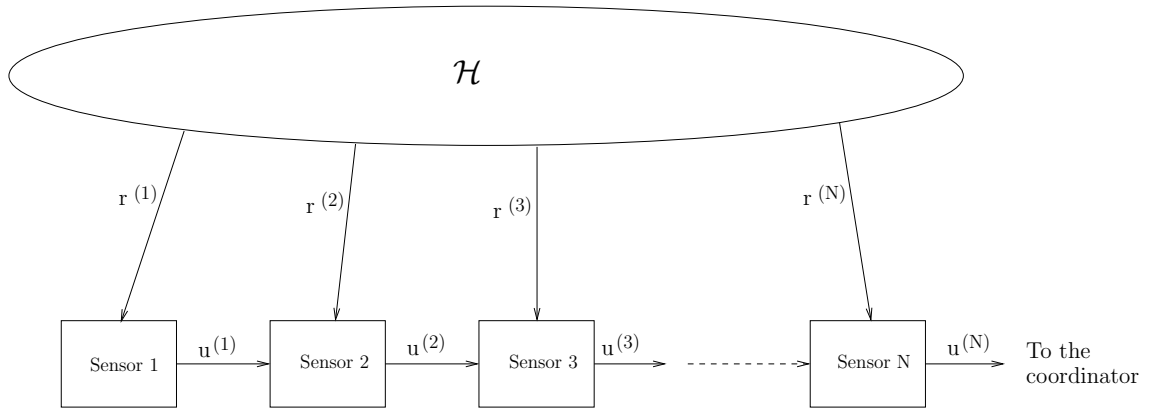


Figure 3.1: Chain Network for Fire Detection.

At the end of the chain, the coordinator reads the decision received by node N and decides for fire present or absent. In other words, if the signal $u^{(N)}$ is equal to 1 the coordinator will transmit the fire alarm to the final user. Fusion rules at each stage of the chain must be designed to reduce the probability of false alarm (P_{fa}) and probability of miss detection (P_{md}) at the coordinator. These two terms are defined as follows:

$$P_{fa} = \Pr\{u^{(N)} = 1 \mid \text{target not present}\}$$

$$P_{md} = \Pr\{u^{(N)} = 0 \mid \text{target present}\}.$$

The use of chain networks in forest fire detection systems allows to minimize energy consumption of the network with the only drawback that, considering a chain with N nodes, the coordinator will receive the final decision from the last node only after $N + 1$ time periods.

In the next sections we present two case of study. In the first we assume that all sensors observe the same phenomenon and we define fusion rules that consider the transmission of one bit in sensor-to-sensor link . In the second case we assume that, as in a more realistic scenario, the phenomenon H_1 is inherent at a limited area and we introduce some rules of decision to minimize the throughput.

3.1 First scenario: all nodes observing the same phenomenon

The first case of study considers that each node of the network observes the same phenomenon. In other words we consider $H^{(1)} = H^{(2)} = \dots = H^{(N)}$. In this scenario we investigate the rules with a 1-bit sensor-to-sensor throughput. Under this constraint, fusion rules should minimize P_{fa} and P_{md}

at the last stage of the chain.

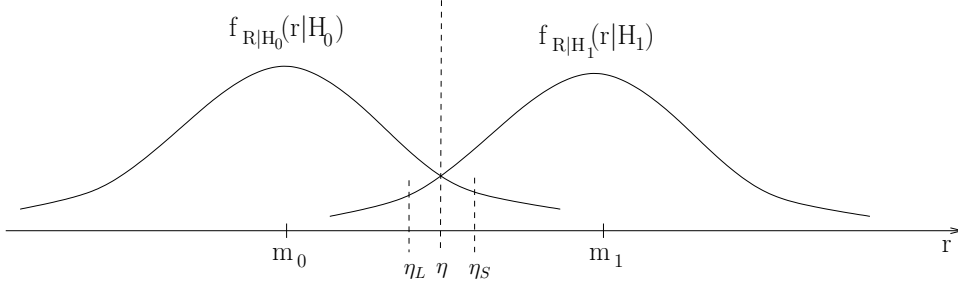


Figure 3.2: Conditional p.d.f. of the observed phenomenon.

We define a conditional p.d.f. related to the generic observation r as $f_{R|H_i}(r|H_i)$ in the hypothesis H_i . Naming m_0 the mean value relating to hypothesis H_0 and m_1 that of hypothesis H_1 , from the next considerations we assume that $m_0 < m_1$.

Obviously, the first node in the chain (node 1) can only take into account for its local decision the observation of the phenomenon. For the other nodes, the p.d.f. of the observation variable r is represented in figure 3.2, where to define fusion rules we consider a threshold η and an uncertainty interval delimited by two thresholds η_L and η_S . The proposed fusion rules are based on the concept that, if the observed $r^{(i)}$ is lower than $\eta_L^{(i)}$ the sensor i decides for H_0 ($u^{(i)} = 0$) irrespectively of the decision $u^{(i-1)}$; similarly, if $r^{(i)}$ is greater than $\eta_S^{(i)}$ the sensor decides for H_1 ($u^{(i)} = 1$) independently of the decision $u^{(i-1)}$. If $r^{(i)}$ is inside the uncertainty interval we can think that the observation is not very reliable, and the sensor transmits a decision $u^{(i)}$ equal to that received from the previous node in the network. Summarizing, the decision rules for node i are

- if $r^{(i)} < \eta_L^{(i)} \Rightarrow u^{(i)} = 0$
- if $r^{(i)} > \eta_S^{(i)} \Rightarrow u^{(i)} = 1$
- if $\eta_L^{(i)} < r^{(i)} < \eta_S^{(i)} \Rightarrow u^{(i)} = u^{(i-1)}$

It is possible to describe the system through a Markov chain as illustrated in figure 3.3, with two states corresponding to the binary possible values of $u^{(i)}$. Consequently we define four transition probabilities deriving from the rules described above.

As previously stated, the first node in the chain does not consider this model and it takes the decision $u^{(1)}$ using only the threshold η . This decision can assume two values and must be compared with the true hypothesis.

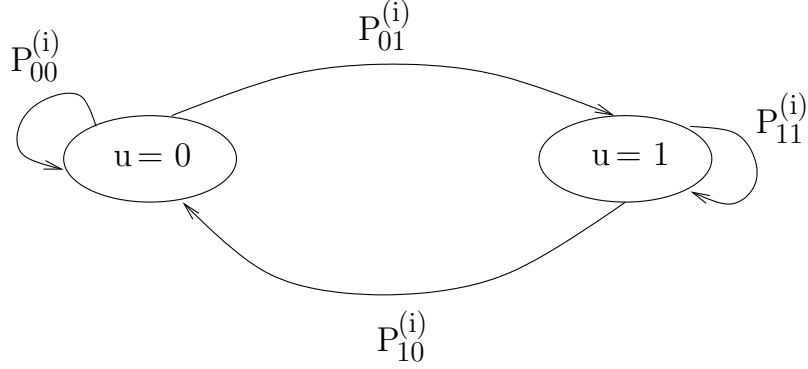


Figure 3.3: Markov chain used to describe the system.

In other words, it is possible that node 1 decides for H_0 (target absent) and the true hypothesis is H_0 (no error in the transmitted decision); or, the same decision can be made when the target is present but in this case the transmitted decision $u^{(1)}$ is wrong (miss detection error). In a formal definition of these possible cases we define with $H_j^{(1)}$, where $j \in \{0, 1\}$, the two possible true hypotheses H_0, H_1 . We introduce:

$$u_0^{(1)}(H_j^{(1)}) = \Pr\{\text{Sensor 1 decides for hypothesis } H_0 | H_j^{(1)}\} = \Pr\{r_1 < \eta | H_j^{(1)}\}$$

$$u_1^{(1)}(H_j^{(1)}) = \Pr\{\text{Sensor 1 decides for hypothesis } H_1 | H_j^{(1)}\} = \Pr\{r_1 > \eta | H_j^{(1)}\}.$$

At each stage the transition probabilities are dependent on the decision received from the previous node in the chain. We define:

$$P_{00}^{(i)}(H_j^{(i)}) = \Pr\{u^{(i)} = 0 | u^{(i-1)} = 0, H_j^{(i)}\} = \Pr\{r^{(i)} < \eta_S^{(i)} | H_j^{(i)}\} \quad (3.1)$$

$$P_{01}^{(i)}(H_j^{(i)}) = \Pr\{u^{(i)} = 1 | u^{(i-1)} = 0, H_j^{(i)}\} = \Pr\{r^{(i)} > \eta_S^{(i)} | H_j^{(i)}\} \quad (3.2)$$

$$P_{10}^{(i)}(H_j^{(i)}) = \Pr\{u^{(i)} = 0 | u^{(i-1)} = 1, H_j^{(i)}\} = \Pr\{r^{(i)} < \eta_L^{(i)} | H_j^{(i)}\} \quad (3.3)$$

$$P_{11}^{(i)}(H_j^{(i)}) = \Pr\{u^{(i)} = 1 | u^{(i-1)} = 1, H_j^{(i)}\} = \Pr\{r^{(i)} > \eta_L^{(i)} | H_j^{(i)}\}. \quad (3.4)$$

Defining the vector

$$\mathbf{u}^{(1)} = \mathbf{u}^{(1)}(H_j^{(1)}) = \begin{pmatrix} u_0^{(1)}(H_j^{(1)}) & u_1^{(1)}(H_j^{(1)}) \end{pmatrix} \quad (3.5)$$

and the matrix

$$\mathbf{P}^{(i)} = \mathbf{P}^{(i)}(H_j^{(i)}) = \begin{pmatrix} P_{00}^{(i)}(H_j^{(i)}) & P_{01}^{(i)}(H_j^{(i)}) \\ P_{10}^{(i)}(H_j^{(i)}) & P_{11}^{(i)}(H_j^{(i)}) \end{pmatrix} \quad (3.6)$$

at the N^{th} node of the chain we have

$$\mathbf{u}^{(N)} = \mathbf{u}^{(1)} \cdot \prod_{i=2}^N \mathbf{P}^{(i)} = \begin{pmatrix} u_0^{(N)} & u_1^{(N)} \end{pmatrix} \quad (3.7)$$

where $u_0^{(N)}$ is the probability that the N^{th} node decides for hypothesis H_0 (target absent) and $u_1^{(N)}$ is the probability that the N^{th} node decides for hypothesis H_1 (target present). Note that $\mathbf{u}^{(N)}$ in (3.7) depends in general on \mathcal{H} .

Since in this scenario we are assuming that all nodes observe the same phenomenon, to evaluate the system performance we can calculate the probability of miss detection and of false alarm at the N^{th} node as

$$P_{md} = P_{md}(\mathcal{H}) = \Pr(u_{(0)}^{(N)} | \mathcal{H} = \{H_1, H_1, \dots, H_1\}) \quad (3.8)$$

$$P_{fa} = P_{fa}(\mathcal{H}) = \Pr(u_{(1)}^{(N)} | \mathcal{H} \rightarrow \{H_0, H_0, \dots, H_0\}). \quad (3.9)$$

We can also define the probability of error

$$P_e = \pi_0 P_{fa} + \pi_1 P_{md} \quad (3.10)$$

where $\pi_0 = \Pr\{\mathcal{H} = \{H_0, H_0, H_0\}\}$ and $\pi_1 = \Pr\{\mathcal{H} = \{H_1, H_1, H_1\}\}$ are the a-priori probabilities of the observed phenomenon.

3.1.1 Results

For the evaluation of some numerical example, we assume that the observed phenomenon has a Gaussian distribution, as in Fig. 3.2, with mean value $m_0 = -1$ for hypothesis H_0 and $m_1 = 1$ for hypothesis H_1 (antipodal mean values). We also assume $\pi_0 = \pi_1$. We consider a signal-to-noise ratio $\text{SNR} = 1/\sigma^2$ and an uncertainty interval defined as $\varepsilon^{(i)} = \eta_S^{(i)} - \eta_L^{(i)}$, for a chain with 10 sensors.

For the Gaussian case the evaluation of the relevant probabilities is easy by means of function $\text{erfc}(\cdot)$ defined as

$$\text{erfc}(x) \triangleq \frac{2}{\sqrt{\pi}} \int_x^\infty e^{-t^2} dt. \quad (3.11)$$

For example, considering the case of target absent (hypothesis H_0), we can write:

$$u_1^{(1)}(H_0^{(1)}) = \Pr\{\text{Sensor 1 decide for } H_1 | H_0^{(1)}\} = \frac{1}{2} \operatorname{erfc} \left(\frac{\eta - m_0}{\sqrt{2\sigma^2}} \right) \quad (3.12)$$

$$P_{00}^{(i)}(H_0^{(i)}) = \Pr\{u_0^{(i)} | u_0^{(i-1)}, H_0^{(i)}\} = 1 - \frac{1}{2} \operatorname{erfc} \left(\frac{\eta_S - m_0}{\sqrt{2\sigma^2}} \right) \quad (3.13)$$

where $\eta = \varepsilon/2 + m_0$.

In terms of performance, we have calculated the results related to the fusion rules presented above in three different schemes. In each of them it has been used a different method to set the uncertainty interval $\varepsilon^{(i)}$ adopted at stage (i) of the chain. These values have been calculated using arithmetical processing.

In the first scheme we consider a fixed value of $\varepsilon^{(i)} = \varepsilon$ for each sensor. Thus, we study the performance in terms of error probability, using expression (3.10), in the case where all the nodes make a local decision using the same thresholds. The values of these thresholds are calculated in order to minimize P_e at stage 10 of the chain. We name this type of scheme "Fixed threshold".

In the second scheme we consider different values of $\varepsilon^{(i)}$ calculated in a static manner at each stage. For example the node i uses a value of $\varepsilon^{(i)}$ that minimizes the error probability in the case the chain ends at this node. We name this scheme "Locally set thresholds".

In the third scheme we consider different values of thresholds calculated in a global manner. In this case the node i uses a value of $\varepsilon^{(i)}$ that minimizes the error probability at its stage considering the value of $\varepsilon^{(i-1)}$ used by node $i - 1$. We name this scheme "Coordinated thresholds".

Figures 3.4, 3.5, 3.6 show the performance related to these three schemes in a chain network with 10 nodes and for three different values of SNR. In these figures we show the P_e calculated at each stage of the chain. It is clear from each of these figures that the "Coordinated thresholds" scheme is the best at each stage of the chain. Differences are more pronounced when it is considered a high value of SNR.

Some results related to this scenario have been also presented in [96]. In [96] the author proposed a distributed detection method for a chain network (that he named "serial network"), and compared the obtained performance in terms of error probability, looking also at three decisions criteria. The first one is the optimum case with parallel scheme (star topology network) where

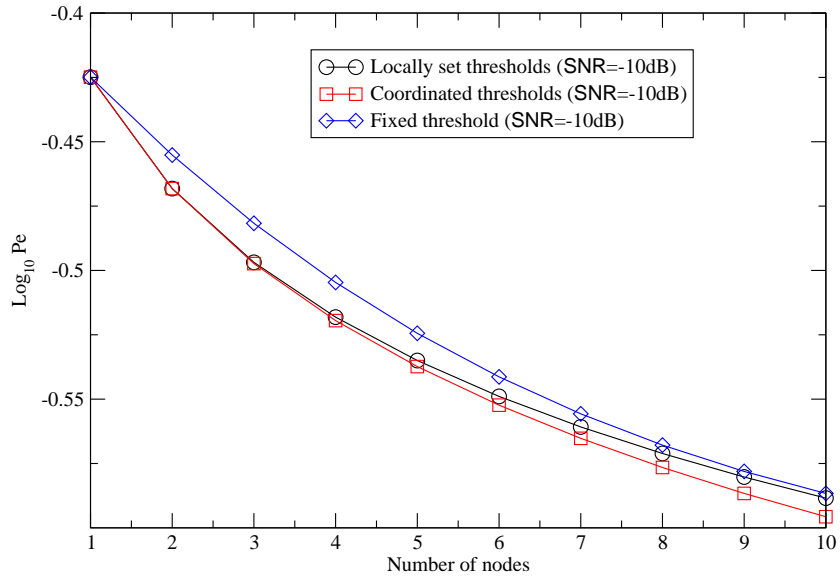


Figure 3.4: Performance for the three schemes with $\pi_0 = \pi_1$ and SNR = -10dB .

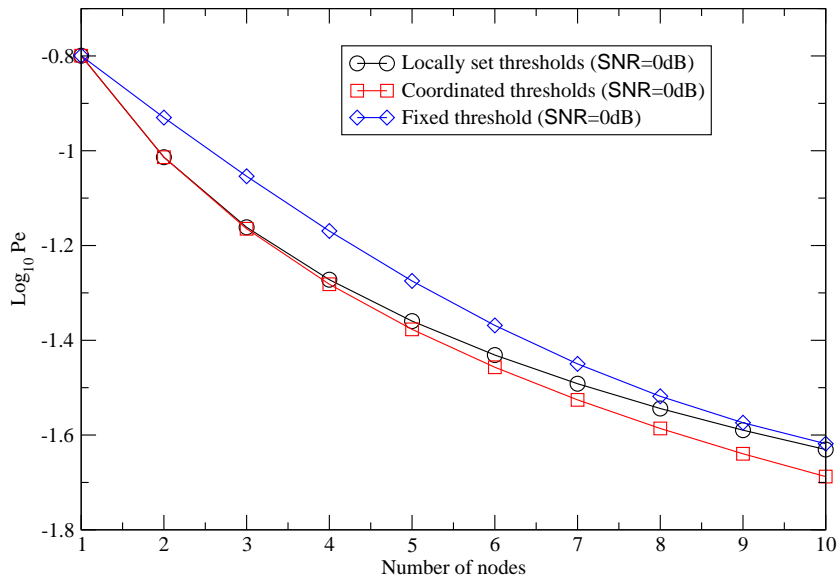


Figure 3.5: Performance for the three schemes with $\pi_0 = \pi_1$ and SNR = 0dB .

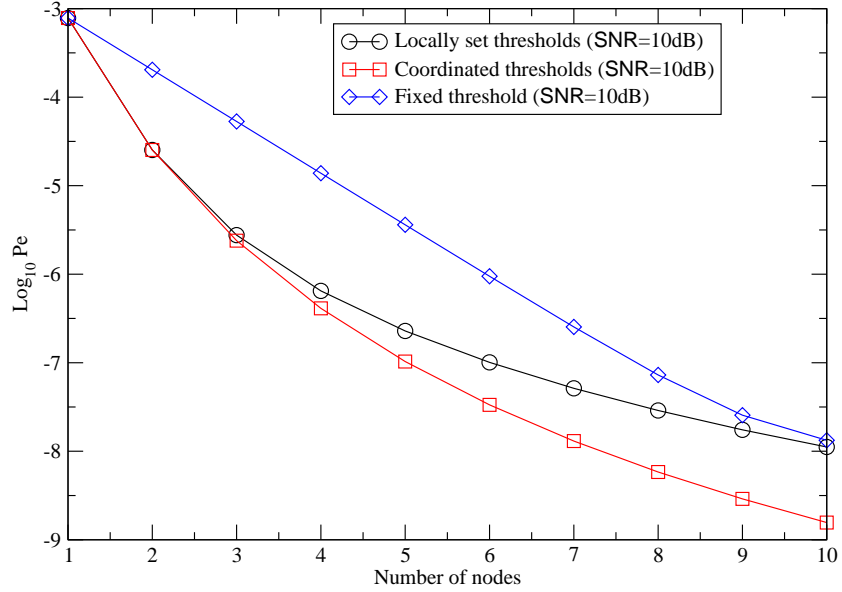


Figure 3.6: Performance for the three schemes with $\pi_0 = \pi_1$ and $\text{SNR} = 10\text{dB}$.

each node transmits the observation directly to the coordinator. The binary decision are made from the coordinator using the optimum test:

$$\sum_{i=1}^N r^{(i)} \underset{H_0}{\overset{H_1}{\geq}} 0.$$

The second criterion is suboptimal, where in a scenario similar to that just presented, sensors transmit to the coordinator the locally taken decisions. In this case the coordinator uses the test:

$$\sum_{i=1}^N \text{sgn}(r^{(i)}) \underset{H_0}{\overset{H_1}{\geq}} 0.$$

The third criteria is that presented in [53].

In Figure 3.7 we show the comparison between the optimum case scheme, Cover's scheme [53], Swaszek's scheme [96] and Coordinated thresholds scheme, considering a $\text{SNR} = 0\text{dB}$. As we can see the performance of our solution are coincident with those of [96] and are better of Cover's results. In the Swaszek's approach the P_e at stage i is calculated using a recursion that contains the value of P_e in the previous stage. In this manner, when it is necessary to evaluate performance in a network with a high number of nodes,

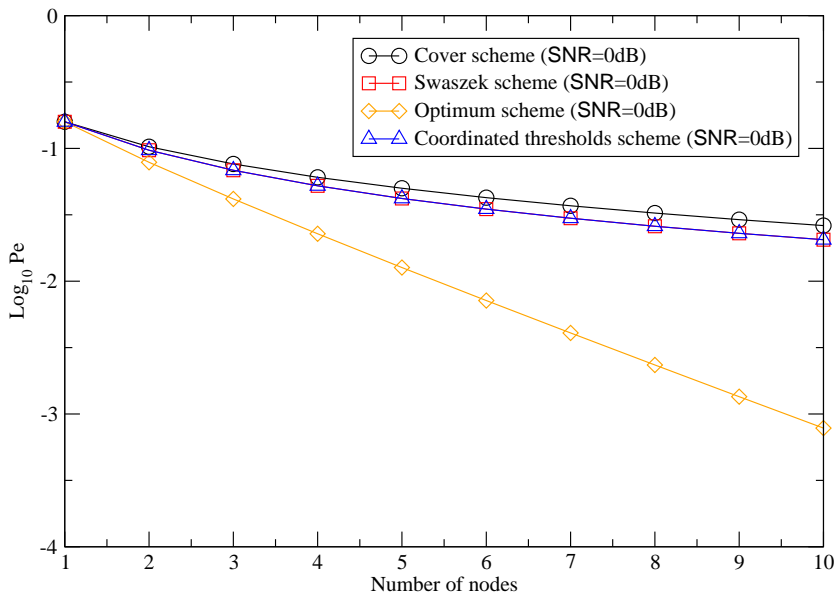


Figure 3.7: Comparison of "Coordinated thresholds" scheme with Cover, Swaszek and optimum schemes.

the computational complexity could become very heavy. Moreover, the results of [96] are valid under the assumption $\pi_0 = \pi_1$. The system description using Markov chain representation, proposed in this work, permits to reduce computational complexity and is valid for all values of a-priori probabilities.

In order to have a complete description of the proposed solution, we have calculated the performance of the system also in the case of unequal a-priori probabilities ($\pi_0 \neq \pi_1$). Figures 3.8, 3.9 and 3.10 show the results obtained with $\text{SNR} = 0\text{dB}$ for different values of a-priori probabilities (remembering that $\pi_0 + \pi_1 = 1$) in the Fixed threshold, Locally set thresholds and Coordinated thresholds schemes, respectively. Note that, the best performance in terms of P_e is achieved with equal a-priori probabilities.

To compare the performance of the three schemes, figure 3.11 shows the results obtained for $\text{SNR} = 0\text{dB}$ and $\pi_0 = 0.7$. We can conclude that Coordinated thresholds is the better scheme both in the case of unequal and equal a-priori probabilities.

To evaluate the performance of the system independently of the a-priori probabilities, we have analytically determined the expressions of P_d and P_{fa} at stage i as a function of those at previous stages. In particular, considering that

$$P_d^{(i)} = \Pr\{u^{(i-1)} = 1, r^{(i)} > \eta_L^{(i)} | H_1^{(i)}\} + \Pr\{u^{(i-1)} = 0, r^{(i)} > \eta_S^{(i)} | H_1^{(i)}\} \quad (3.14)$$

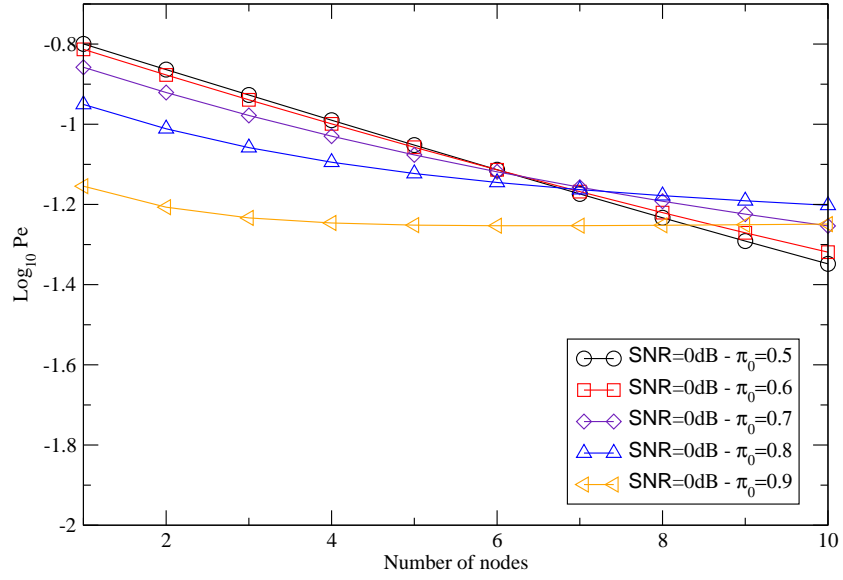


Figure 3.8: Fixed threshold scheme for different a-priori probabilities.

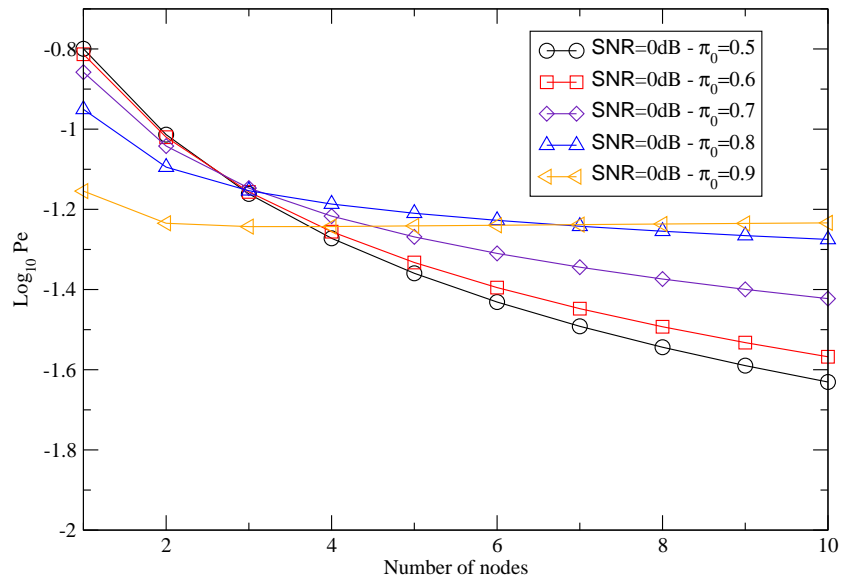


Figure 3.9: Locally set thresholds scheme for different a-priori probabilities.

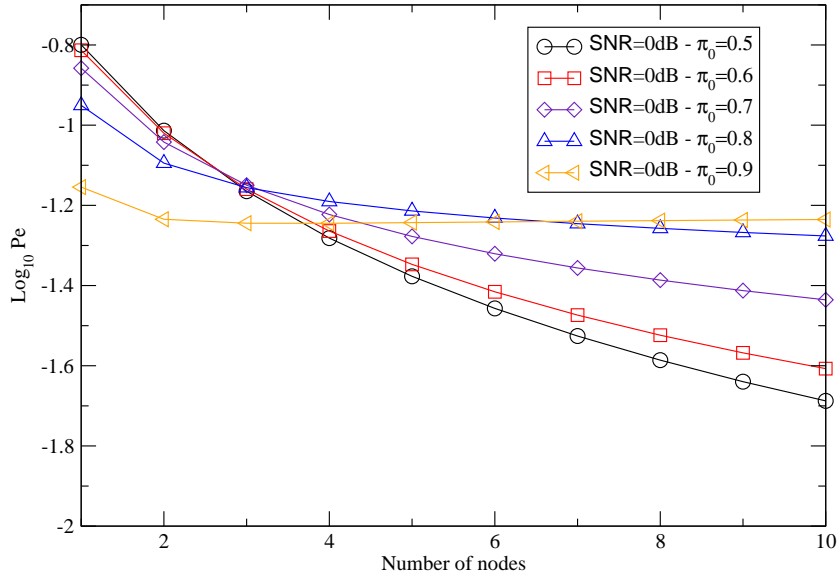


Figure 3.10: Coordinated thresholds scheme for different a-priori probabilities.

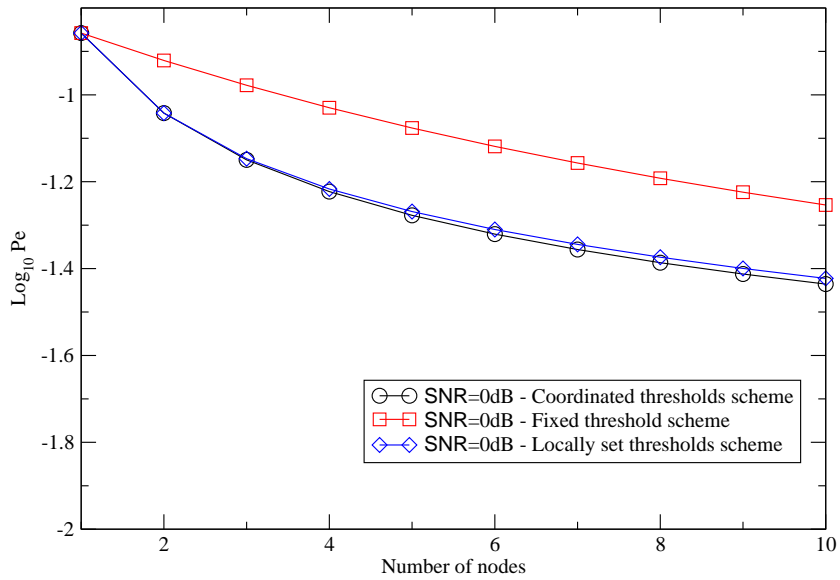


Figure 3.11: Comparison of the three cases with SNR= 0dB and $\pi_0 = 0.7$.

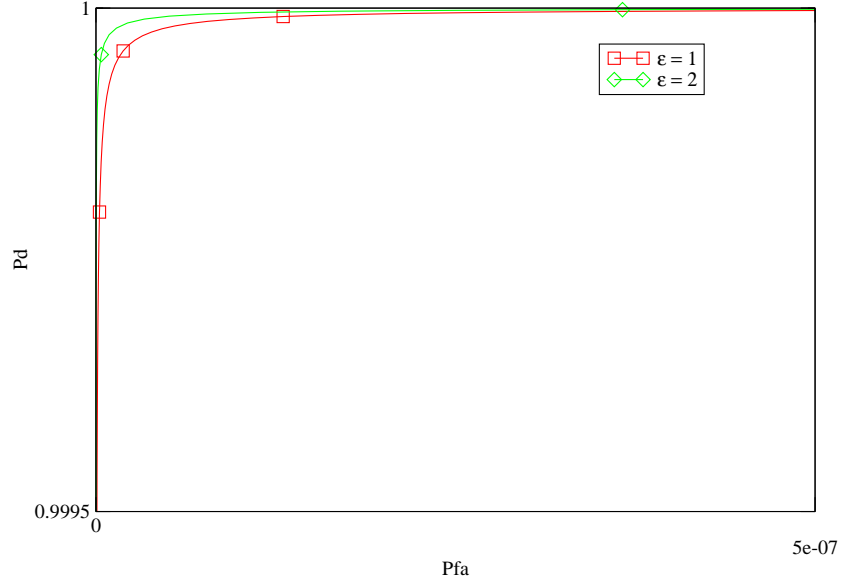


Figure 3.12: ROC curves obtained with an SNR=10dB.

and applying some basic probabilistic rules we can obtain that

$$P_d^{(i)} = \Pr\{r^{(i)} > \eta_L^{(i)} | H_1^{(i)}\} \cdot P_d^{(i-1)} + \Pr\{r^{(i)} > \eta_S^{(i)} | H_1^{(i)}\} \cdot (1 - P_d^{(i-1)}). \quad (3.15)$$

We can conclude that P_d and P_{fa} at stage i depend on $\eta_L^{(i)}$, $\eta_S^{(i)}$ and on their values at previous stages. We can write

$$P_d^{(i)} = f_1(P_d^{(i-1)}, \eta_L^{(i)}, \eta_S^{(i)})$$

$$P_{fa}^{(i)} = f_2(P_{fa}^{(i-1)}, \eta_L^{(i)}, \eta_S^{(i)})$$

To evaluate performance in terms of P_d and P_{fa} we use ROC curves, realized by varying the value of threshold η . More precisely, we fix the interval ε (the same for all stages) and assume that η is in the middle of this interval. At the first node we consider only threshold η with $\varepsilon = 0$.

Figures 3.12, 3.13 and 3.14 show ROC curves for three different values of SNR, with different values of ε . Remembering that in this graphs the optimal curve passes for the point with coordinates $P_{fa} = 0$ and $P_d = 1$, in the presented figures it is possible locate an optimum value of ε .

To derive the optimum threshold value that optimize performance for each curve, and than must be used in the hypothesis tests, we consider the MinMax criterion. The MinMax equation is

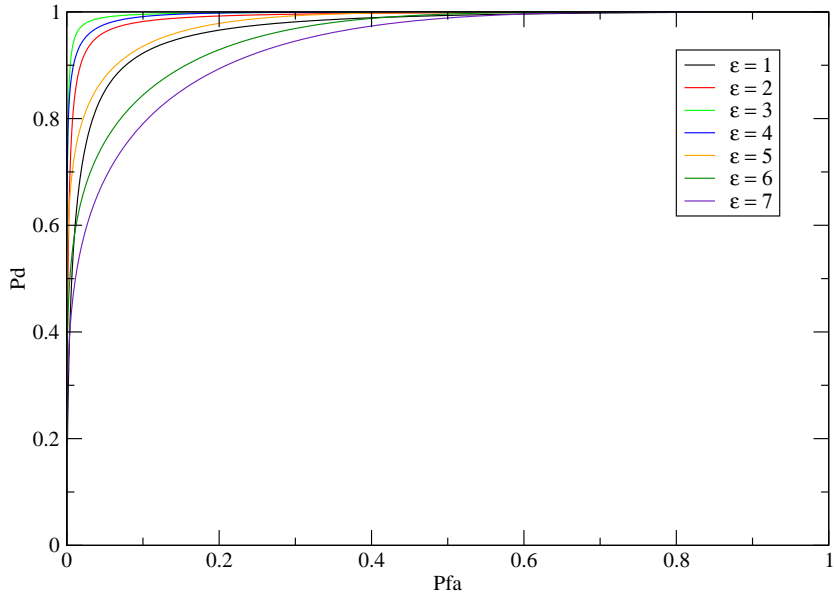


Figure 3.13: ROC curves obtained with an SNR=0dB.

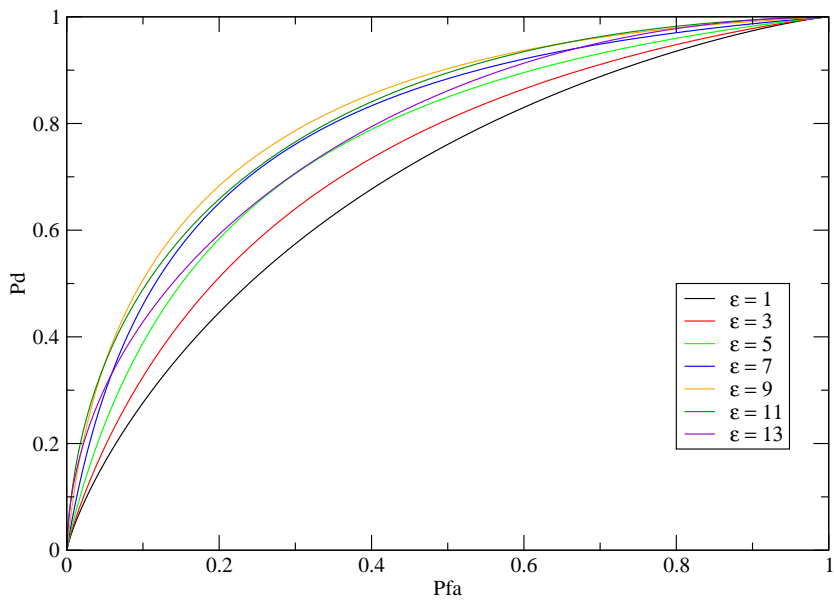


Figure 3.14: ROC curves obtained with an SNR=-10dB.

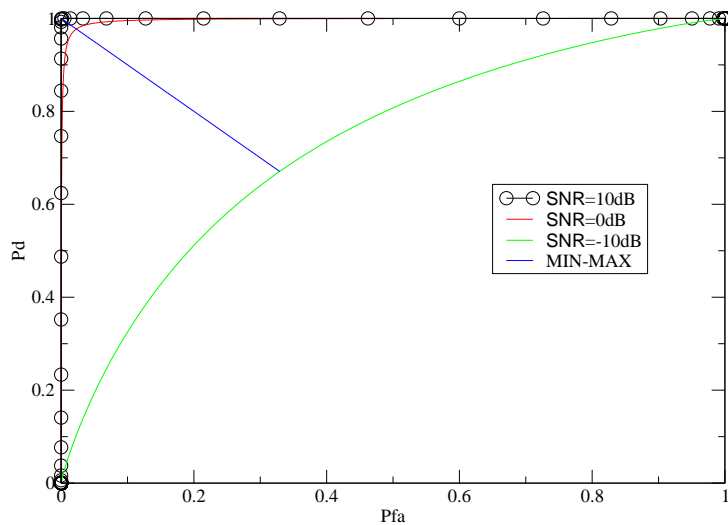


Figure 3.15: ROC curves obtained with $\varepsilon = 3$ for different SNR values.

$$C_{01}P_{md} = C_{10}P_{fa},$$

where C_{01} is the cost in choosing H_0 given H_1 and C_{10} is the cost in choosing H_1 given H_0 . If we assume $C_{10} = C_{01}$, we can write the expression

$$P_d = 1 - P_{fa}$$

that defines a line that cross the ROC curves in the values that minimize the maximum error.

Figures 3.15 and 3.16 show the MinMax line and ROC curves obtained varying SNR and ε values respectively. Figures 3.17 and 3.18 show curves obtained for different SNR values and for each stage of the network. These curves are obtained choosing the value of ε that maximize the performance (derived with results presented in figures 3.12, 3.13, 3.14). MinMax line determines the optimum value of threshold η for each stage. As expected, the optimal value of threshold η is 0.

3.2 Second scenario: observation of a local phenomenon

In the second case of study we consider that only a restricted number of nodes can sense the presence of the target. The decision rules used for the first case

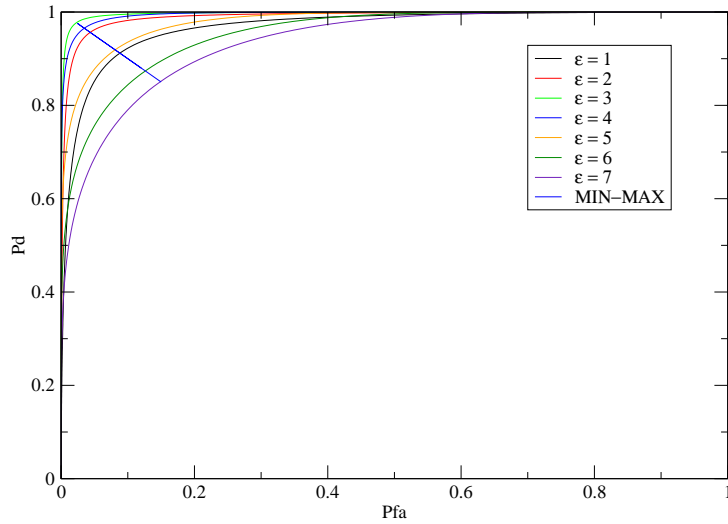


Figure 3.16: ROC curves obtained with SNR= 0dB for different values of ϵ .

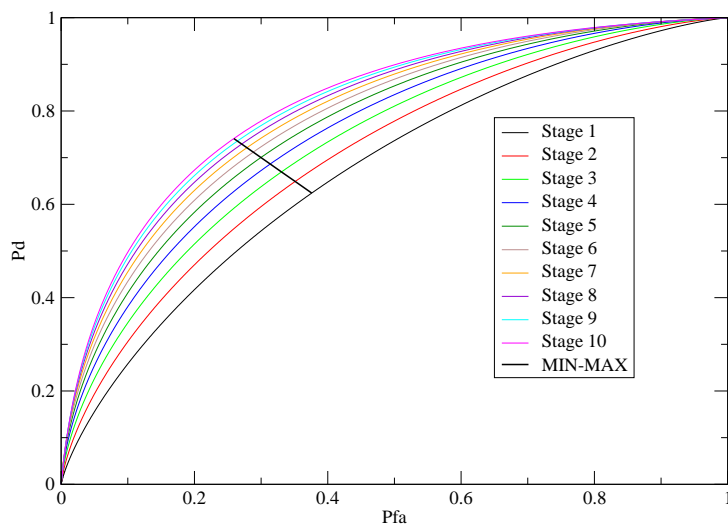


Figure 3.17: ROC curves obtained with $\epsilon = 9$ and SNR=-10dB, for each stage of the chain.

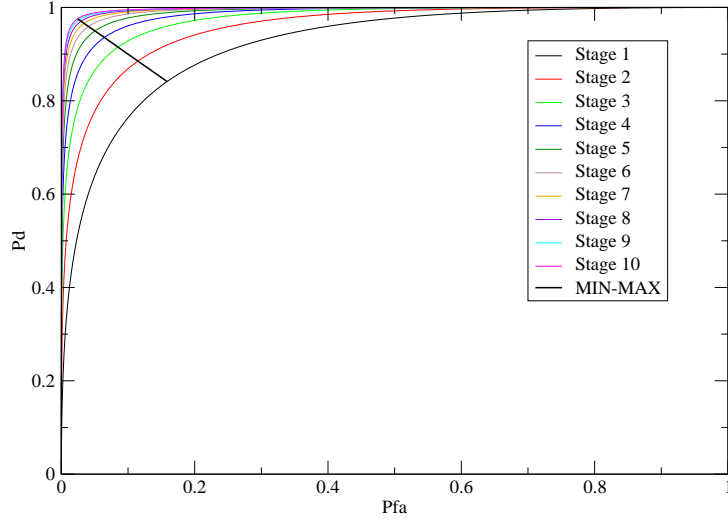


Figure 3.18: ROC curves obtained with $\varepsilon = 3$ and $\text{SNR}=0\text{dB}$, for each stage of the chain.

of study are not valid, because in this case we want advise the user that there is a fire in a restricted region, where only a limited number of nodes are sensing, while most of the nodes are not in a region where there is fire. Consequently we will obtain an increase of the miss detection probability.

We propose a solution for this scenario that considers the transmission of two bits, related to two consecutive nodes decisions (node i receives $u^{(i-1)}$ composed of two bits inherent to the decision taken by nodes $i-2$ and $i-1$). We assume that if two adjacent nodes of the network decide for hypothesis H_1 this decision has to be forwarded by the other following nodes until the coordinator. In other words if a node i receives a combination of two bits equal to 11 (nodes $i-2$ and $i-1$ have decided for the hypothesis H_1), it decides for H_1 irrespectively on its observation, retransmitting these two bits to the following sensor in the chain.

This choice derives by the consideration that when two consecutive nodes decide for hypothesis H_1 , it is more likely that they have detected a fire rather than both produce a false alarm.

To validate the last consideration it is important that each node of the network decides for hypothesis H_1 only in the presence of a reliable observation. Consequently, in decision rules, sensor decides for hypothesis H_1 when $r^{(i)} > \eta_S^{(i)}$. When the observation is inside the uncertainty interval the node decides for H_0 .

We assume that the first two nodes of the chain decide only observing

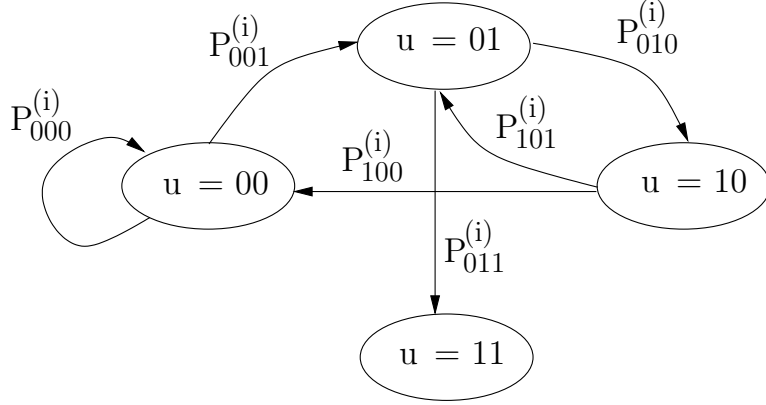


Figure 3.19: Markov chain used to describe network in the second scenario.

the phenomenon and the proposed "detection strategy" begins at node 3.

Table 3.1 resumes decision rules for this scenario.

$\mathbf{u}^{(i-1)}$	$\mathbf{r}^{(i)}$	$\mathbf{u}^{(i)}$
00	$> \eta_S^{(i)}$	01
00	$< \eta_S^{(i)}$	00
01	$> \eta_S^{(i)}$	11
01	$< \eta_S^{(i)}$	10
10	$> \eta_S^{(i)}$	01
10	$< \eta_S^{(i)}$	01
11	—	11

Table 3.1: Fusion rules for local phenomenon scenario

We can describe the system through a Markov chain as illustrated in figure 3.19. It is possible to define four states and eight transition probabilities deriving from the rules described above. As previously stated, the first two nodes in the chain do not consider this model as they take the decision independently, using the threshold $\eta_S^{(i)}$ in order to minimize the false alarm probability.

The signal $u^{(2)}$, composed of two bits, that the sensor 2 transmits to the sensor 3, can assume four values:

$$\begin{aligned}
 u_{00}^{(2)}(H_j^{(i)}) &= \Pr\{r^{(1)} < \eta_S^{(i)}, r^{(2)} < \eta_S^{(i)} | H_j^{(i)}\} \\
 u_{01}^{(2)}(H_j^{(i)}) &= \Pr\{r^{(1)} < \eta_S^{(i)}, r^{(2)} > \eta_S^{(i)} | H_j^{(i)}\} \\
 u_{10}^{(2)}(H_j^{(i)}) &= \Pr\{r^{(1)} > \eta_S^{(i)}, r^{(2)} < \eta_S^{(i)} | H_j^{(i)}\}
 \end{aligned}$$

$$u_{11}^{(2)}(H_j^{(i)}) = \Pr\{r^{(1)} > \eta_S^{(i)}, r^{(2)} > \eta_S^{(i)} | H_j^{(i)}\}$$

where for example the term $u_{01}^{(2)}$ indicates that the decision made by nodes 1 is 0 (hypothesis H_0) while the decision made by node 2 is 1 (hypothesis H_1).

The transition probabilities are ¹:

$$P_{000}^{(i)}(H_j^{(i)}) = \Pr\{u^{(i)} = 00 | u^{(i-1)} = 00, H_j^{(i)}\} = \Pr\{r^{(i)} < \eta_S^{(i)}\} \quad (3.16)$$

$$P_{001}^{(i)}(H_j^{(i)}) = \Pr\{u^{(i)} = 01 | u^{(i-1)} = 00, H_j^{(i)}\} = \Pr\{r^{(i)} > \eta_S^{(i)}\} \quad (3.17)$$

$$P_{010}^{(i)}(H_j^{(i)}) = \Pr\{u^{(i)} = 10 | u^{(i-1)} = 01, H_j^{(i)}\} = \Pr\{r^{(i)} < \eta_S^{(i)}\} \quad (3.18)$$

$$P_{011}^{(i)}(H_j^{(i)}) = \Pr\{u^{(i)} = 11 | u^{(i-1)} = 01, H_j^{(i)}\} = \Pr\{r^{(i)} > \eta_S^{(i)}\} \quad (3.19)$$

$$P_{100}^{(i)}(H_j^{(i)}) = \Pr\{u^{(i)} = 00 | u^{(i-1)} = 10, H_j^{(i)}\} = \Pr\{r^{(i)} < \eta_S^{(i)}\} \quad (3.20)$$

$$P_{101}^{(i)}(H_j^{(i)}) = \Pr\{u^{(i)} = 01 | u^{(i-1)} = 10, H_j^{(i)}\} = \Pr\{r^{(i)} > \eta_S^{(i)}\} \quad (3.21)$$

$$P_{110}^{(i)}(H_j^{(i)}) = \Pr\{u^{(i)} = 10 | u^{(i-1)} = 11, H_j^{(i)}\} = 0 \quad (3.22)$$

$$P_{111}^{(i)}(H_j^{(i)}) = \Pr\{u^{(i)} = 11 | u^{(i-1)} = 11, H_j^{(i)}\} = 1 \quad (3.23)$$

Defining a vector

$$\mathbf{u}^{(2)} = \mathbf{u}^{(2)}(H_j^{(i)}) = \left(u_{00}^{(2)}(H_j^{(i)}) \quad u_{01}^{(2)}(H_j^{(i)}) \quad u_{10}^{(2)}(H_j^{(i)}) \quad u_{11}^{(2)}(H_j^{(i)}) \right) \quad (3.24)$$

and the matrix

$$\mathbf{P}^{(i)} = \mathbf{P}^{(i)}(H_j^{(i)}) = \begin{pmatrix} P_{000}^{(i)}(H_j^{(i)}) & P_{001}^{(i)}(H_j^{(i)}) & 0 & 0 \\ 0 & 0 & P_{010}^{(i)}(H_j^{(i)}) & P_{011}^{(i)}(H_j^{(i)}) \\ P_{100}^{(i)}(H_j^{(i)}) & P_{101}^{(i)}(H_j^{(i)}) & 0 & 0 \\ 0 & 0 & P_{110}^{(i)}(H_j^{(i)}) & P_{111}^{(i)}(H_j^{(i)}) \end{pmatrix} \quad (3.25)$$

at the N^{th} node of the chain we have

$$\mathbf{u}^{(N)} = \mathbf{u}^{(2)} \cdot \prod_{i=3}^N \mathbf{P}^{(i)} = \left(u_{00}^{(N)} \quad u_{01}^{(N)} \quad u_{10}^{(N)} \quad u_{11}^{(N)} \right) \quad (3.26)$$

where $u_{00}^{(N)}$ and $u_{10}^{(N)}$ are the probabilities that the N^{th} node decides for hypothesis H_0 (target absent) while $u_{01}^{(N)}$ and $u_{11}^{(N)}$ are the probabilities that the N^{th} node decides for hypothesis H_1 (target present).

¹Note that for nodes on the boundaries, terms $u^{(i)}$ and $P^{(i)}$ are also dependent on the phenomena observed by the two previous nodes.

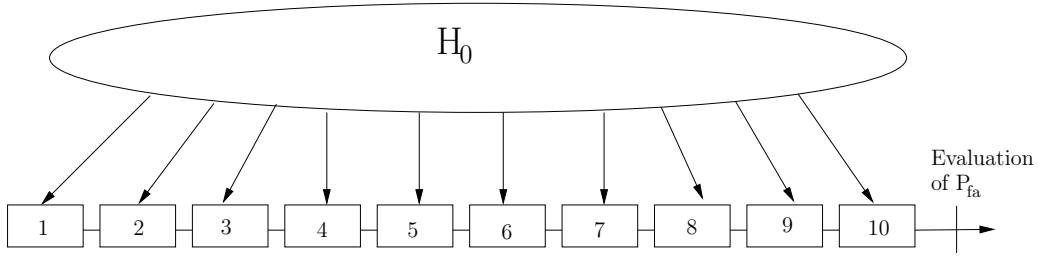


Figure 3.20: Scheme of chain network used to evaluate P_{fa} .

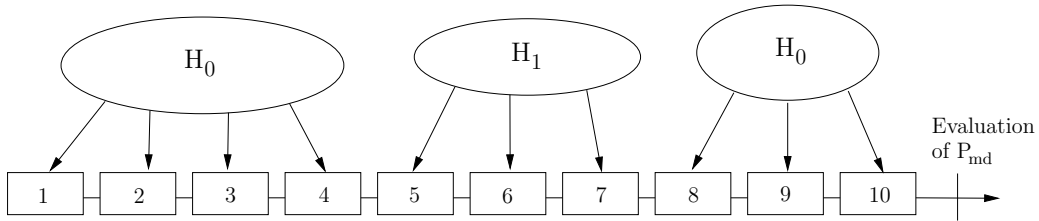


Figure 3.21: Scheme of chain network used to evaluate P_{md} .

3.2.1 Results

To evaluate the performance in terms of probabilities of miss detection and false alarm we consider a network composed of 10 nodes and we analyze the two schemes presented in figures 3.20 and 3.21. In the first we consider the absence of fire and we want to evaluate the probability of false alarm deriving by the use of the decision rules above presented. The second scheme considers the presence of fire. In particular we assume that nodes 1, 2, 3, 4, 8, 9, 10 observe phenomenon H_0 (absence of fire) and nodes 5, 6, 7 observe phenomenon H_1 (presence of fire). Considering a Gaussian case, we assume that for hypothesis H_0 the mean value m_0 is -1 , for hypothesis H_1 the mean value m_1 is equal to 1. We assume that all the nodes use the same thresholds, that is $\eta_S^{(i)} = \eta_S$, $\eta^{(i)} = \eta$ and $\eta_L^{(i)} = \eta_L$. Figure 3.2 resumes the case of study where for the rules defined in this paragraph we consider only threshold η_S . In Gaussian case the evaluation of transition probabilities and terms $u_{ij}^{(2)}$ can be expressed by using the function $\text{erfc}(\cdot)$. For example, for hypothesis H_0

$$u_{00}^{(2)} = \left[1 - \frac{1}{2} \text{erfc} \left(\frac{\eta_S - m_0}{2\sigma^2} \right) \right]^2$$

$$P_{000} = 1 - \frac{1}{2} \text{erfc} \left(\frac{\eta_S - m_0}{2\sigma^2} \right).$$

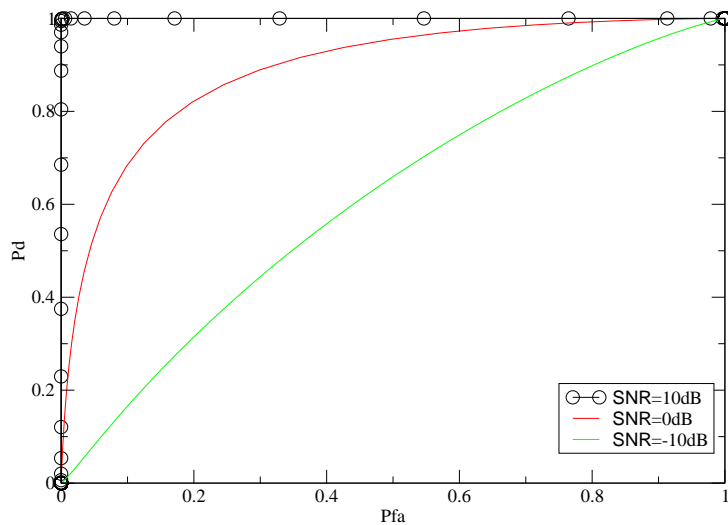


Figure 3.22: ROC curves relative to the proposed decision criterion for different SNR values.

For performance evaluation we calculate the probability of false alarm at the N^{th} node in scenario 3.20 as

$$P_{fa} = u_{(01)}^{(N)} + u_{(11)}^{(N)}$$

and the probability of miss detection at the N^{th} node in scenario 3.21 as

$$P_{md} = u_{(00)}^{(N)} + u_{(10)}^{(N)}.$$

Figure 3.22 shows ROC curves relative to this approach for different values of SNR.

To validate the idea of transmitting two bits and to use decision rules based only on the threshold η_S , we have also calculated the performance in the "local phenomenon" scenario in terms of P_d and P_{fa} using the rules defined in the one bit case.

Figure 3.23 shows the comparison between two cases for the two different values of SNR. In particular, we compare the optimum curve from the one-bit case with that of two bits case maintaining fixed SNR.

It is possible to note that the two bits scheme has the better performance; however, its drawback is due to the throughput, that it is the doubled. Actually this is not completely true, since as we can see in table 3.1, the transmission of two bits is necessary only when a single node takes a local decision equal to 1. Therefore, the average throughput is actually less than two bits per link.

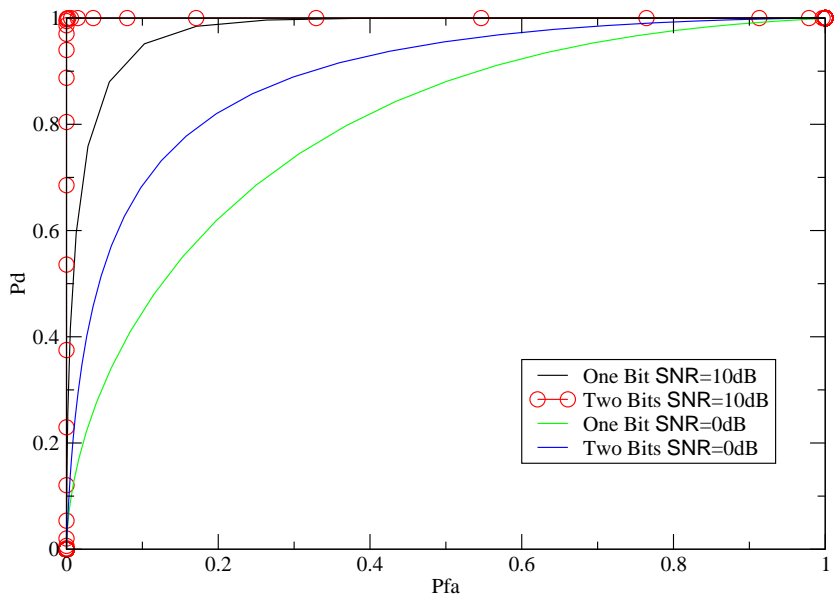


Figure 3.23: ROC curves to compare the two types of decision criterion.

Chapter 4

Experimental results of WSNs

As presented in chapter 1, WSNs are suitable for a high number of applications. In this chapter it is presented the realization of an application for an agricultural scenario, with results obtained from an on-field experimentation of several months.

Before to describe the characteristics of the realized work, in the first two sections we will review the main aspects of the IEEE802.15.4 standard that regulates the MAC and PHY layers of WSNs, and present the commercial platforms Crossbow and Chipcon.

The first of these it has been used to realize the agriculture application, whose main features are:

- Monitoring of air temperature, soil temperature and humidity.
- Minimization of sensors consumptions, in order to guarantee a lifetime of the network of the order of 1 year.
- Creation of a remote control system, in order to allow reading of data network through a web site.

With regard to the implementation layer, WSN applications are divided into two main categories:

- Applications that use a predefined network layer implementation and need the creation of the user application.
- Applications that are created directly on MAC layer, where we need to implement both the network layer and the user application.

Relatively to the first category, at the moment, there are different producers that provide platforms with dedicated network protocol. A number of

important electronic companies in 2004 have created an alliance named Zigbee, with the goal to define a common network protocol. The characteristics of this protocol can be found in [97].

The Crossbow platform, that it has been used for the agriculture application, belongs to the first category. Using their "mesh" network protocol, we realized the user application according to the above presented specifications.

The Chipcon platform allows to create applications for both categories. For the future works, it will be considered to realize applications belonging at the second category, in order to build a dedicated platform that guarantees high flexibility.

4.1 Standard IEEE802.15.4

In this section we describe the main characteristics of the standard that regulates the WSNs. Standard IEEE802.15.4 [98] defines the specifications relatively to MAC and PHY layers for low-rate WPANs that include WSNs. It uses carrier sense multiple access with collision avoidance (CSMA-CA) medium access mechanism and supports star as well as peer-to-peer topologies.

It includes four optional PHYs:

- An 868/915 MHz DSSS PHY employing binary phase shift keying (BPSK) modulation.
- An 868/915 MHz DSSS PHY employing offset quadrature phase-shift keying (O-QPSK) modulation.
- An 868/915 MHz parallel sequence spread-spectrum (PSSS) PHY employing BPSK and amplitude shift keying (ASK) modulation.
- An 2450 MHz DSSS PHY employing O-QPSK modulation.

The 868/915 MHz PHYs support over-the-air data rates of 20 kb/s, 40 kb/s, and optionally 100 kb/s and 250 kb/s. The 2450 MHz PHY supports an over-the-air data rate of 250 kb/s. The PHY choice depends on local regulations and user preference.

There are 16 channels in the 2450 MHz band, 30 channels in the 915 MHz band, and 3 channels in the 868 MHz band. In the more used 2450 MHz PHY the 16 channels are large 2 MHz and are spaced of 5 MHz.

The IEEE802.15.4 standard imposes a range of transmission power between -32 and 0 dBm.

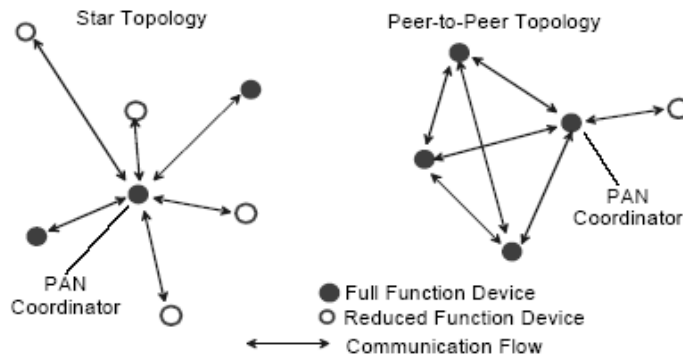


Figure 4.1: Types of network defined by IEEE802.15.4 standard

Two different types of devices can participate in an IEEE802.15.4 network; a full-function device (FFD) and a reduced-function device (RFD). The FFD can operate in three modes serving as a personal area network (PAN) coordinator, a coordinator, or a device. An FFD can talk to RFDs or other FFDs, while an RFD can talk only to an FFD. An RFD is intended for applications that are extremely simple, such as a light switch or a passive infrared sensor; they do not have the need to send large amounts of data and may only associate with a single FFD at a time. Consequently, the RFD can be implemented using minimal resources and memory capacity. Usually a WPAN shall include at least one FFD, operating as the PAN coordinator.

Depending on the application requirements, the IEEE802.15.4 standard may operate in either of two topologies: the star topology and the peer-to-peer topology. Both are shown in Figure 4.1. In the star topology the communication is established between devices and a single central controller, called PAN coordinator. A device typically has some associated application and is either the initiation point or the termination point for network communications. A PAN coordinator may also have a specific application, but it can be used to initiate, terminate, or route communications around the network. The PAN coordinator is the primary controller of the PAN. All devices operating on a network of either topology shall have unique 64-bit address. This address may be used for direct communication within the PAN, or a short address may be allocated by the PAN coordinator when the device is associated. The PAN coordinator might often be mains powered, while the devices will most likely be battery powered. Applications that benefit from a star topology include home automation, personal computer (PC) peripherals, toys and games, and personal health care.

The peer-to-peer topology also has a PAN coordinator; however, it differs

from the star topology in that any device may communicate with any other device as long as they are in range of one another. Peer-to-peer topology allows more complex network formations to be implemented, such as mesh networking topology. Applications such as industrial control and monitoring, asset and inventory tracking, intelligent agriculture, and security would benefit from such a network topology. A peer-to-peer network can be ad hoc, self-organizing, and self-healing. It may also allow multiple hops to route messages from any device to any other device on the network. Such functions can be added at the higher layer, but are not part of the standard.

Since in the greater part of the applications, devices are battery powered, and battery replacement or recharging in relatively short intervals is impractical, the power consumption is a primary aspect. The standard was developed with limited power supply availability in mind. Battery-powered devices will require duty-cycling to reduce power consumption. These devices will spend most of their operational life in a sleep state; however, each device periodically listens to the RF channel in order to determine whether a message is pending. This mechanism allows the application designer to decide on the balance between battery consumption and message latency. Higher powered devices have the option of listening to the RF channel continuously.

From a security perspective, wireless ad hoc networks are no different from any other wireless networks. They are vulnerable to passive eavesdropping attacks and potentially even active tampering because to access at physical communication channel it is not required to participate in communications. The very nature of ad hoc networks and their cost objectives impose additional security constraints, which perhaps make these networks the most difficult environments to secure. Devices are low-cost and have limited capabilities in terms of computing power, available storage, and power drain; and it cannot always be assumed they have a trusted computing base nor a high-quality random number generator aboard. Communications cannot rely on the online availability of a fixed infrastructure and might involve short-term relationships between devices that may never have communicated before. These constraints might severely limit the choice of cryptographic algorithms and protocols and would influence the design of the security architecture because the establishment and maintenance of trust relationships between devices need to be addressed with care. In addition, battery lifetime and cost constraints put severe limits on the security overhead these networks can tolerate, something that is of far less concern with higher bandwidth networks. Most of these security architectural elements can be implemented at higher layers and may, therefore, be considered to be outside the scope of the standard.

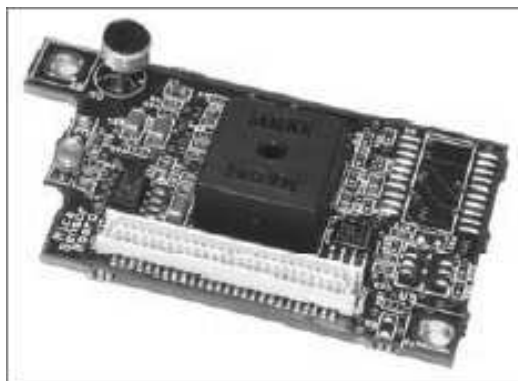


Figure 4.2: Sensor board MTS300

4.2 Description of two commercial WSN platforms

At the moment, there are many WSN platforms that can be used to realize applications for this type of networks. We will focus mainly on the Crossbow and Chipcon platforms. The first one it has been used to realize environmental application that will be described in the next section, while the second one is a new platform that guarantees better performance. In the last section future works on this one will be sketched.

4.2.1 Crossbow Platform

One of the first producers of sensor nodes is Crossbow [99]. This company defines three different modules: the sensor board, the radio board and the coordinator board. The main characteristics of these components are:

- **Sensor Board.** This module is intended to sense environmental parameters. Crossbow has produced different types of these boards, each of them contains different types of sensors with different accuracies. Fig. 4.2 shows MTS300CA board that includes sensors to monitor light, temperature, acoustic and sounder. This board as other Crossbow sensor boards is used with radio board MICAz and MICA2. The connection is done through a 51 pin connector.
- **Radio Board.** This module contains both radio part and CPU. The radio board MICAz (showed in Fig. 4.3) is a 2.4 GHz, IEEE802.15.4 compliant module used to create low-power, wireless, sensor networks. It includes:

- IEEE802.15.4/Zigbee compliant RF transceiver that works with frequencies from 2.4 to 2.4835 GHz, globally compatible with ISM band and support a range of powers transmission between -25 and 0 dBm;
- direct sequence spread spectrum radio which is resistant to RF interference, provides inherent data security and guarantees 250 kbps data rate;
- hardware security obtained through the use of AES-128;
- tinyOS as operating system to program nodes;
- reliable mesh networking stack software. In this manner users must program only on application level.

In term of CPU, radio board MICAz contains a microcontroller ATMega128L that has these characteristics:

- 8 MHz frequency clock;
- RISC architecture with 133 instructions;
- 4K bytes of SRAM;
- 4K bytes of EEPROM;
- 2 timer/counter of 8 bits;
- 2 PWM channels of 8 bits;
- 8 ADC channels of 10 bits;
- 128K bytes of internal flash memory.

Radio boards support plug and play connection with all of Crossbow's sensor boards, data acquisition boards and coordinator boards. Radio boards MICA2 and TELOS have similar characteristics.

- **Coordinator Board.** Crossbow considers two types of modules to send data to final user, MIB510 board uses serial port while MIB600 adopts Ethernet connection. The MIB600CA board (showed in Fig. 4.4) provides Ethernet (10/100 Base-T) connectivity and support both MICAz and MICA2 radio boards to exchange data with the network. This module allows remote access to sensor network data via TCP/IP. The MIB600CA is also used to program sensor nodes. The built-in Power Over Ethernet (POE) feature eliminates the need for an external power source, simplifying installation and maintenance.



Figure 4.3: Radio board MicaZ



Figure 4.4: Coordinator board MIB600

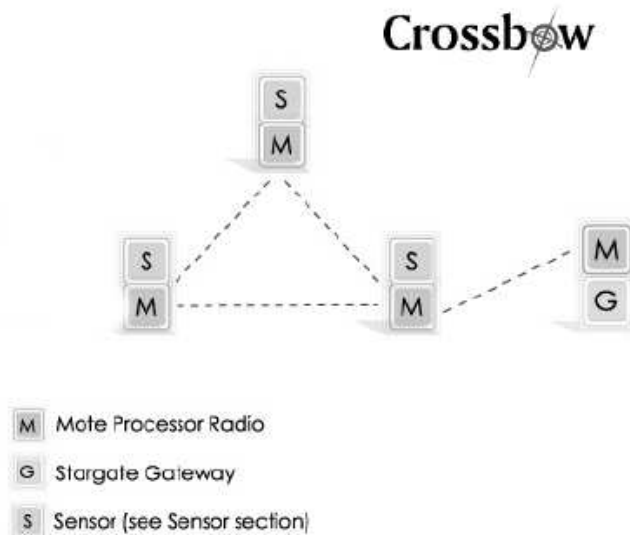


Figure 4.5: Crossbow network

Figure 4.5 shows a typical Crossbow’s network, where sensor nodes include both sensor board (part S) and radio board (part M), while sink include radio board and coordinator board (part G).

As above mentioned, to program sensor nodes, Crossbow platform considers to use operating system TinyOs. This is an open-source operating system designed for wireless embedded sensor networks. It features a component-based architecture which enables rapid innovation and implementation, minimizing code size as required by the severe memory constraints inherent in sensor networks. TinyOS component library includes network protocols, distributed services, sensor drivers, and data acquisition tools, all of which can be used as-is or be further refined for a custom application. TinyOS event-driven execution model enables fine-grained power management yet allows the scheduling flexibility made necessary by the unpredictable nature of wireless communication and physical world interfaces.

4.2.2 Chipcon Platform

Chipcon platform [100] uses the same modular approach and defines three types of boards:

- Radio board. As for Crossbow platform, this module contains both radio part and CPU. The chip CC2431 (Fig. 4.6) is smaller than that



Figure 4.6: Chipcon radio board

of Crossbow platform and supports an antenna circuit that permits to reach higher radio distances. It uses the 2.4 GHz ISM band and can support Zigbee protocol stack. The CPU unit is composed of a microcontroller 8051 that has these characteristics:

- 32 Kbyte of flash memory;
- 8 Kbyte of RAM memory;
- 32 MHz frequency clock;
- 4 operating modes, with a current consumption that can reach as minimum value $5\mu\text{A}$;
- 4 timer/counter (of 8 and 16 bits);
- 21 I/O pin.

For the creation of MAC application, it is used the operating system OSAL.

- Battery board. This is a module where radio board is inserted. It contains two I/O ports used for the connection of external sensors.
- Evaluation board. This module (shown in Fig. 4.7) is equivalent to coordinator board of Crossbow platform. It is used both to program radio board through USB connection and to transmit network data to the user through serial port.

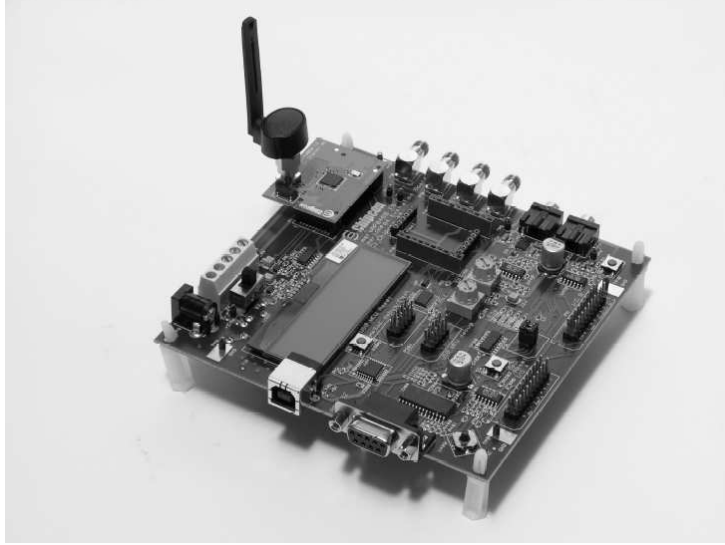


Figure 4.7: Chipcon smart evaluation board

4.3 Application tests on Crossbow Micaz platform

Before to describe the agricultural application, realized during the Ph.D. period, in this section some application tests are presented in order to verify the performance of Crossbow's nodes. These tests have been carried out by using Micaz radio boards.

4.3.1 Interference test

Given that the ISM band is used both by WSNs and by other types of wireless networks (for example WiFi), the first test had the goal to verify the reliability of WSN transmissions in an interference environment.

We used 2.4 GHz Micaz radio boards in a star configuration and in an indoor environment covered by a WLAN network. Nodes were at a distance of few meters from coordinator. Figure 4.8 shows the comparison of WSN and WLAN channels frequencies. For the test it was necessary to consider overlapped channels, consequently it was chosen channel 7 for WLAN, that has a carrier frequency at 2.442 GHz, and channel 18 for WSN, that has carrier frequency at 2.44 GHz. The parameter used to verify communications reliability is the packet error rate (PER), calculated in each sensor-to-coordinator link as the ratio between the number of non-received packets and the number

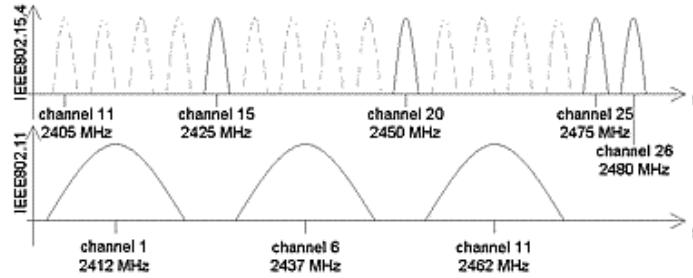


Figure 4.8: WSN and WLAN overlapped channels frequencies

Transmission Power	0dBm	-5dBm	-10dBm	-15dBm	-25dBm
Distance	100m	42m	20m	10m	2m

Table 4.1: Results on distance test

of transmitted packets.

From repeated tests, it has been obtained a maximum value of PER equal to 5.5% with nodes that transmit with a power of 0 dBm, and a maximum value equal to 15% with a transmission power of -25 dBm.

To avoid transmission interference, where it is possible, it is suggested to use non-overlapped channels, as for example, channels 15, 20 and 25.

4.3.2 Radio distance

Another important test is related to the maximum distance that it is possible to reach in a sensor-to-sensor link. This parameter depends on the transmission power. Table 4.1 shows tests results obtained with nodes that transmitted with different powers in a free space environment. Nodes were positioned at an height of 1.7 meters from the soil, in order to avoid multipath effects. The receiver sensitivity was -90dBm.

Considering that, at the moment, sensor nodes have high costs, in a WSN application it becomes important to minimize the number of used nodes, that usually are positioned in a chain configuration. For this reason, nodes are programmed to transmit with the maximum power. This choice increases energy consumptions. From these observations, it is clear as in this scenario it is important to define a trade-off between the number of employed nodes, radio distances and energy consumptions.

In agricultural environment it is possible that communications are ob-

Component	Consumption (mA)
ATMega128L full operation	12
ATMega128L sleep	0.010
Radio, receive	19.7
Radio, transmit (0dBm)	17
Radio, sleep	0.001
Flash memory, write	15
Flash memory, read	4
Flash memory, sleep	0.002

Table 4.2: Energy consumption on Micaz components

structured by trees or foliage. In general, it is important to perform on-field tests to evaluate the maximum radio distance that it is possible to reach in a sensor-to-sensor link in the presence of these obstacles, and consequently define a propagation model for WSNs in agricultural scenarios.

4.3.3 Energy consumptions

As specified in chapter 1 and highlighted in each section of this thesis, energy efficiency is the primary factor to consider in WSNs. Consequently, before to use sensor nodes in a specific application, it is necessary to evaluate nodes consumptions, in order to estimate the lifetime of the network, given the energy resources of each sensor.

Micaz radio boards are supplied by 2 AA batteries and have a practical operating voltage range from 3.6 to 2.7 volt. Table 4.2 shows current consumptions of each radio board component, extracted from Crossbow datasheets [101]. Sensor boards have a consumptions of 5 mA in full operation mode and 5 μ A in sleep mode.

Defining a duty cycle of 1%, that is, considering nodes that are in full operation mode for 1% of simulation time, with a supply capacity of 3000mA-hr Crossbow has estimated a sensor lifetime equal to 17 months.

From tests carried out in the agricultural scenario, described in next section, we have obtained a maximum lifetime of each single node equal to less than a month. The difference with the Crossbow data is due to the fact that, in the realized application, it has been not possible to reach in sleep mode the declared consumptions. From this point of view, the use of a platform that permits to create a MAC application (as e.g. Chipcon), guarantees more flexibility.

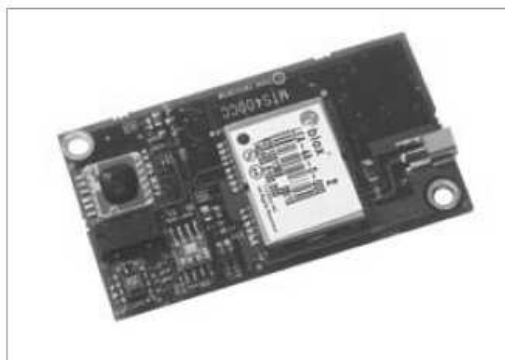


Figure 4.9: MTS420 sensor board

Physical parameter	Sensor type	Range	Resolution	Accuracy
Pressure	Intersema MS5534AM	300-1100 mbar	0.01 mbar	$\pm 1.5\%$ at 25°C
Light	TAOS TSL2550D	400-1000 nm	-	-
Humidity	Sensirion SHT11	0-100% RH	0.03% RH	$\pm 3.5\%$ RH
Temperature	Sensirion SHT11	-10°C to $+60^{\circ}\text{C}$	0.01°C	$\pm 0.5^{\circ}\text{C}$ at 25°C

Table 4.3: Sensor characteristics of MTS420 sensor board

4.4 Agricultural Application

By using the Crossbow platform, we realized an application for agricultural scenarios, that it has been tested on-field for a period of six months.

It is possible to divide this application in four parts:

1. Considering the type of scenario, it was necessary to choose a sensor board with appropriate sensors, and to connect to the ADC channels the possible useful sensors that weren't in the chosen board. Using a Crossbow sensor board MTS420 (showed in Fig. 4.9), it is possible to sense air temperature, humidity, barometric pressure and light. The main characteristics of these sensors are presented in table 4.3. For agricultural application it has been necessary to include soil temperature and rain gauge.
2. To cover a wide area, it has been necessary to create a chain network as that presented in chapter 3. Crossbow "mesh" network protocol implementation it has been modified to support a duty cycle of 1%, that is, it alternated active periods of 10 seconds followed by sleep periods with very low current consumptions ($300 \mu\text{A}$).

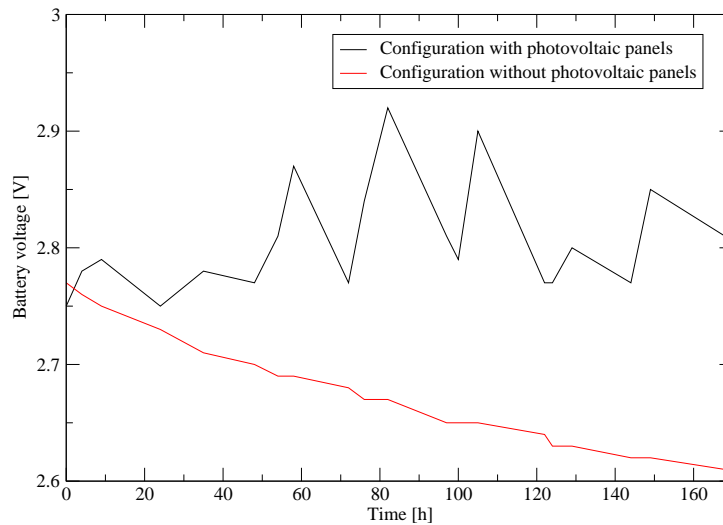


Figure 4.10: Comparison of energy consumptions of nodes with and without photovoltaic panels

3. To guarantee lifetimes on the order of 10 – 12 months, each sensor node has been equipped with photovoltaic panels and rechargeable batteries. Figure 4.10 shows a comparison in terms of energy consumptions between sensor nodes with and without this supply system. Data are related to a period of 170 hours. It is possible to see as, during the day, photovoltaic panels are able to completely recharge batteries, guaranteeing an amount of energy higher than that spent during the night. Theoretically, the nodes could have an infinite duration, but in the real cases it is necessary to consider weather conditions and that batteries can support a finite number of recharges.
4. It has been created a remote transmission system that sends network data to a web site through a GPRS connection in determined intervals.

4.4.1 Results

Figure 4.11 shows the application scenario, with six nodes in a chain configuration. Each of them was at a distance of 30 meters from the next, and at a height of 1.7 meters. The data were gathered at intervals of 15 minutes and transmitted to the coordinator, that forwarded all to the web site every two hours.

Figure 4.12 shows an example of a network data, displayed on the web



Figure 4.11: Agricultural application scenario

site. Each line of the table contains one node information, and in particular, its identification number (ID), its temperature and humidity data, its voltage capacity and the time when data are gathered. The batteries voltage it has been used to estimate energy consumptions.

This application have guaranteed detailed real time control of a large area for agriculture. These data are extremely valuable, for example to monitor insect infections and possible diseases of fruit trees.

Figures 4.13 and 4.14 show air temperature and humidity data recorded over one month of monitoring.

4.5 Evolution: the path towards a dedicated platform

To reduce energy consumptions and to have a more flexible network, after the realization of the agricultural application we realized that it would be very useful to study Chipcon nodes to create a dedicated platform, working directly on the MAC layer.

From the radio distance test, it has been evaluated that, fixing the transmission power, the Chipcon nodes can reach higher distances then the Crossbow. Table 4.4 presents the results obtained. For this implementation we use the Texas Instruments API relative to IEEE802.15.4 MAC layer commands.

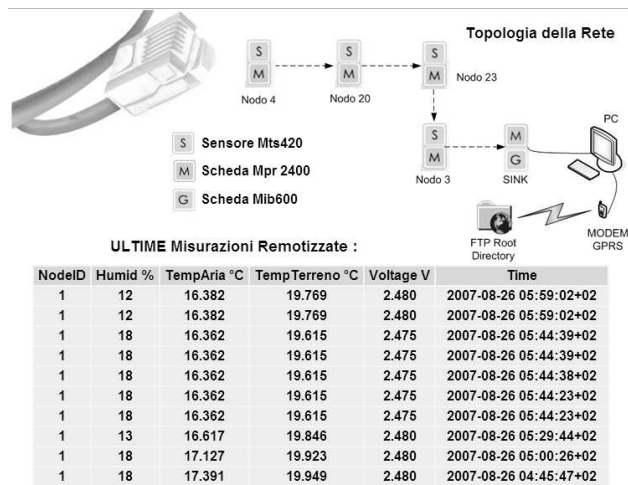


Figure 4.12: Example of a network data displayed on the web site

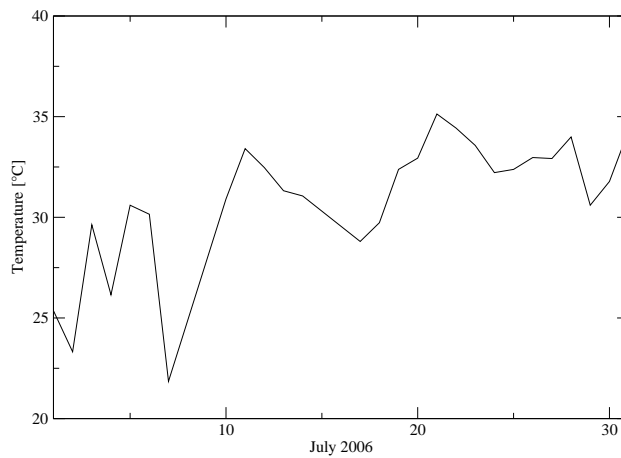


Figure 4.13: Temperature values recorded over one month of monitoring

Transmission Power	0dBm	-6dBm	-15dBm	-25dBm
Distance	200m	50m	25m	10m

Table 4.4: Results on distance test with Chipcon nodes

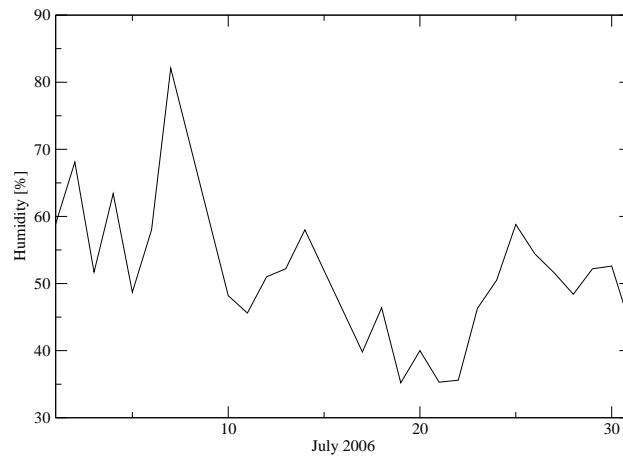


Figure 4.14: Humidity values recorded over one month of monitoring

The main parts of this evolution should include:

- Easy start of the network. When nodes come switched on, it is necessary to define an association procedure that guarantees the creation of each sensor-to-sensor link.
- Fault tolerance. It is important to implement procedures that guarantee correct behavior in presence of a discharge or breaking of some nodes.
- Implementation of a routing algorithm that guarantees minimum energy consumptions and a uniform discharge of the nodes in the network.
- Synchronization. To implement low consumption algorithms, it is important to define synchronization procedures that have to mitigate clock nodes drifts.
- Connection with the user. Data received by coordinator will have to be transmitted to the user. Two solutions are envisaged. In the first one, data are saved on a computer connected to the coordinator; in the second, data are transmitted to a web site through a GPRS/UMTS connection. Independently from the solution, it will be necessary to guarantee transmission of data from coordinator to computer or GPRS/UMTS modem, e.g. through serial port.
- Connection of several types of sensors. Depending on the type of desired application, it will be important to guarantee the connection of different types of sensors to the ADC channels.

- Creation of a user application. User application will have to show the network data and elaborate them in order to obtain some useful information. For example, it could be interesting to calculate the mean temperature or the maximum night humidity values.

This dedicated platform could be used to test the applications described in chapters 2 and 3.

Conclusion

In this thesis, two WSN scenarios have been investigated. For each of them, we have studied problems and goals, and have been presented solutions that it has been validated with simulation results. Moreover, it has been presented a practical implementation of a WSN platform, that it has been used for an on-field trial showing the usage of WSNs in agriculture.

In Chapter 1, the WSN environment has been studied, describing the main characteristics, the protocol stack for this type of networks and several possible applications. In Chapter 2, the UAV scenario has been presented with analytical results showing that it is possible to exploit cooperative diversity for high throughput, low BEP and very low energy nodes consumptions. In Chapter 3, the use of a chain network for a forest fire alarm scenario has been investigated. We considered two cases of study and for each of them we proposed fusion rules that have been shown to give good results, in terms of both throughput in sensor-to-sensor link and error probability. To evaluate the performance of this distributed detection scenario, we introduced a system description that guarantees low computational complexity, making possible the simulation of a high number of nodes. In Chapter 4, WSNs have been studied under a practical point of view, describing the main characteristics of IEEE802.15.4 standard and two commercial WSN platforms. By using a commercial WSN platform we realize an agricultural application that has been tested in a six months on-field experimentation.

Acknowledgments

During my doctoral course period I have been constantly encouraged, supported and advised by several people: had it not been for them, I would not have never made this thesis. I want to express my gratitude to all of them. I am deeply indebted to my supervisor, Prof. Marco Chiani, for offering me the study chance and the research environment, for supporting me, for continuously stimulating me with his instructions. I wish to dedicate a special thank to my telecommunication group-mates Enrico Paolini, Matteo Mazzotti, Gianluigi Liva, Stefano Severi, Matteo Fabbri, Paola Pulini, Michela Varrella and to Prof. Davide Dardari and Andrea Giorgetti for never denying me their precious suggestions any time I needed them. I also wish to thank all my lab-mates, colleagues and friends at university in Cesena, especially Gillo, Nicola Zanolla, Francesco Lodesani, Enrico Vitucci, Emanuele Tavelli, Pablo Gonzalez, Enrico Oliva and all the people carrying out every day their working activity at the II Engineering Faculty of the University of Bologna. I also wish to thank all the friends I have outside the work, and here the list would be really too long. In particular Nicolò, Sheila and their very lovely kids Camilla and Alessandro, Filippo, Sara, Andrea, Gabriella, Gianluca. Finally, I would like to express boundless thanks to my girlfriend and future wife Stefania, whose love and infinite patience enabled this work, to my parents Loris and Fernanda, my brother Alex, for their encouragement in getting a doctoral degree.

Bibliography

- [1] I. F. Akyildiz, W. Su, Y. Sankarasubramaniam, and E. Cayirci, “A survey on sensor networks,” *IEEE Commun. Mag.*, vol. 40, no. 8, pp. 102–114, Aug. 2002.
- [2] M. Tubaishat and S. Madria, “Sensor networks: an overview,” *IEEE Potentials*, vol. 22, no. 2, pp. 20–23, Apr./May 2003.
- [3] R. Verdone, D. Dardari, G. Mazzini, and A. Conti, in *Wireless Sensor and Actuator Networks: technologies, analysis and design*. Elsevier, 2008.
- [4] H. Karl and A. Willig, “A short survey of wireless sensor networks,” Technical University Berlin, Telecommunication Networks Group, Tech. Rep., Oct. 2003.
- [5] C. Y. Chong and S. P. Kumar, “Sensor networks: evolution, opportunities, and challenges,” *Proceedings of the IEEE*, vol. 91, no. 8, pp. 1247–1256, Aug. 2003.
- [6] I. Demirkol, C. Ersoy, and F. Alagöz, “Mac protocols for wireless sensor networks: A survey,” *IEEE Commun. Mag.*, pp. 115–121, Apr. 2006.
- [7] E. Fasolo, M. Rossi, J. Widmer, and M. Zorzi, “In-network aggregation techniques for wireless sensor networks: a survey,” *IEEE Trans. Wireless Commun.*, pp. 70–87, Apr. 2007.
- [8] S. Hedetniemi, S. Hedetniemi, and A. Liestman, “A survey of gossiping and broadcasting in communication networks,” *Networks*, vol. 18.
- [9] W. R. Heinzelman, J. Kulik, and H. Balakrishnan, “Adaptive protocols for information dissemination in wireless sensor networks,” in *Proceedings of ACM MobiCom '99*, pp. 174–185.

- [10] T. Arampatzis, J. Lygeros, and S. Manesis, "A survey of applications of wireless sensors and wireless sensor networks," in *Proceedings of the 13th Mediterranean Conference on Control and Automation*, June 2005, pp. 719–724.
- [11] D. Li, K. Wong, Y. H. Hu, and A. Sayeed, "Detection, classification, and tracking of targets," *IEEE Signal Processing Mag.*, vol. 19, no. 2, pp. 17–29, Mar. 2002.
- [12] T. He, S. Krishnamurthy, J. A. Stankovic, T. Abdelzaher, L. Luo, R. Stoleru, T. Yan, L. Gu, J. Hui, and B. Krogh, "Energy-efficient surveillance system using wireless sensor networks," in *Proceedings of the 2nd international conference on Mobile systems, applications, and services MobySys'04*, pp. 270 – 283.
- [13] B. Sinopoli, C. Sharp, L. Schenato, S. Schaffert, and S. Sastry, "Distributed control applications within sensor networks," in *Proc. IEEE*, vol. 91, Aug. 2003, pp. 1235 – 1246.
- [14] A. Rytter, "Vibration based inspection of civil engineering structures," Ph.D. dissertation, Dept. of Building Technology and Structural Eng., Aalborg University. Denmark, 1993.
- [15] A. Mainwaring, J. Polastre, R. Szewczyk, D. Culler, and J. Anderson, "Wireless sensor networks for habitat monitoring," in *Proc. of ACM Inter. Workshop on Wireless Sensor Networks and Applications (WSNA'02)*, Atlanta GA, USA, 2002.
- [16] J. Burrell, T. Brooke, and R. Beckwith, "Vineyard computing: sensor networks in agricultural production," *Pervasive Computing IEEE*, vol. 3, no. 1, pp. 38–45, 2004.
- [17] L. Schwiebert, S. K. Gupta, and J. Weinmann, "Research challenges in wireless networks of biomedical sensors," in *Mobile Computing and Networking*, 2001, pp. 151–165.
- [18] M. B. Srivastava, R. R. Muntz, and M. Potkonjak, "Smart kindergarten: sensor-based wireless networks for smart developmental problem-solving environments," in *Mobile Computing and Networking*, 2001, pp. 132–138.
- [19] J. K. Perng, B. Fisher, S. Hollar, and K. S.J.Pister, "Acceleration sensing glove (ASG)," in *ISWC International Symposium on Wearable Computers*, 1999, pp. 178–180.

- [20] C. Buratti, A. Giorgetti, and R. Verdone, "Simulation of an energy efficient carrier sensing multiple access protocol for clustered wireless sensor networks," in *Proc. IEEE Int. Work. on Wireless Ad-hoc Networks (IWWAN2004)*, Oulu, Finland, June 2004, pp. 325–329.
- [21] —, "Cross layer design of an energy efficient cluster formation algorithm with carrier sensing multiple access for wireless sensor networks," *EURASIP Journal on Wireless Communications and Networking*, no. 5, pp. 672–685, Dec. 2005.
- [22] T. Q. S. Quek, M. Z. Win, and M. Chiani, "Distributed diversity in ultrawide bandwidth wireless sensor networks," in *Proc. IEEE Vehicular Tech. Conf. (VTC2005-Spring)*, vol. 2, Stockholm, Sweden, May 2005, pp. 1355–1359.
- [23] S. D. Servetto, "Distributed signal processing algorithms for the sensor broadcast problem," in *Proc. of the 37th Annual Conf. on Information Sciences and Systems (CISS)*, Baltimore, MD, Mar. 2003.
- [24] J. Barros and S. D. Servetto, "Network information flow with correlated sources," *IEEE Trans. Inform. Theory*, vol. 52, no. 1, pp. 155–170, Jan. 2006.
- [25] Z. Yang and L. Tong, "Cooperative sensor networks with misinformed nodes," *IEEE Trans. Inform. Theory*, vol. 51, no. 12, pp. 4118–4133, Dec. 2005.
- [26] A. Scaglione and Y.-W. Hong, "Opportunistic large array: Cooperative transmission in wireless multihop ad hoc networks to reach far distances," *IEEE Trans. Signal Processing*, vol. 51, no. 8, pp. 2082–2092, Aug. 2003.
- [27] T. Q. S. Quek and M. Z. Win, "Analysis of UWB transmitted-reference communication systems in dense multipath channels," *IEEE J. Select. Areas Commun.*, vol. 23, no. 9, pp. 1863–1874, Sept. 2005.
- [28] T. Q. S. Quek, D. Dardari, and M. Z. Win, "Energy efficiency of dense wireless sensor networks: To cooperate or not to cooperate," *IEEE JSAC (Special Issue on Cooperative Communications and Networking)*, vol. 25, no. 2, Feb 2007.
- [29] J. N. Laneman and G. W. Wornell, "Distributed space-time-coded protocols for exploiting cooperative diversity in wireless networks," *IEEE Trans. Inform. Theory*, vol. 49, no. 10, pp. 2415–2425, Oct. 2003.

- [30] H. E. Gamal and D. Aktas, “Distributed space-time filtering for cooperative wireless networks,” in *Globecom 2003*, vol. 4, San Francisco, USA, Dec. 2003, pp. 1826–1830.
- [31] A. Sendonaris, E. Erkip, and B. Aazhang, “User cooperation diversity-part I: System description,” *IEEE Trans. Commun.*, vol. 51, no. 11, pp. 1927–1938, Nov. 2003.
- [32] —, “User cooperation diversity-part II: Implementation aspects and performance analysis,” *IEEE Trans. Commun.*, vol. 51, no. 11, pp. 1939–1948, Nov. 2003.
- [33] A. Bletsas, H. Shin, and M. Z. Win, “Outage-optimal cooperative communications with regenerative relays,” in *Proc. of 40th Conf. on Information Sciences and Systems (CISS 2006)*, Princeton NJ, USA, Mar. 2006.
- [34] —, “Cooperative communications with outage-optimal opportunistic relaying,” *IEEE Trans. Wireless Commun.*, vol. 6, no. 9, pp. 3450 – 3460, sep 2007.
- [35] —, “Outage optimality of opportunistic amplify-and-forward relaying,” *IEEE Commun. Lett.*, vol. 11, no. 3, pp. 261–263, Mar. 2007.
- [36] P. A. Bello, “Aeronautical channel characterization,” *IEEE Trans. Commun.*, vol. 21, no. 5, pp. 548–563, May 1973.
- [37] E. Haas, “Aeronautical channel modeling,” *IEEE Trans. Veh. Technol.*, vol. 51, no. 2, pp. 254–264, Mar. 2002.
- [38] J. L. Cuevas-Ruíz and J. A. Delgado-Penín, “Channel modeling and simulation in HAPS systems,” in *Proc. The Fifth European Wireless Conf.*, Barcelona, Spain, Feb. 2004.
- [39] G. L. Stuber, *Principles of Mobile Communication*, 2nd ed. Norwell, MA 02061: Kluwer Academic Publishers, 2001.
- [40] M. Pursley, “The role of spread spectrum in packet radio networks,” *Proceedings of the IEEE*, vol. 75, no. 1, pp. 116–134, Jan. 1987.
- [41] M. Z. Win and R. Scholtz, “Impulse radio: How it works,” *IEEE Commun. Lett.*, vol. 2, no. 2, pp. 36–38, Feb. 1998.

- [42] ———, “Ultra-wide bandwidth time-hopping spread-spectrum impulse radio for wireless multiple-access communications,” *IEEE Trans. Commun.*, vol. 48, no. 4, pp. 679–691, Apr. 2000.
- [43] J. R. Foerster, “The performance of a direct-sequence spread ultra wideband system in the presence of multipath, narrowband interference, and multiuser interference,” in *Proc. IEEE Conf. on Ultra Wideband Sys. and Tech. (UWBST’02)*, Baltimore MD, USA, May 2002, pp. 87–92.
- [44] M. Z. Win, G. Chrisikos, and N. R. Sollenberger, “Performance of Rake reception in dense multipath channels: Implications of spreading bandwidth and selection diversity order,” *IEEE J. Select. Areas Commun.*, vol. 18, no. 8, pp. 1516–1525, Aug. 2000.
- [45] W. E. Ryan, L. Han, and P. A. Quintana, “Design of a low-orbit-to-geostationary satellite link for maximal throughput,” *IEEE Trans. Commun.*, vol. 45, no. 8, pp. 988–996, Aug. 1997.
- [46] L. H. Ozarow, S. Shamai, and A. D. Wyner, “Information theoretic considerations for cellular mobile radio,” *IEEE Trans. Veh. Technol.*, vol. 43, no. 2, pp. 359–378, May 1994.
- [47] A. Giorgetti, P. J. Smith, M. Shafi, and M. Chiani, “MIMO capacity, level crossing rates and fades: The impact of spatial/temporal channel correlation,” *Int. Journal of Communications and Networks (special issue on Coding and signal processing for MIMO systems)*, vol. 5, no. 2, pp. 104–115, June 2003.
- [48] S. Wang and A. Abdi, “On the second-order statistics of the instantaneous mutual information of time-varying fading channels,” in *Proc. IEEE Int. Work. on Signal Processing Advances for Wireless Communications (SPAWC’05)*, New York City, NY, June 2005, pp. 405–409.
- [49] J. G. Proakis, *Digital Communications*, 4th ed. McGraw-Hill, 2001.
- [50] M. Chiani, D. Dardari, and M. K. Simon, “New exponential bounds and approximation for the computation of error probability in fading channels,” *IEEE Trans. Wireless Commun.*, vol. 2, no. 4, pp. 840–845, July 2003.
- [51] Y. Li, Z. Wang, and Y. Song, “Wireless sensor network design for wildfire monitoring,” in *IEEE Proceedings of the 6th World Congress*

- on *Intelligent Control and Automation*, Dalian, China, June 2006, pp. 109–113.
- [52] Z. Chaczko and F. Ahmad, “Wireless sensor network based system for fire endangered areas,” in *IEEE Proceedings of the Third International Conference on Information Technology and Applications (ICITA’05)*.
- [53] T. M. Cover, “Hypothesis testing with finite statistics,” *The Annals of Mathematical Statistics*, vol. 40, no. 3, pp. 828–835, June 1969.
- [54] P. K. Varshney, *Distributed Detection and Data Fusion*. Springer, 1996.
- [55] J.-F. Chamberland and V. V. Veeravalli, “Wireless sensors in distributed detection applications,” *IEEE Signal Processing Mag.*, pp. 16–25, May 2007.
- [56] R. R. Tenney and N. R. Sandell, “Detection with distributed sensors,” *IEEE Trans. Aerosp. Electron. Syst.*, vol. 17, no. 4, pp. 501–510.
- [57] J. N. Tsitsiklis, “Decentralized detection,” *Adv. Statistical Signal Processing*, vol. 2, pp. 297–344.
- [58] R. Viswanathan and P. K. Varshney, “Distributed detection with multiple sensors: Part I-fundamentals,” in *Proc. IEEE*, vol. 85, Jan. 1997, pp. 54–63.
- [59] R. S. Blum, S. A. Kassam, and H. V. Poor, “Distributed detection with multiple sensors: Part II-advanced topics,” in *Proc. IEEE*, vol. 85, Jan. 1997, pp. 64–79.
- [60] Z. Chair and P. K. Varshney, “Distributed Bayesian hypothesis testing with distributed data fusion,” *IEEE Trans. Syst., Man, Cybern.*, vol. 18, no. 5, pp. 695–699, 1988.
- [61] J. N. Tsitsiklis, “Decentralized detection by a large number of sensors,” *Math. Control, Signals, Syst.*, vol. 1, no. 2, pp. 167–182.
- [62] J.-F. Chamberland and V. V. Veeravalli, “Asymptotic results for decentralized detection in power constrained wireless sensor networks,” *IEEE J. Select. Areas Commun.*, vol. 22, no. 6, pp. 1007–1015, Aug. 2004.
- [63] ———, “Decentralized detection in sensor networks,” *IEEE Trans. Signal Processing*, vol. 51, no. 2, pp. 407–416, Feb. 2003.

- [64] B. Chen and P. Willett, “On the optimality of the likelihood-ratio test for local sensor decision rules in the presence of nonideal channels,” *IEEE Trans. Inform. Theory*, vol. 51, no. 2, pp. 693 – 699, Feb. 2005.
- [65] P. Willett, P. Swaszek, and R. Blum, “The good, bad and ugly: distributed detection of a known signal in dependent Gaussian noise,” *IEEE Trans. Signal Processing*, vol. 48, no. 12, pp. 3266 – 3279, Dec. 2000.
- [66] J.-F. Chamberland and V. Veeravalli, “How dense should a sensor network be for detection with correlated observations?” *IEEE Trans. Inform. Theory*, vol. 52, no. 11, pp. 5099 – 5106, Nov. 2006.
- [67] K. Liu and A. Sayeed, “Asymptotically optimal decentralized type-based detection in wireless sensor networks,” in *Proc. Int. Conf. Acoustics, Speech, Signal Processing (ICASSP '04)*, vol. 3, May 2004, pp. 873–876.
- [68] H. Hashemi and I. Rhodes, “Decentralized sequential detection,” *IEEE Trans. Inform. Theory*, vol. 35, no. 3, pp. 509 – 520, May 1989.
- [69] V. Veeravalli, T. Basar, and H. Poor, “Minimax robust decentralized detection,” *IEEE Trans. Inform. Theory*, vol. 40, no. 1, pp. 35 – 40, Jan. 1994.
- [70] V. Aalo and R. Viswanathou, “On distributed detection with correlated sensors: two examples,” *IEEE Trans. Aerosp. Electron. Syst.*, vol. 25, no. 3, pp. 414 – 421, May 1989.
- [71] S. Alhakeem and P. K. Varshney, “A Bayesian formulation of decentralized detection systems with feedback,” in *Proc. 1990 Conf. on Info. Sciences and Systems*, Princeton, Mar. 1990.
- [72] R. S. Blum and S. A. Kassam, “Optimum distributed detection of weak signals in dependent sensors,” *IEEE Trans. Inform. Theory*, vol. 38, no. 3, pp. 1066–1079, May 1992.
- [73] R. S. Blum, “Necessary conditions for optimum distributed sensor detectors under the Neyman-Pearson criterion,” *IEEE Trans. Inform. Theory*, vol. 42, no. 3, pp. 990–994, May 1996.
- [74] T. M. Cover and J. A. Thomas, *Elements of Information Theory*. New York: John Willet & Sons, 1991.

- [75] H. Delic and P. Papantoni-Kazakos, "Robust decentralized detection by asymptotically many sensors," *IEEE Trans. Signal Processing*, vol. 33, no. 2, pp. 223–234, Aug. 1993.
- [76] W. Irving and J. Tsitsiklis, "Some properties of optimal thresholds in decentralized detection," *IEEE Trans. Automat. Contr.*, vol. 39, no. 4, pp. 835–838, Apr. 1994.
- [77] J. Papastavrou and M. Athans, "Distributed detection by a large team of sensors in tandem," *IEEE Trans. Aerosp. Electron. Syst.*, vol. AES-28, no. 3, pp. 639–653, July 1992.
- [78] —, "On optimal distributed decision architectures in a hypothesis testing environment," *IEEE Trans. Automat. Contr.*, vol. 37, no. 8, pp. 1154–1169, Aug. 1992.
- [79] J. Papastavrou, "Decentralized decision making in a hypothesis testing environment," Ph.D. dissertation, M.I.T., Boston, MA, USA, May 1990.
- [80] G. Polychronopoulos and J. Tsitsiklis, "Explicit solutions for some simple decentralized detection problems," *IEEE Trans. Aerosp. Electron. Syst.*, vol. AES-26, pp. 282–292, Mar. 1990.
- [81] A. Reibman and L. Nolte, "Optimal detection and performance of distributed sensor systems," *IEEE Trans. Aerosp. Electron. Syst.*, vol. AES-23, pp. 24–30, Jan. 1987.
- [82] —, "Design and performance comparison of distributed detection networks," *IEEE Trans. Aerosp. Electron. Syst.*, vol. AES-23, pp. 789–797, Nov. 1987.
- [83] —, "Optimal design and performance of distributed signal detection systems with faults," *IEEE Trans. Acoust., Speech, Signal Processing*, vol. 38, no. 10, pp. 1771–1783, Oct. 1990.
- [84] R. Srinivasan, "A theory of distributed detection," *Signal Processing*, vol. 11, pp. 319–327.
- [85] —, "The detection of weak signals using distributed sensors," in *Proc. of the Conf. on Info. Sciences and Systems*, Princeton, Mar. 1990.
- [86] —, "Distributed detection with decision feedback," *IEE Pro.*, vol. 137, no. 6, pp. 427–432, Dec. 1990.

- [87] J. Tsitsiklis and M. Athans, "Convergence and asymptotic agreement in distributed decision problems," *IEEE Trans. Automat. Contr.*, vol. 29, no. 1, pp. 42–50, Jan. 1984.
- [88] ———, "On the complexity of decentralized decision making and detection problems," *IEEE Trans. Automat. Contr.*, vol. AC-30, pp. 440–446, May 1985.
- [89] J. Tsitsiklis, "On threshold rules in decentralized detection," in *Proc. 25th IEEE Conf. on Decision and Control*, vol. 1, pp. 232–236.
- [90] S. Thomopoulos, R. Viswanathan, and D. Bougoulas, "Optimal distributed decision fusion," *IEEE Trans. Aerosp. Electron. Syst.*, vol. AES-25, pp. 761–765, Sept. 1989.
- [91] H. V. Trees, *Detection, Estimation, and Modulation Theory*. New York: John Willet & Sons, 1968.
- [92] V. Veeravalli, "Topics in decentralized detection," Ph.D. dissertation, University of Illinois, Illinois, USA, apr 1992.
- [93] R. Viswanathan and A. Ansari, "Distributed detection of a signal in generalized Gaussian noise," *IEEE Trans. Acoust., Speech, Signal Processing*, vol. 37, no. 5, pp. 775–779, May 1989.
- [94] R. Viswanathan, S. Thomopoulos, and R. Tumuluri, "Optimal serial distributed decision fusion," *IEEE Trans. Aerosp. Electron. Syst.*, vol. AES-24, pp. 366–375, July 1988.
- [95] P. Willet and D. Warren, "Decentralized detection: An information theoretic approach," in *Proc. of the Conf. on Info. Sciences and Systems*, Princeton, Mar. 1988.
- [96] P. F. Swaszek, "On the performance of serial networks in distributed detection," *IEEE Trans. Aerosp. Electron. Syst.*, vol. 29, no. 1, pp. 254–260, Jan. 1993.
- [97] "Zigbee alliance." [Online]. Available: <http://www.zigbee.org>
- [98] "IEEE standard for information technology - telecommunications and information exchange between systems - local and metropolitan area networks - specific requirement part 15.4: Wireless medium access control (MAC) and physical layer (PHY) specifications for low-rate wireless personal area networks (WPANs)," *IEEE Std 802.15.4-2006 (Revision of IEEE Std 802.15.4-2003)*, pp. 1–305, 2006.

- [99] “Crossbow WSN platform.” [Online]. Available: <http://www.xbow.com>
- [100] “Chipcon WSN platform.” [Online]. Available: <http://www.ti.com>
- [101] “Crossbow WSN platform datasheets.” [Online]. Available: http://www.xbow.com/support/Support_pdf_files/MPR-MIB_Series_Users_Manual.pdf